A Sheffield Hallam University thesis

SHEFFIELD HALLAM UNIVERSITY

Mass spectrometry methods for profiling xenobiotic distribution in biofluids and whole tissues

A thesis submitted in partial fulfilment of the requirements of Sheffield Hallam University for the degree of Doctor of Philosophy

John G. Swales

December 2017

Abstract

Historically, studies of drug biodistribution are traditionally carried out in the later stages of pre-clinical pharmaceutical research and development (R&D) using radio-labelled techniques. Such studies are often slow, expensive and unselective, meaning resulting data can be complicated to deconvolute and too late in the development pipeline to change the medicine under investigation.

Mass spectrometry imaging (MSI) has the potential to provide an unlabelled, multiplex method of mapping and quantifying molecular distributions within tissues at a much earlier stage in the R&D timeline, informing researchers of exposure in target tissue or providing evidence of localised and accumulated drug concentration in tissues exhibiting symptoms of toxicity.

The research presented in this thesis begins by exploring the use of MALDI, DESI and LESA-MSI in early pharmacokinetic cassette dosing studies. Furthermore, MSI techniques were applied to blood brain barrier penetration studies to assess compound penetration profiles. Quantitative MSI (qMSI) methods were studied using tissue mimetics to generate accurate calibration lines and produce *in situ* concentration data. Finally, region specific qMSI was used to quantify endogenous metabolite concentrations and evaluate tumour heterogeneity in several different tumour models, identifying a model that would be used in pre-clinical efficacy studies.

The results indicate that MSI drug distribution studies can be performed much earlier in the lead optimisation stage of the drug discovery process. This was done using a range of MSI platforms with different sensitivity, spatial resolution and chemical scope. The use of LESA-MSI to assess drug blood brain barrier penetration revealed benefits

over non-spatially resolved analytical methods. The multiplex nature of MSI analysis was shown to mitigate residual blood contamination in brain tissue sections giving greater differentiation of poorly BBB permeable drugs. Development of quantitative LESA and DESI-MSI methods were used in conjunction with tissue mimetics to show that qMSI is a reliable way of generating in-tissue concentration data. qMSI results compared favourably with 'gold standard' LC-MS approaches. Finally, MALDI-qMSI was shown to be capable of generating region-specific concentration data of endogenous metabolites in heterogeneous tumour tissues. This culminated in drug project selection of a tumour model with a less heterogeneous lactate distribution, less intra-tumour lactate variability and a better platform to discriminate lactate modulation in drug dosed animals versus control in efficacy studies.

The research presented in this thesis has shown that the MSI methodology developed can be successfully applied to pharmaceutical R&D. The validated protocols can be employed earlier in the development timeline allowing researchers time to evaluate and react to any data produced. Furthermore, MSI has been shown to be applicable in pharmacokinetic, pharmacodynamic and toxicity studies, offering spatially enhanced results that complement the data generated using existing analytical techniques and hence can make a contribution to safer, more efficacious medicines being brought to patients.

ACKNOWLEDGEMENTS

ear when I needed one. You have been an inspiration over the course of my studies and career, I value our friendship immensely.

The unsung heroes of a PhD story are family and friends. Mark Denn, Caroline Smith, Louise Moss and Kerry Frost have provided much needed distraction over the years. I'd also like to thank my oldest friend Professor Chris Van Der Gast for his inspiration and unconditional kinship since the age of 4.

I could not have done most of the things I've done without firm foundations, for that I give thanks to my mum and dad, Jean and John Swales for being the best parents anyone could wish for, they have offered advice, love and support throughout my life, they have also told me straight over the years when I needed to concentrate on things. You have both been an inspiration and made me the man I am.

Finally I would like to thank my beautiful girls. PhD's take some time and effort on the part of the student, but inevitably that impacts on someone else. Helen Scoble is my partner and rock, she has never complained when I've disappeared to study or left to go and showcase my research in far flung places, she keeps our family together and is a fantastic and much loved partner and mum. That brings me to the two people I hope will take the most inspiration from their dad doing this work. Jessica and Emily Swales my beautiful daughters, I love you both so much, it's a pleasure to be your dad and I hope you both grow up to be happy, healthy and wise!

Table of Contents

LIST OF FIGURES

LIST OF TABLES

ABBREVIATIONS

3D	3-Dimensional
9-AA	9-Aminoacridine
AC	Acetyl carnitine
ATP	Adenosine triphosphate
CASI	Continuous Accumulation of Selected Ions
CHCA	α-cyano-4-hydroxycinnamic acid
CID	Collision Induced Dissociation
Da	Daltons
DAN	1,5-diaminonapthalene
DESI	Desorption Electrospray Ionisation
DHB	2,5-dihydroxybenzoic acid
DNA	Deoxyribonucleic acid
EPR	Enhanced permeability and retention
ESI	Electrospray Ionisation
FFPE	Formalin Fixed Paraffin Embedded
FTICR	Fourier Transform Inductively Coupled Resonance
GB	Gigabytes
H&E	Haematoxylin & Eosin
HPLC	High Performance Liquid Chromatography
Hrs	Hours
ICP	Inductively coupled plasma
IDO1	indoleamine-2,3-dioxygenase1
IHC	Immunohistochemistry

IP	Isopentane
IS	Internal Standard
IV	Intravenous
kHz	Kilohertz
LA	Laser Ablation
LAESI	Laser Ablation Electrospray Ionisation
LC	Liquid Chromatography
LESA	Liquid Extraction Surface Analysis
LN	Liquid Nitrogen
LTQ	Linear Trap
m/z	mass to charge ratio
MALDI	Matrix Assisted Laser Desorption Ionisation
MPS	Micro Physiological Systems
MS	Mass Spectrometry
MSI	Mass Spectrometry Imaging
nm	Nanometres
OCT	Optimum Cutting Temperature
PD	Pharmacodynamics
pHPMA	Poly[N-(2-hydroxypropyl)methacrylamide]
PK	Pharmacokinetics
ppm	Parts Per Million
Q1,Q2,Q3	quadrupole 1, 2, 3
QE	Q-Exactive
qMSI	quantitative mass spectrometry imaging

QqQ	Triple quadrupole
QqToF	Quadrupole Time of Flight
qWBA	quantitative Whole Body Autoradiography
R&D	Research & Development
REIMS	Rapid Evaporative Ionisation Mass Spectrometry
RF	Radio Frequency
RNA	Ribonucleic acid
RoC	Receiver operating characteristic
SIMS	Secondary Ion Mass Spectrometry
SRM	Selected Reaction Monitoring
TEC	Tissue Extinction Coefficient
TIC	Total Ion Current
ToF	Time of Flight
μm	Micrometres
UV	Ultraviolet

1. INTRODUCTION

1.1 Introduction to mass spectrometry imaging and its application in pharmaceutical research and development

During pharmaceutical research and development (R&D) it is essential to have a detailed understanding of drug pharmacology, toxicity and distribution. In order to exert an effect drug molecules must reach target receptors at the site of action at a sufficiently high unbound concentration to deliver efficacy whilst it should not be so high that they instigate a toxic response. Plasma concentration measurements have traditionally been used as a surrogate for the concentration of drug in tissues but this does not always accurately represent the levels within specific organs or sub-compartments and therefore additional assays are required in the development of an understanding of the efficacy or toxicology of a new chemical entity *in vivo*. Drug distribution studies are typically performed in later stages of the development pipeline using radio-labelled compounds in techniques such as quantitative Whole Body Autoradiography (qWBA)[1,2] or by using tissue homogenisation followed by LC-MS[3,4]. Whilst these analytical techniques still have relevance in the progression of a new chemical entity, they are often time consuming, costly and misleading due to the non-specific method of detection being used. Radiolabelled drugs have the potential to undergo metabolism, often their primary metabolites can contain the radiolabel and this can misrepresent the distribution profile of the drug rendering the data ambiguous.

In a rapid moving R&D environment it is beneficial to have this drug distribution information at an early stage to confirm drug delivery at the active site or to highlight drug accumulation in an organ where toxicity may have been encountered. Furthermore, it is essential to have an indication of efficacy in target tissues to limit attrition further down the R&D process.

Mass Spectrometry Imaging (MSI) is a technique that is used to visualise the two-dimensional (and 3D) molecular distribution of endogenous compounds[5], drugs[6], lipids[7], proteins[8] and peptides[9] in biological tissue. It encompasses a range of mass spectrometry based platforms all based on different surface sampling ion sources, each variation offering similar but slightly different properties in terms of speed, sensitivity, chemical scope and spatial resolution. Essentially, each technique rasters or continuously scans across tissue sections acquiring a constant full mass spectrum at each pixel or coordinate, each mass peak within the spectrum is assigned an arbitrary intensity that can be colour coded into a heat map image describing the relative abundance of an analyte within the tissue.

Matrix Assisted Laser Desorption/Ionisation (MALDI) is arguably the most predominant MSI technique used in research. MALDI is a 'soft' ionisation technique allowing the detection of large, non-volatile and labile molecules by mass spectrometry. It was introduced in the early 1980's[10], but the first reported use of MALDI for imaging was made in 1984, it did not however gain widespread attention until the seminal paper from the Caprioli group in 1997[11]. MALDI uses a pulsed, high repetition rate laser beam focused at the required spatial resolution making it ideal for microscopic interrogation of chemical entities from tissue sections. MALDI initially suffered from poor reproducibility which cast a cloud over its application within the imaging field but the technique has been developed significantly over the intervening years with changes in instrumentation and improved sample preparation overcoming these initial concerns and constituting a reliable, robust and widely applicable MSI platform capable of qualitative and quantitative analysis.

Since its inception MALDI-MSI has been joined by various complementary imaging capable ion sources. Desorption Electrospray Ionisation (DESI) is being increasingly

employed in various academic and industrial laboratories. As its name suggests, DESI is an ambient ionisation technique based on traditional electrospray ionisation[12] and as such has a wide and varied chemical applicability. Its use was once viewed by researchers as being something of a 'dark art' but recent years have seen it being developed by instrument manufacturers and researchers into a robust analytical technique capable of molecular imaging at spatial resolutions of ~50-100 µm[13]. The technique was first reported in 2004[14] and has grown to become a primary method of MSI. DESI has been widely applied to areas such as lipid profiling[7], neurotransmitter analysis[15], metabolic phenotyping of tumours[16] and xenobiotic drug distribution studies[17]. NanoDESI[18] is a further development of the technique, it is also fundamentally related to Liquid Extraction Surface Analysis (LESA) discussed further below. NanoDESI has been used in quantitative drug analysis[19] as well as a variety of other applications[20,21]. Spatial resolution is higher than DESI at around 12µm[22].

LESA is an MSI technique that has been successfully shown to be applicable in the areas of metabolic profiling[23], identification of proteins[24] and drug imaging[6]. Like DESI it is based upon traditional ESI, giving the technique wide applicability. LESA is sometimes referred to as liquid micro-junction surface sampling[25] and essentially uses a robotic pipette tip to introduce an extraction solvent to predefined areas on a tissue section. The extraction liquid is dispensed onto the tissue whilst maintaining a liquid junction with the pipette tip, it is then aspirated and sprayed into the mass spectrometer usually via a nanoelectrospray chip[26]. The main drawback of the LESA technique is its low spatial resolution, effectively restricted by the diameter of the pipette tip/syringe needle (typically 1000µm) being used to transfer the liquid extraction solvent. A fundamental benefit of this low spatial resolution is the introduction of high amounts of analyte into the mass spectrometer rendering the technique as a high sensitivity

alternative to MALDI and DESI which are both limited by inherent limit of detection thresholds for different chemical classes.

Many other MSI platforms have been developed to perform similar analyses, secondary ion mass spectrometry[27] (SIMS), which pre-dates MALDI as an MSI tool, laser ablation electrospray ionisation[28] (LAESI) and laser desorption ionisation[29] (LDI) are but a few that are being used but have yet to find widespread implementation, usually due to high costs or limited applicability. There are far too many other techniques to discuss in this thesis so this introduction will focus on the primary techniques used in this research project. For a full description of all MS imaging modalities see the recent review by Paine et al.[30].

An important factor in any MSI platform is the mass analyser that is used in conjunction with the ion source. Various different mass analysers are used including time of flight[31], triple quadrupole[32], ion trap[33] and ion cyclotron resonance[34] instruments. Each offer differences in sensitivity, mass resolution, mass accuracy and scan rate and care must be taken when choosing which instrument to purchase, tailor making an MSI platform to the research being undertaken.

Sample pre-treatment is another fundamental part any MSI workflow (a typical MSI workflow can be seen in figure 1). As mentioned earlier most of the techniques employed have benefitted from development of robust sample preparation methods including normalisation of the mass spectrometer response by applying internal standards to the tissue[35], stabilisation of endogenous compounds[36,37], tissue thickness[38] and sample storage[39]. This has helped MSI gain a good reputation as a viable alternative to traditional methods of analysis within industry, with the main pharmaceutical companies now establishing MSI groups to facilitate drug discovery.

Figure 1: A typical Mass Spectrometry Imaging Workflow showing the different steps involved in an MSI experiment from study design to final report.
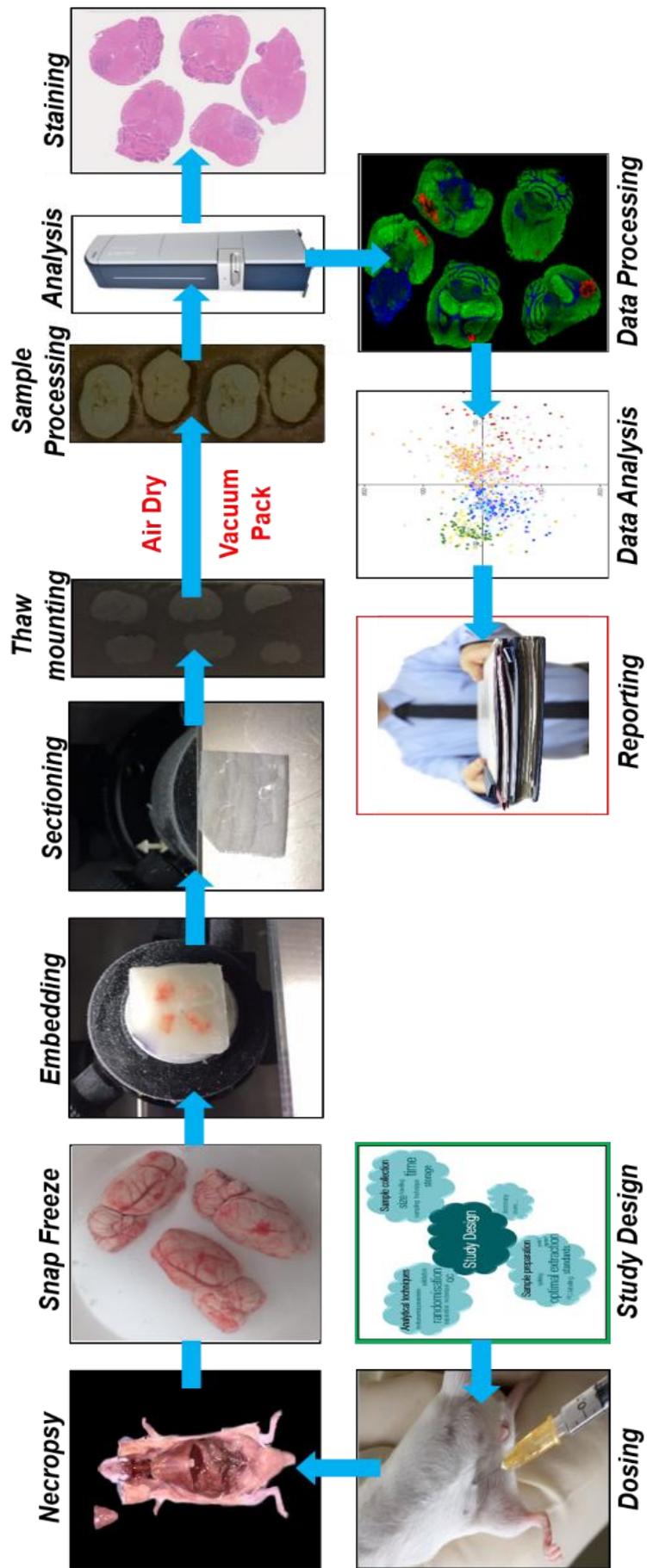
1.2   Ionisation mechanisms and interfaces

1.2.1   Matrix assisted laser desorption ionisation (MALDI)

The MALDI ionisation interface is described in figure 2a. The ionisation process requires the application of large concentrations of an energy absorbent organic compound, called the MALDI matrix, which is coated across the surface of the sample to be analysed (in the case of MSI a tissue section). The MALDI matrix is applied as a solution that promotes extraction of the analytes from the tissue, subsequent evaporation of the solvent causes the matrix and analytes to co-crystallise in a spatially representative way. A pulsed UV laser beam (usually 337 or 355 nm) is used to strike the surface of the matrix in an evacuated chamber. The matrix crystals absorb the ultraviolet light and convert it to heat energy, heating rapidly and vaporising, ionisation occurs in the resulting vaporisation plume, effectively ablating the sample into the mass spectrometer[40]. In the case of MSI the laser pulse is repeated in a raster pattern at spatially distinct intervals across the tissue.

1.2.2   Desorption Electrospray Ionisation (DESI)

The DESI interface is described in figure 2b. The technique is referred to as an ambient ionisation source in contrast to MALDI which is performed under high vacuum. A charged nebulising solvent (usually 95% *v/v* methanol/water) is sprayed from an emitter probe directly at the sample surface extracting the analytes and creating secondary droplets which dry and release the ions in the gas phase into the mass spectrometer. The sample is usually situated on a freely moving sample stage which in the case of DESI-MSI moves from one side of the tissue to the other in spatially separated rows whilst the mass spectrometer acquires a continuous spectrum.

Ionisation occurs via different mechanisms for small and large molecules[41]. Large molecules are ionised by desorption in the liquid phase where multiple charges in the droplet can be transferred to the analyte. Smaller molecules undergo charge transfer of an electron or proton either between the solvent ions and the analyte on the sample surface or between gas phase ions and the analyte on the sample surface or between a gas phase ion and the analyte in the gas phase.

1.2.3   Liquid Extraction Surface Analysis (LESA)

The LESA interface is described in figure 2c. It is essentially a robotic pipetting system. A volume of extraction solvent is aspirated into a conductive pipette tip. The robot moves to a predetermined coordinate and dispenses a small volume of the extraction solvent onto the sample surface whilst maintaining a liquid junction between the tip and the tissue, extraction occurs following the normal principles of solvent extraction. After a slight delay the solvent is re-aspirated into the pipette tip and the robot takes it to a nano-electrospray chip where it follows the normal principles of electrospray ionisation into the mass spectrometer[12]

Figure 2: A schematic of a) the MALDI interface, b) the DESI interface, c) the LESA interface. These surface sampling techniques form the basis of the MSI platforms discussed in this thesis.
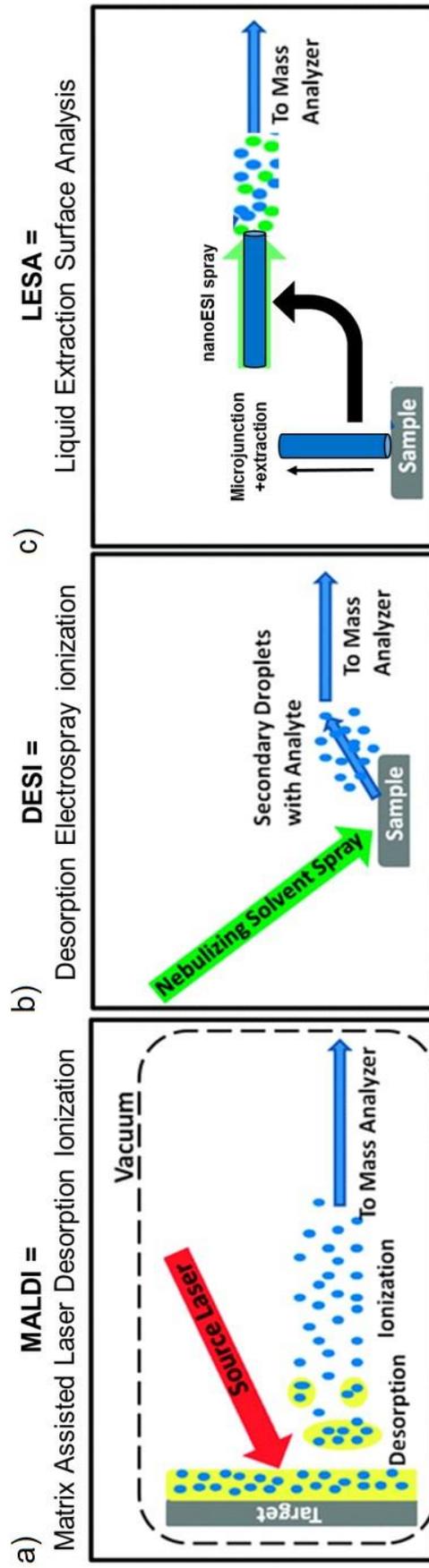
1.3   Mass Analysers

Ions generated by the various ionisation sources described in the previous section are detected by their different mass/charge (*m/z*) ratios. A range of MSI compatible mass analysers, each offering different mass accuracy, mass resolution, sensitivity and signal to noise ratio are available (Table 1). The main variants that have played a part in the research covered in this thesis are discussed, although many other combinations and hybrids are available[42].

Table 1: Comparison of different mass analysers used in MSI

Analyser	Resolving power	Mass Range	Mass accuracy (ppm)	Acquisition frequency (Hz)
ToF	10^3 - 10^4	0 – 20 kDa	1-5	>10
Triple Quadrupole	10^2 - 10^3	0 – 5 kDa	2	>100
Orbitrap (QE)	10^4 - 10^5	$\sim$50 – 6 kDa	1	>10
FTICR	10^4 – 10^6	$\sim$20 Da – 10 kDa	≤1	>1

High mass accuracy, usually expressed as parts per million (ppm) or essentially a 1 mDa error margin on a mass measured at 1000 Da, combined with high mass resolving power, measured as mass at peak centre/width of peak at half height, is highly desirable when performing MSI analyses. The two terms are closely interlinked, with any degradation in one having a negative effect on the other[43]. Thousands of ion images can be generated during a single analytical run, high mass accuracy and

resolving power are required to deconvolute isobaric peaks or overlapping isotopic distributions within the resulting spectra[44].

Sensitivity and signal to noise ratio are largely governed by the sample that is being analysed and not the instrument hardware. Most commercially available instruments have inherently good sensitivity in ideal test conditions, however, when more complex biological matrices are analysed various factors such as ionisation suppression and salt content can vastly change the response and spectra obtained.

1.3.1 Time-of-flight (ToF) mass analysers

ToF mass analysers are arguably the most highly used instrument for MSI[41,45,46]. ToF analysers offer parallel, high detection efficiency, which leads to high inherent instrument sensitivity. Essentially ions are separated by their flight time in a field free region known as a flight tube. Mass to charge ratios are determined by measuring the time it takes for the ions to move through the flight tube and hit the detector and is governed by the following equation:

$m/z = At^2 + B$

Where m/z is the mass/charge ratio, A is the calibration constant calculated by least squares fitting of a series of measured (arrival times) peaks of known m/z values, t is arrival time and B is a second calibration constant accounting for the velocity of the ablation plume.

ToF instruments can have axial or orthogonal geometry. Axial instruments[47] allow ions to directly enter the flight tube from the ion source and travel to the detector (Figure 3). Orthogonal instruments[48] transmit the ions generated from the ion source via ion

optics (often a quadrupole) to a pusher where the ion beam is deflected sideways into the flight tube and on to the detector (Figure 4). Many ToF mass analysers can operate in what is known as linear and reflectron modes, utilising two detectors (Figure 5), linear mode measures *m/z* ratio via flight time to detector one, whereas a ToF analyser operating in reflectron mode does not use detector one, instead ions are reflected back down the flight tube to a second detector via a series of ring electrodes, effectively doubling the length of the flight tube and improving resolution. The reflectron diminishes the spread of flight times of ions with the same *m/z* caused by differences in the kinetic energy of these ions, essentially allowing ions of higher energy (which have a longer flightpath) to reach the detector at the same time as lower energy ions at the same mass.

Figure 3: A schematic of an axial time of flight mass analyser. Ions enter a high vacuum, field free region where they are separated by their flight time prior to detection.
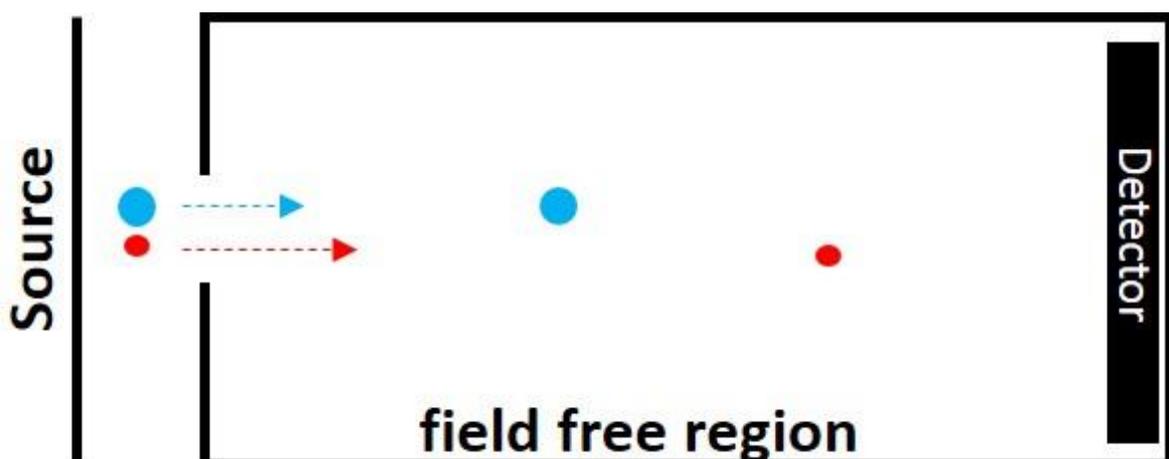
Axial and orthogonal analysers can both operate in full scan only mode (MS) but some instruments are capable of performing tandem mass spectrometry experiments (MS/MS). Axial instruments can form product ions by the introduction of a collision cell directly into the flight tube, splitting the tube into two drift sections, this type of configuration is often referred to as a ToF/ToF instrument. The first drift section separates ions with the same flight time into different groups, entry into the collision cell is controlled by an ion gate that only allows passage of the desired precursor ion for subsequent collision induced dissociation fragmentation. Product ions then enter a second reflectron drift section where they are separated and detected.

Figure 4: A schematic of an axial reflectron time of flight mass analyser capable of MS/MS showing the field free separation regions and the collision cell where precursor ions undergo collision induced dissociation.
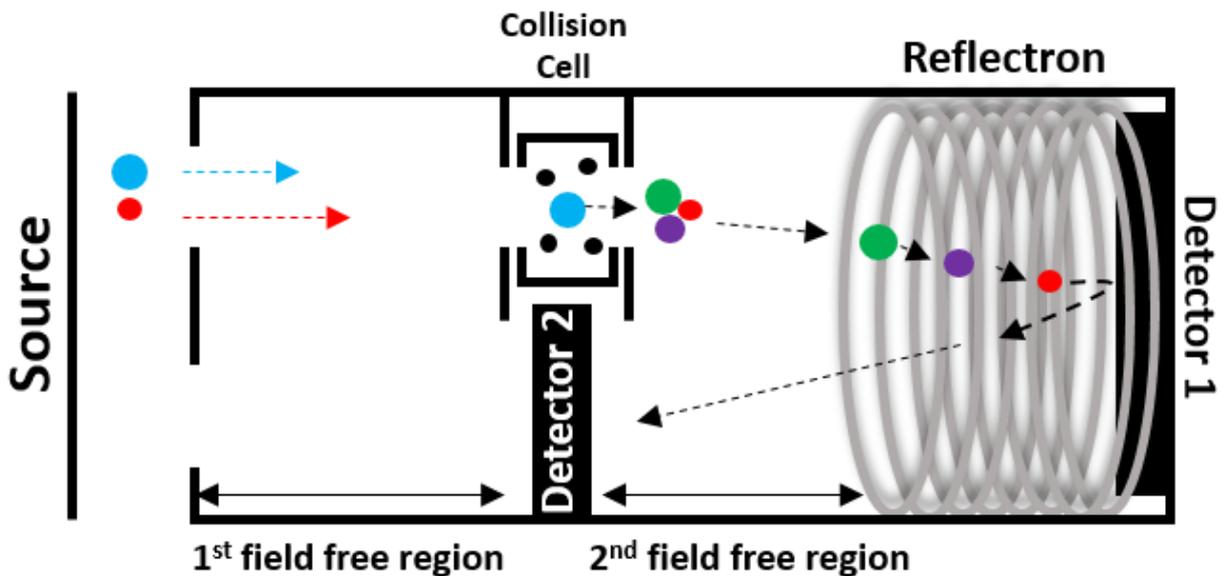
Orthogonal ToF instruments generally use a quadrupole (discussed later) mass filter to select precursor ions generated in the source for entry to the collision cell prior to fragmentation. Product ions subsequently enter the flight tube for separation and detection.

Figure 5: A schematic of an orthogonal reflectron time of flight mass analyser capable of MS/MS. The ion optics region used to select precursor ions is usually a quadrupole mass filter.
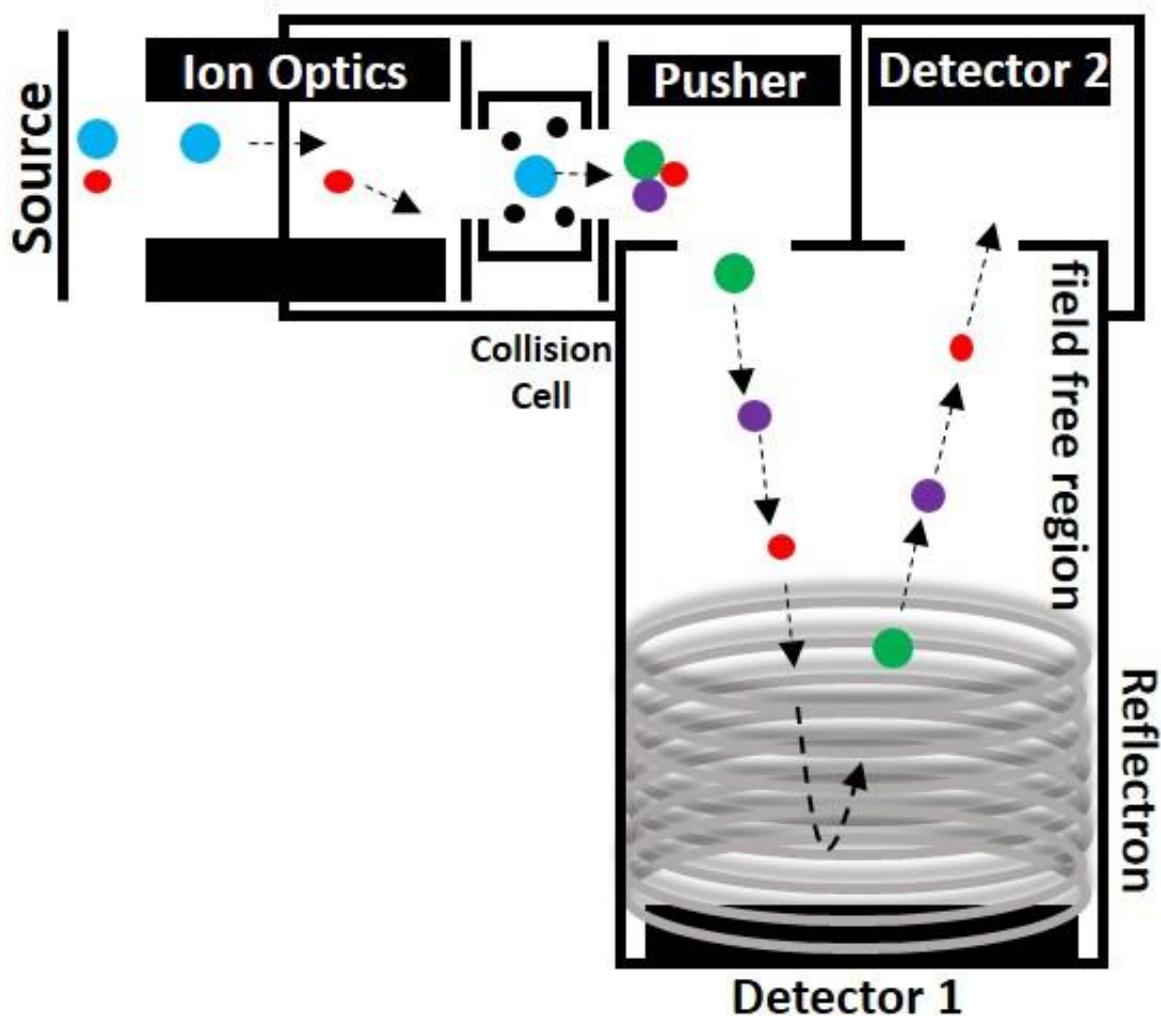
MALDI sources and ToF mass analysers are an ideal combination for performing mass spectrometry imaging experiments due to a variety of reasons. Probably the most significant is that the high duty cycle of the ToF analyser is perfectly coupled to the pulsed repetition rates (as high as 10 kHz) of the MALDI laser process. The ToF analyser allows all ions to be detected almost simultaneously giving it a distinct advantage over scanning mass analysers such as a quadrupole or ion trap instrument. ToF analysers can also be combined with DESI and LESA ion sources.

1.3.2　Quadrupole mass analysers

Quadrupole mass analysers[49] consist of four parallel (ideally) hyperbolic rods (Figure 6) that are used to electronically focus ions of a specific *m/z* ratio through the quadrupole. The opposing rods are electrically linked and specific radio frequencies and voltages are applied intermittently to induce oscillation of selected ions through the quadrupole region. Any ions that are not induced to oscillate assume an unstable trajectory and collide with the rods, resulting in the ions not being transmitted through the quadrupole.

Quadrupoles are used in various hybrid mass analysers usually as mass filters for ions that are selected for subsequent MS/MS experiments, they are also, as the name suggests, and the main mass filter used in triple quadrupole instruments (QqQ). QqQ mass spectrometers are configured using Q1 and Q3 as mass filters whilst Q2 is operated in radio frequency only mode, Q2 can be flooded with an inert 'collision' gas allowing it to act as a collision cell for collision induced dissociation (CID) making MS/MS experiments possible. Mass resolution in quadrupole mass spectrometers is usually lower than that achieved in ToF instruments, typically around unit mass

resolution. QqQ instruments do however offer several different scan modes in addition to full scan mode. Precursor ion scanning, product ion scanning, constant neutral loss and selected reaction monitoring, the most commonly used scan mode on QqQ for MSI. Selected reaction monitoring mode offers high sensitivity, specificity and low signal to noise. QqQ instruments have been shown to be effective in MSI detection, and can be easily combined with MALDI, DESI and LESA ion sources[50-52].

Figure 6: A schematic of a typical quadrupole mass analyser. The quadrupole rods intermittently change polarity and radio frequency to induce ions of a selected mass to pass through to the detector whilst other ions are lost.
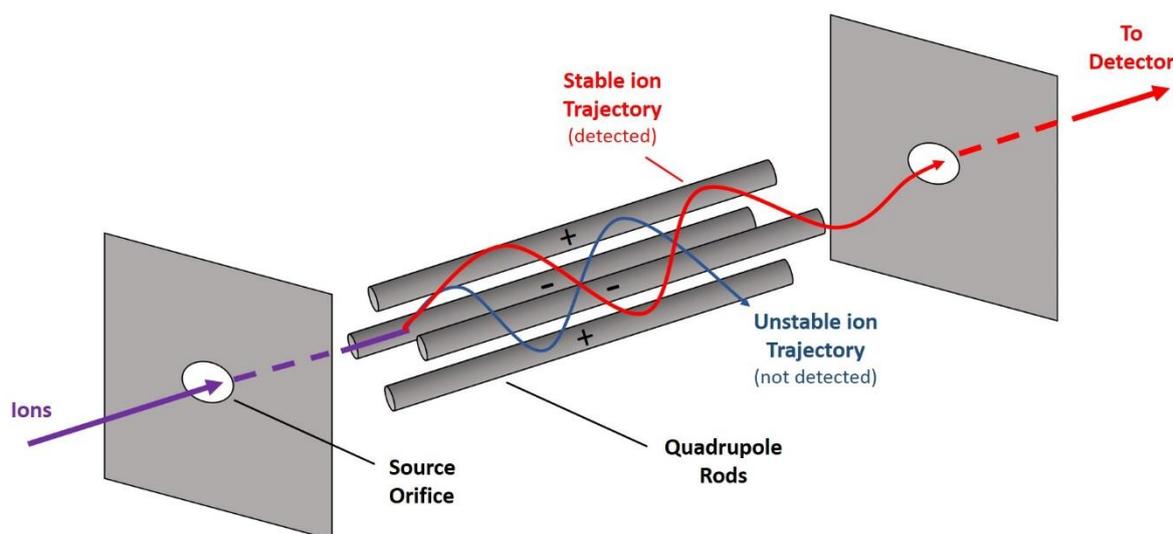
1.3.3 Ion trap mass analysers

There are three different types of ion trap mass analyser, 3D-quadrupole ion traps (Paul traps), Penning traps typically used in FTICR instruments (discussed later) and Kingdon traps used in instruments such as the Orbitrap™.

All ion trap mass analysers operate by storing ions in the trap and by using carefully timed changes in voltage, magnetic field and radiofrequency to manipulate the ions and ultimately deliver them to the detector. Ion traps have the ability to perform MS^n experiments, allowing acquisition of CID data on a particular ion followed by its product ions and any ions resulting from further CID of those product ions, this differentiates ion traps from other mass analysers such as the ToF and QqQ.

Orbitrap based instruments such as the Q-Exactive (Figure 7) offer high mass resolving power (up to 140K at m/z 200) and good mass accuracy. They are increasingly being used in conjunction with DESI ion sources for MSI. The Orbitrap consists of two outer electrodes around an interior spindle shaped electrode connected to independent voltage supplies. The space between the electrodes is at high vacuum. A voltage can be applied to the outer and inner electrodes creating an electric field that can be used to focus the ions in the direction of the central spindle electrode, the circular motion of the ions creates an opposing centrifugal force. An applied axial electric field guides the ions to the widest part of the central spindle creating oscillations concurrently with the circular motion. The outer electrodes measure the ion current in the time domain which is Fourier transformed into the frequency domain then converted into a mass spectrum[53].

Ion trap mass spectrometers can be used with MALDI, DESI and LESA ion sources for MSI analysis.

Figure 7: A schematic of a Q-Exactive mass spectrometer with an Orbitrap mass analyser. The Q-Exactive incorporates a quadrupole mass filter, collision cell and Orbitrap allowing both MS/MS analysis and MS^n.
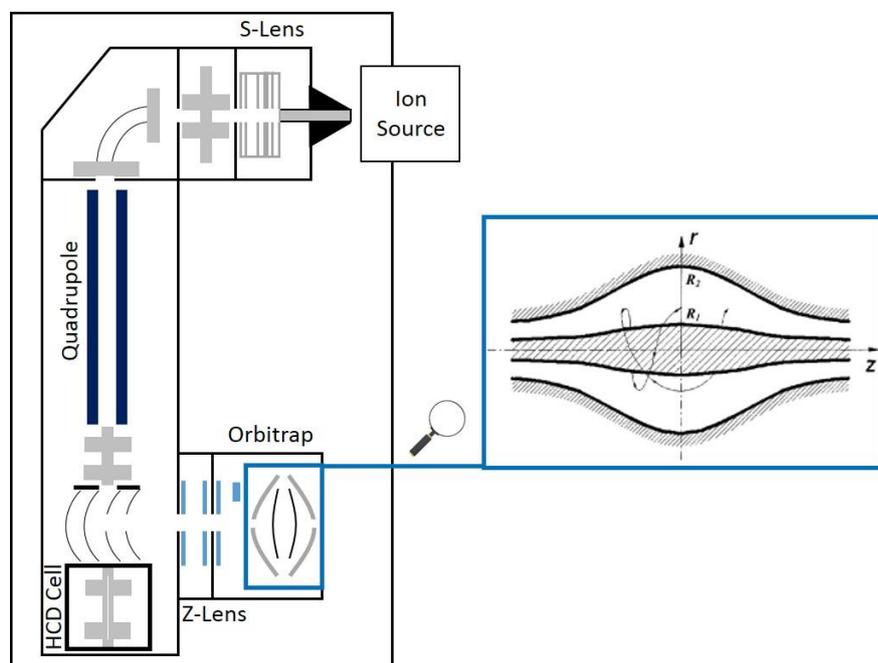
1.3.4   Fourier transfer ion cyclotron resonance (FTICR) mass analysers

FTICR mass analysers are becoming increasingly popular for MSI experiments and widely used in pharmaceutical MSI R&D. FTICR instruments are capable of extremely high mass accuracy and resolving power. FTICR-MS offer new identification strategies that are not reliant on fragmentation, the superior mass resolution offered by the instruments allows identification of unknown structures by elemental composition[54]. FTICR fundamentals are complex and are extensively covered and reviewed elsewhere[55], only the basics are covered here.

FTICR instruments consist of an ICR cell located in the centre of a super-conducting magnet which provides a stable and uniform magnetic field. Ions can undergo cyclotron motion in a stable magnetic field, this motion causes the ions to travel in a circular orbit with a frequency that is dependent on the ions mass.

A typical open cylindrical ICR cell (Figure 8a) consists of several sets of plates known as trapping electrodes, excitation electrodes and detection electrodes. Ions are trapped in the ICR cell by applying a small voltage to the trapping electrodes at either end of the cell. A sweeping radio-frequency potential is applied to the excitation electrodes at a resonant frequency covering all of the ions in the cell, the ions are excited into cyclotron motion with increasing orbital radius (Figure8b) until they either hit the walls and are neutralised or the RF potential is switched off, at which point the ions continue to oscillate and generate a small electric field on the detection electrodes. The data is Fourier transformed from time to frequency domain data from which a *m/z* ratio can be mathematically calculated.

Figure 8: A schematic of Fourier transform ion cyclotron mass spectrometry a) A typical open cylindrical cell where ions are trapped and excited into cyclotron motion, b) Typical Excite/Detect geometry with an ion in cyclotron motion.
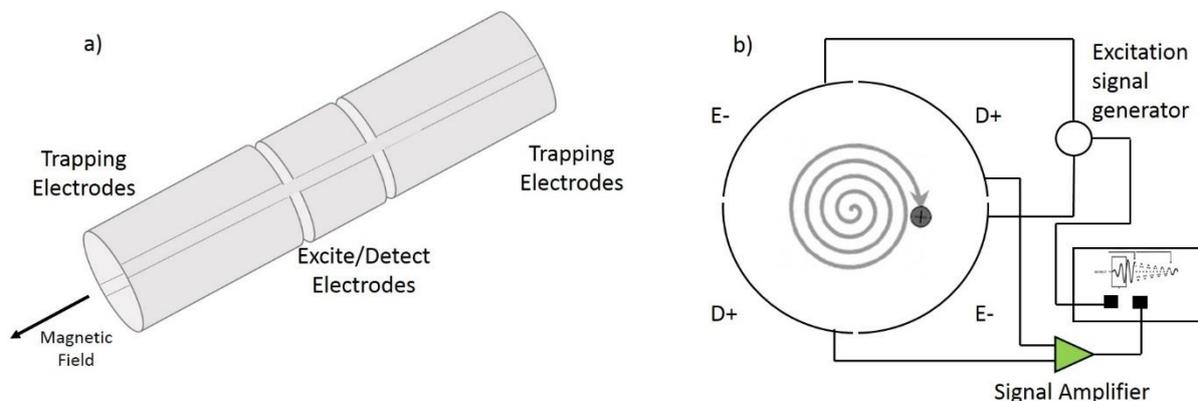
Most FTICR Instruments such as the Bruker SolariX FTICR combine a quadrupole analyser and collision cell with the ICR cell to allow ion isolation, accumulation and MS/MS analysis. Fragmentation can also be done in the ICR cell itself after the introduction of a suitable gas to promote Collision Induced Dissociation (CID). A relatively new introduction to the SolariX platform is Continuous Accumulation of Selected Ions (CASI®)[56], this technique has shown results of up to 10-fold higher sensitivity in comparison with full scan acquisition mode. The CASI mode separates targeted ions from any chemical background noise generated from the sample thereby lowering the limit of detection for the analytes. FTICR instruments are typical used with ESI[57] and MALDI ion sources[58] but can also be linked to LESA.

1.4 Sample preparation

Sample preparation is an important factor when embarking on any MSI analysis[37]. It is essential to adhere to strict sample collection protocols to maintain tissue integrity and minimise any endogenous or exogenous compound degradation within the tissue. Fundamentally MSI analysis requires a flat surface to sample from, so cryomicrotome sectioning under controlled temperature conditions must be performed. DESI and LESA analysis require little sample pre-treatment other than cryomicrotome sectioning prior to standard analysis, although occasionally all MSI techniques benefit from sample washing to remove lipids and salts. Further sample pre-treatment may be required to aid detection such as proteolytic digestion or chemical derivatisation. MALDI-MSI additionally requires the coating of a matrix across the tissue to promote ionisation, this essential step needs careful consideration of factors such as matrix choice, analyte extraction, analyte delocalisation and what spatial resolution is required. Matrix selection, wetness and thickness can take several iterations to fully optimise but with automated systems can be performed reproducibly. The specific considerations of MALDI sample preparation are discussed later.

1.4.1 Sample collection and storage

MSI is best performed on fresh, snap frozen tissue. Snap freezing can be carried out in several different ways to ensure adequate maintenance of the tissue structure and minimal degradation. Essentially different solvent systems can be used to exert different temperatures on the tissue to ensure no tissue fracturing occurs.

Tissues must be snap frozen free floating to avoid any deformation caused by the solvent container. Several different solvents can be used in MSI sample collection but

typically liquid nitrogen (LN) and dry-ice chilled isopentane (IP) are employed depending on the size of the tissue being frozen. Generally small organs or tissue samples can be snap frozen by free floating in LN. Dry-ice chilled IP offers a faster rate of cooling, so is more suitable for larger tissues. Often the freezing rate for more fragile tissues can be too quick so an alternative to IP such as isopropyl alcohol can be used to bring the temperature down more slowly, this is often followed by a short time submerged in LN or IP to bring the temperature of the tissue closer to -80°C. Care must be taken to adequately dry the frozen tissue to ensure no residual solvent is left on the sample that could compromise any subsequent sectioning.

Whole body samples can be frozen in dry-ice chilled hexane. Freezing whole body samples can be a lengthy process often taking as long as 15 mins due to the insulating effect of hair, fat and the outer organs resulting in the risk of continuing metabolic processes[59].

MSI tissue samples are usually stored at -80°C post snap freezing. The samples have been shown to be stable for approximately a year[60], after this period effects on protein and peptide stability has been reported[61].

1.4.2 Other stabilisation methods and formalin fixed paraffin embedded samples

Formalin fixed paraffin embedded (FFPE) samples are the mainstay of traditional histology and as such, extensive libraries of tissue samples exist around the world offering a massive opportunity for MSI analysis to have an impact on the etiology of disease. Successful MSI analysis has been reported using FFPE samples but results have largely been in the area of proteomics[39,61-63]. Extensive covalent cross linking

within proteins in FFPE samples is a significant challenge for MSI analysis. Concerns also exist within the MSI community about delocalisation of smaller molecules and drugs brought about by the formalin fixation process itself and the de-waxing process that is needed prior to analysis. FFPE tissues have however been shown to be effective in lipidomic analysis[64,65], where no signs of delocalisation or interference where observed, despite the higher prevalence of sodium adduct ions arising from the buffers used in the formalin fixation process.

Although snap frozen tissue is considered stable when stored at -80°C cellular degradation restarts when the sample is thawed (when thaw mounting for example)[66]. A method pf preventing proteolytic activity by rapid heating under vacuum to denature tissue proteins and enzymes has been developed[36,67,68]. This method has seen some success but concerns still exist with respect to post stabilisation tissue quality[69]. Incorporation of preservation solvents into MALDI matrices has also been explored as a histologically relevant way of simultaneously stabilising (fixing) the tissue and depositing the MALDI matrix enabling subsequent proteomic analysis[70,71].

1.4.3 Tissue embedding

The time spent cryo-sectioning tissues individually at moderate low temperature (~ -20°C) can sometimes lead to molecular and optical changes to the tissue sections, sometimes called 'freezer burn'. Furthermore, some tissues are small and quite fragile making them hard to cryo-section, it is therefore often necessary to embed several tissues from the same study in a supportive embedding media. Several different embedding media have been successfully used with MSI. Gelatin and carboxymethylcellulose (CMC) are widely used. Optimal cutting temperature (OTC)

media has been used with MSI but severe ion suppression has been observed in several studies as the media coats the cutting blade of the cryostat and contaminates the sections[72]. Recently a new embedding media Poly[N-(2-hydroxypropyl)methacrylamide] (pHPMA) has been developed especially for MSI application[73]. pHPMA has some excellent physical properties making it a good embedding media, unlike other media it is a liquid to around -8°C thus minimising the chance of any outer thawing of the tissue during the embedding process. Practically, pHPMA cuts very nicely on the cryostat and maintains a solid support around the tissue. It has also been shown to have little or no ion suppression effects when used for MSI.

Figure 9: Figure showing several rat kidneys embedded in pHPMA prior to sectioning. The embedding media allows simultaneous sectioning of multiple tissue at the same time, maintaining tissue structure and reducing time spent in the cryostat.
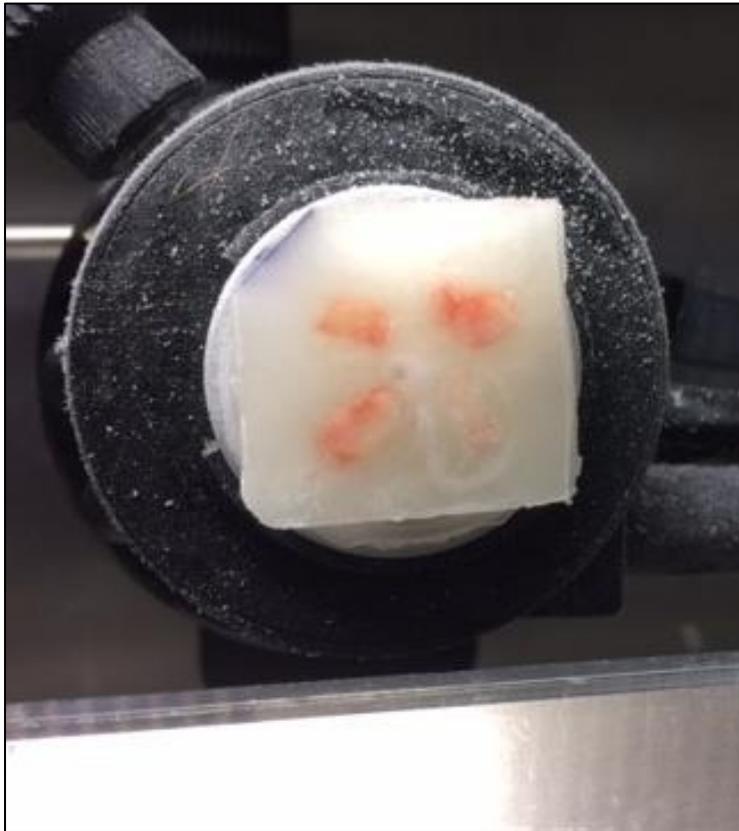
1.4.4   Cryo-sectioning, post sectioning stabilisation and section storage

Cryo-sectioning is an important part of MSI sample preparation. Tissue sections are produced from frozen tissue in a cryomicrotome or cryostat, the tissue is usually mounted onto the cryostat cutting block using a small amount of distilled water. Sections are usually taken at around 10-20 µm thickness and thaw-mounted (gentle warming of the slide under surface) onto glass microscope slides for DESI, LESA and MALDI-MSI or indium tin oxide (ITO) coated glass slides for MALDI-MSI on axial ToF instruments. Stoeckli et al. described the optimum tissue thickness for MSI as being 12 µm[74], although tissue thicknesses ranging from 3-50 µm have been reported[38].

Tissue orientation and cutting depth are sectioning parameters that should be considered prior to embarking on an experiment. Thought should be given to which geometry e.g. sagittal or coronal sectioning will most easily show the required organ features to answer the questions being posed.

Temperature is another sectioning variable that needs to be controlled to allow production of the highest quality sections possible. The temperature at which sections are cut is tissue dependant but generally ranges between -15 to -25°C. In our laboratories we generally cut sequential sections for DESI, MALDI, LESA and histology all at the same time to minimise any potential disorientation caused by remounting the sample at a later date. Sections should be randomised as much as possible on the slide to eliminate any degradation bias caused by time in the cryostat.

Once a section has been cut, it can be dried/desiccated in a stream of nitrogen prior to re-freezing for the addition of further sections. This process stops any build-up of frost on the slides, minimising delocalisation by surface water when the slide is brought back to room temperature, it also stabilises small endogenous metabolites within the

tissue. Once the required sections are cut and the final drying process completed the slides can be vacuum packed and stored at -80°C in individual slide mailers to minimise any freeze/thaw cycles when the slides are used. Care should be taken when removing the slides from -80°C storage to allow the slides to reach room temperature prior to breaking the vacuum pack seal, again minimising any condensation build-up that could cause delocalisation.

1.4.5 Sample washing

Washing mounted sections to remove lipids and salts in order to increase sensitivity and reduce ion suppression has been reported to be effective in the analysis of proteins and peptides[60,72,75,76]. Washing procedures in general should be avoided when analysing small molecules such as drugs, although some successful washing approaches have been applied to such molecules by Shariatgorji et al.[77]. Ammonium salt solution washes have been used to to enhance the sensitivity of negative ion MALDI-MSI lipid analysis[78].

1.4.6 On-tissue tryptic digestion

Protein and peptide analysis are not the focus of this thesis but it is relevant to mention that intact proteins can be detected with reasonable sensitivity up to around the 25-30 kDa mass range. It is also possible to detect larger proteins by using on-tissue enzymatic digestions (generally carried out using the enzyme trypsin), effectively cleaving the larger proteins into their constituent peptides. A good review of the relevant techniques has been published by Diehl et al.[79]

1.4.7   On-tissue chemical derivatisation

On-tissue chemical derivatisation has been recognised as a good method for enhancing analyte sensitivity and detection in MSI analysis. Derivatisation reagents are liquids so concerns exist about the impact on MSI images caused by delocalisation of the analytes. Its popularity has however grown over recent years, with methods being largely based on established LC-MS derivatisation procedures. The reaction schemes are usually functional group specific and have been applied to various different chemical classes including peptides[80], N-glycans[81], amino acids[82], steroids[83] and drug molecules[84]. Building on this success, MALDI-MSI researchers have found compounds that can act as both an on-tissue derivatisation reagent and a MALDI matrix[85-87].

1.4.8   MALDI matrix selection

Matrix selection is an essential step in MALDI-MSI sample preparation. Successful detection of analyte molecules is dependent on which matrix is applied to the sample. An ideal matrix should absorb UV light at the appropriate laser wavelength and be able to isolate and extract the analytes under investigation, it should also not sublime under vacuum, it should be a proton acceptor or donator and its solubility should be high in the same solvents as the analytes. Small organic molecules work well, many have been evaluated over the years, a list of commonly used matrices can be found in Table 2, along with typical applications and operating polarity. 2,5-dihydroxybenzoic acid (DHB), α-cyano-4-hydroxycinnamic acid (CHCA), 9-aminoacridine (9AA) and 1,5-diaminonapthalene (DAN) are the most commonly used for pharmaceutical applications because of their ability to extract and ionise small endogenous

metabolites, drugs and lipids. In an industrial R&D environment it is often not possible to screen large numbers of matrices for compatibility with new chemical entities, instead ionisation testing is limited to the four main matrices listed above, if none are found to be effective alternative imaging platforms such as DESI and LESA-MSI are then attempted.

The solvent system used to dissolve a matrix is another parameter that can effect analyte extraction. Typically 50 – 80% *v/v* mixtures of acetonitrile, methanol, ethanol and water are used with a small amount of organic acid such as trifluoroacetic acid[60] (0.1-1% *v/v*) for proton enrichment in positive ion mode. The amount of organic acid used can greatly influence the spectra obtained from direct tissue analysis so careful optimisation is required. Matrix concentration usually ranges between 5-50 mg/mL depending on the matrix being used.

Table 2 List of typical MALDI-MSI matrices for different applications and polarities

Matrix	Molecular Weight (Da)	Ionisation mode	Typical applications	References
2,5-dihydroxybenzoic acid	154.1	Positive	Drugs, lipids, peptides	88-90
α-cyano-4-hydroxycinnamic acid	189.1	Positive	Drugs, peptides, Oligonucleotides	90,91
9-aminoacridine	194.2	Negative	Lipids, drugs	92-94
1,5-diaminonaphthalene	158.2	Negative	Amino acids, lipids	95-97

Sinapinic acid	224.2	Positive	Proteins	90,98
2-mercaptobenzothiazole	158.2	Positive	Lipids	99,100
2,6-dihydroxyacetophenone	152.1	Positive	Lipids	45,101
2,4-dinitrophenylhydrazine	198.1	Positive	peptides	61,102

1.4.9 MALDI matrix application

Matrix deposition for MALDI-MSI analysis should be carefully considered. Any method should ensure a homogeneous coverage of the tissues to be studied to minimise variations in response in different regions of the sample. Crystal size is all important when performing MSI, if the crystals are too large this will affect the spatial resolution that can be achieved with the analysis. Crystal sizes as low as 1 µm have been reported[103] but typical matrix crystal sizes of between 5-150 µm are more usual depending on the deposition method. The deposition method must also be reproducible to ensure high quality images are produced and inter slide comparison in larger studies or across different laboratories can be performed. The main matrix deposition methods available will be discussed below.

Matrix can be deposited in various different ways, with the most commonly reported being administration by pneumatic nebulisation. This can be done manually with the use of a pneumatically assisted thin layer chromatography sprayer or airbrush or matrix deposition can be done robotically with various commercially available systems such as the TMsprayer (HTX Technologies, Chapel Hill, NC, USA) or the SunCollect

sprayer (SunChrom, Friedrichsdorf, Germany). All use the common principle of multiple, differing direction, passes across the slide to deposit the matrix. These systems are rapid and highly reproducible but as always require method optimisation for each matrix being applied, measures must be taken to ensure the application is not too wet as any accumulation of surface solvent could result in delocalisation of the analytes within the tissue. Pneumatically assisted sprayers can also suffer from intermittent blockages, altering the amount of matrix being dispensed, so rigorous instrument hygiene procedures must be adhered to.

Other methods of depositing liquid matrices include piezoelectric[104] and acoustic spotters[105] which can dispense pL volumes of matrix, they typically produce matrix spots in the region of 100-150 µm spot centre to spot centre so limit the spatial resolution of any subsequent analysis. An automated system based on vibrational vaporisation (ImagePrep, Bruker Daltonics, Bremen, Germany) is commercially available offering droplet sizes of ~20 µm, it comes with an optical sensor to control deposition periods and intervals, matrix layer thickness, wetness and drying rate in real time[106].

In addition to these 'wet' application techniques there are also several 'dry' application techniques worthy of note. Matrix sublimation has grown in popularity over recent years, as advances in laser technology lead to reduced laser beam diameter (min. 5 µm) and increased laser repetition rate (max. 10kHz). Higher spatial resolution imaging is becoming a viable and valuable asset to the researcher as biological processes become more focussed on changes at the cellular level[107]. Sublimation offers a rapid, robust and dry way of homogeneously coating slides with matrix, importantly the crystal size achieved can be in the low micron region, making high resolution analysis possible[108] and the solvent free nature of the technique minimises

any potential delocalisation of analytes. The equipment needed to make sublimation apparatus is readily available, with most industrial and academic groups building in-house kits at low cost[109]. Commercially available sublimation instruments have recently been introduced, notably the iMLayer™ (Shimadzu, Cheadle Hulme, UK). Such instruments offer a viable alternative to home-built apparatus but are fairly expensive to acquire and concerns exist over inter matrix contamination. Sublimation protocols need to be strictly controlled in terms of time, vacuum (pressure and duration) and matrix amount and must be developed for each different matrix[95,110].

A further 'dry' matrix deposition method is dry coating. This simple method involves milling the dry matrix crystals using a mortar and pestle and subsequently passing through a fine sieve onto the tissue sections[111]. A drawback of dry matrix application techniques is that the absence of a liquid interface does not allow extraction of analytes into the crystals from the tissue surface, making the techniques unsuitable for some applications. However it has been successfully applied to detection of drugs in tissues that were undetectable by standard matrix application[112]. Ferguson et al. have built upon the dry matrix application method for forensic applications, developing a 'dry-wet' application method when preparing and analysing latent fingermarks my MALDI-MSI[113].

All of the matrix application techniques discussed are usually performed post-sectioning, however, some academic groups have developed processes that use slides pre-coated with sublimated matrix prior to sectioning[114]. Crystal sizes of 1-2 µm are reported. The advantage of this procedure versus post-sectioning sublimation is that the tissue sections become wet on thaw mounting allowing analyte extraction making the process more widely applicable.

Matrix deposition quality control is important and can easily be done simply by weighing the slide before and after coating or by measuring the optical transparency throughout the application process[8], crystal size can be checked using an optical microscope, ensuring reproducibility from slide to slide.

1.5   Quantitative MSI methods

MSI has rapidly developed into a valuable and versatile technique for exploring molecular distributions in animal tissues. This qualitative data gives the researcher valuable insight, especially in pharmaceutical R&D where quick and robust assessments of a drug or metabolite distribution can confirm efficacy in a target tissue at an early stage or accumulation in tissue where toxicity has been encountered. Scientists within industry have become familiar with the kind of qualitative information MSI offers but require quantitative information to calculate parameters like dose to man predictions, pharmacodynamic models of efficacy and the assessment of drug toxicity thresholds. Quantitative MSI (qMSI) is an area of considerable research at the moment, simultaneous extraction of both qualitative spatial distribution information and quantitative exogenous/endogenous compound levels has been shown to be possible but has proven to be difficult in practice, largely because of ion suppression effects caused by the changing molecular environments within complex tissue sections. Numerous methods of qMSI have been reported, most follow a tried and tested formula of spotting a calibration standard[111] or set of calibration standards[112,115] onto control tissue which is then run alongside any unknowns. Further quantitative methods have been reported that utilise tissue mimetics[17,116,117] or surrogates[118], essentially tissue homogenates or an inert media such as gelatin with varying levels

of the analyte spiked into them prior to freezing, sectioning and analysis at the same time as the unknowns. Alone these methods offer relative quantitation but do not contend with the issues of variable MS response caused by ion suppression effects or local variations in analyte extraction. In order to address this complex factor most methods have adopted different normalisation strategies to provide absolute quantitation.

1.5.1   Normalisation

Arguably the most accepted method of qMSI normalisation utilises a stable isotope-labelled version of the analyte or a structurally similar compound to the analyte as an internal standard (IS). The IS is mixed with the matrix solution and homogeneously sprayed over the slide prior to sectioning[119] or over the tissue sections after sectioning and calibration standard addition[15]. The IS can then be used for the pixel to pixel correction of the analyte intensity (calculated as analyte intensity/IS intensity) across the tissue sections. Pirman et al. reported using a deuterated version of acetyl-L-carnitine (AC) applied prior to sectioning when quantifying endogenous levels of AC in piglet brain tissue[120]. The principle was successfully used again for the quantitation of cocaine in human brain tissue sections[121]. Prideaux et al. used Levofloxacin as a structurally similar analogue as an internal standard for the quantitation of moxifloxacin in lung tissue taken from a rabbit tuberculosis model[122]. Addition of IS and calibration standards prior to and after sectioning has recently been explored by Chumbley et al. who explored different matrix and calibration standard addition protocols using an acoustic spotter to *in vitro* dosed rabbit liver tissue sections[119]. Post-sectioning addition of the standards, stable-labelled IS and matrix was found to be the optimum sequence

for ripaficin quantitation, results generated by MSI correlated well with those generated by LC-MS/MS.

Although pixel to pixel normalisation with a stable-labelled version of the analyte is the gold standard of absolute quantitation in qMSI, several groups have used alternative normalisation methods in qMSI analysis. Takai et.al. used a representative DHB matrix peak to normalise the response of octreotide, a therapeutic peptide, when quantifying in mouse liver and kidney[118]. Concentrations calculated using DHB normalisation compared favourably with those determined by LC-MS/MS. Tissue specific endogenous marker compounds have also been used to normalise drug response in qMSI. Wang et al. reported using an endogenous brain tissue peak when analysing the distribution of chlorisondamine in rat brain sections[123], although concerns exist that such endogenous markers are not evenly distributed throughout the tissue biasing any data that is normalised against them.

Hamm et al. reported the novel use of a tissue extinction coefficient (TEC) when quantifying olanzapine and propranolol in rat and mouse whole body sections by MALDI-MSI[124]. This technique involves spraying a homogeneous amount of a compound mixed with the matrix over control whole body tissue sections. Once analysed the TEC can be calculated for different organ regions of the section by dividing the average intensity of the compound on tissue by the average intensity of the compound on the glass slide. The regional TEC values can then be used to scale the intensities obtained in dosed tissue, which in turn can be back calculated against an adjacent, off-tissue, spotted calibration range.

A summary of the different qMSI methods is presented in Table 3.

Table 3 Summary of different qMSI methods used to quantify drugs in tissues

Drug	Normalisation	Calibration Curve	Tissue	MSI Platform	Validated by LC-MS/MS	Ref.
Clozapine	None	Yes, control	Brain (rat)	MALDI	✓	[125]
Cocaine	Stable-label	Yes	Brain (human)	MALDI	✓	[121]
Erlotinib	None	Yes, mimetic	Liver (rat)	LESA/ DESI	✓	[17]
Lapatinib	Stable-label	Yes, mimetic	Liver (dog)	MALDI	✓	[116]
Moxifloxacin	Non	Yes, mimetic	Liver (rat)	LESA/ DESI	✓	[17]
Olanzapine	TEC None	Yes Yes, mimetic	Whole body (rat) Liver (rat)	MALDI LESA/ DESI	✓,✓	[17,124]
Octreotide	Matrix peak	Yes, gelatin	Liver, kidney (mouse)	MALDI	✓	[118]
Paclitaxel	Stable isotope	Yes	Licer, spleen, tumour (mouse)	MALDI	✓	[126]
Propranolol	TEC	Yes	Whole body (mouse)	MALDI	✓	[124]
Raclopride	Compound IS	Yes, mimetic	Liver (mouse)	MALDI	✓	[127]
Rifampicin	Stable-label	Yes	Liver (rabbit)	MALDI	✓	[119]
Terfenadine	None None	Yes Yes, mimetic	Whole body (rat & mouse), Liver (rat)	MALDI LESA/ DESI	✓, x	[17,128]
Tiotropium	TIC	Yes	Lung (rat)	MALDI	✓	[115]

Triamcinolone acetonide	Stable label	Yes	Cartilage	MALDI	✓	[129]

1.6   Data processing

Sample preparation and subsequent acquisition of multiplex mass spectrometry data from MSI experiments is a complex process, however, this is a precursor to data processing and analysis that is needed to generate images and interrogate the data. MSI data files are often tens of gigabytes (GB) in size and can be as large as 100 GB in older instruments, creating data storage problems and making data handling slow and difficult. Instrument vendors have developed platform specific data processing software solutions that allow scientists to create images and perform limited multivariate analysis. Vendor software packages concentrate on bringing together the spatial coordinates with the spectral data acquired in the analysis and generate a colour map image based on the relative abundance of the peak of interest in the mass spectrum. This has several drawbacks, foremost the software is designed to process data from the vendors specific file type, rendering it unsuitable for multimodal imaging workflows that adopt different MS platforms and secondly, the software solutions don't allow any additional data processing options to enable further data mining.

The MSI community have introduced a common data format designed especially for MSI analysis. Imaging mass spectrometry mark-up language[130,131] (imzML) has been embraced by scientists eager to use more sophisticated data processing techniques. Most instrument vendors now provide imzML convertors embedded into their own software and various academically derived convertors are available that can be used to convert older data formats[132]. The advantage of this data conversion is that imzML

files can be read by a multitude of different MSI software packages and furthermore data can be easily shared between collaborating institutions.

Various imzML capable software suites are now available as freeware. Robichaud et al. published a report on an open source interface to visualise MSI data called MSiReader based on Matlab, a popular multi-paradigm numerical computing environment[133]. MSiReader is constantly evolving[134] and has found widespread use with both MALDI and DESI-MSI data. SpectralAnalysis is another visualisation software that operates within a Matlab environment[135]. It is versatile software, offering an entire data processing workflow including data smoothing, baseline correction, normalisation, and image generation to multivariate analysis (eg principal component analysis (PCA), non-negative matrix factorisation (NMF), maximum autocorrelation factor (MAF), and probabilistic latent semantic analysis (PLSA))[136]. The software can be used for single experiment data sets and large multi-instrument, multimodality, and multicenter studies. MSiQuant is a purpose built quantitation software package that is also available as freeware[137]. It allows the user to select regions of interest (ROI) around calibration spots typically used in qMSI workflows. ROI are then used to generate mean relative abundances and calibration curve generation for the back calculation of unknowns. Baseline corrections, subtractions, denoising, smoothing, recalibration and normalisation can all be performed within the software.

In addition to the various types of freeware available to MSI scientists, several companies have developed powerful software for MSI data processing. Notable among these companies are Bruker and ImaBiotech. Bruker market a MSI software solution called SCiLS Lab. This is an extremely powerful software suite originally confined to data generated on Bruker MS platforms but now avaiable as multivendor software based on the imzML format. It enables users to perform regular targeted data

analysis but offers a variety of different options to perform downstream untargeted data processing such as spectral segmentation, discriminative RoC analysis and tissue classification using models based on training data[138].

1.7   Complementary optical techniques

It is often necessary to co-register MSI data with classical histology data in order to differentiate the heterogeneous cell populations in complex tissues. The integration of histology and MSI is well documented[139]. Staining can be performed on tissue sections prior to MSI analysis, however, careful attention must be given to the compatibility of the staining protocols with mass spectrometry techniques. Staining with reagents such as methylene blue or cresyl violet have been applied in this way[139,140]. Typically histological staining is performed post analysis. Non-destructive DESI-MSI analysis lends itself well to this protocol although staining post MALDI-MSI requires pre-staining removal of the MALDI matrix. This can be done by gently washing the slide in a 70% ethanol solution to dissolve the deposited matrix, the sections can then be dehydrated by submerging the slide in a sequence of increasing ethanolic solutions[72]. Staining the slide that has been analysed by MSI represents the best way to ensure accurate co-registration, although, some damage can occur to the tissue during analysis. It is therefore regular practice to take adjacent sections for staining either before and/or after the one being analysed[141], although accurate co-registration may be difficult post analysis due to the differences in the structure and cellular morphology of the adjacent sections, especially when performing high resolution MSI.

1.7.1 Haematoxylin and eosin staining

Haematoxylin and eosin (H&E) staining is the most common staining procedure used in pathological examination. Haematoxylin is a violet coloured stain that is used to stain basophilic substances that carry a negative charge such as DNA/RNA in the nuclei of cells. Eosin, in contrast is a pink stain that is used to stain acidophilic substances with a positive charge such as amino acids, it thus highlights intracellular membranes and cytoplasmic filaments that often contain amino acid residues.

H&E staining in MSI experiments is generally carried out post analysis or on adjacent sections as it interferes with the MS response and the subsequent observed mass spectra[140]. H&E staining has been employed extensively alongside MSI data in the classification of different tumour species at the molecular level by MALDI-MSI[142-144] and DESI-MSI[145,146].

1.7.2 Immunohistochemical staining

Immunohistochemistry (IHC) is the selective staining of antigens within the cells of tissues using antibodies[147] that are specific for a particular cellular marker. It is used in pathology to understand and highlight the distribution and location of biomarkers in different regions of tissue. The antibodies are usually labelled with a reporter molecule that can change colour or has the ability to fluoresce for selection. The technique has been widely used to complement MSI analysis in the areas of oncology[148] and nephrotoxicity[149].

Imaging mass cytometry is an emerging technique based on laser ablation inductively coupled plasma mass spectrometry (LA-ICP-MS)[150]. Antibodies are raised to target specific molecular species within tissues (based on the same principles as IHC), the

antibodies can be labelled with metal isotopes such as gold which in turn can be used as reporters for detection by LA-ICP-MS (often referred to as cytometry by time of flight or CyToF). Cocktails of antibodies labelled with different metals can be used to 'stain' a tissue section making the technique both specific and multiplex[151]. The technique has already been used to map the distribution of cisplatin in various tissues including tumour[152]. Imaging mass cytometry offers much promise for the future in pharmaceutical R&D where the trend is towards development of large molecule drugs and drugs based on new modalities such as micro-RNA.

1.8   Validation of MSI against other techniques

When a new analytical technique begins to make progress from an interesting idea to use in academia and subsequent commercialisation it must be compared and validated against a technique that performs a similar role. MSI is no exception and has been extensively validated against alternative imaging technologies such as qWBA and quantitatively against LC-MS/MS based homogenate analysis. These are considered the 'gold standard' techniques over which MSI should offer enhanced or superior analytical properties. qWBA is a radio-labelled based analytical technique that is used to spatially map the distribution of drugs in tissues. The main drawback of the technique is that the radio-labelled version of the drug can undergo metabolism *in vivo* and subsequently form a labelled metabolite that confuses the distribution profile of the parent drug making the data ambiguous. Homogenisation analysis by LC-MS/MS is extensively used to provide researchers with tissue concentrations but the technique results in the loss of all spatial information within the tissue. MSI has the potential to

complement these two techniques offering quantitative, label free distribution data. Validation of MSI against the different techniques will be discussed further below.

1.8.1   Validation vs. Quantitative whole body autoradiography

Comparison of MSI data with traditional qWBA data has been extensive. Hsieh et al. first reported a good correlation between MSI data generated by MALDI-ToF and qWBA in the analysis of clozapine in rat brain tissue, even going a step further and comparing the intensity difference in different areas of the brain to the concentration differences observed by HPLC-MS/MS[125]. Kertesz et al. similarly compared the distribution of propranolol in rat whole bodies sections by DESI-MSI and qWBA. This showed nominal agreement between the relative abundance of the drug by DESI and the amount of radioactivity detected by qWBA in brain, lung and liver tissue. Kidney tissue however showed a disparity between the two techniques that could possibly be attributed to accumulation of a metabolite and subsequent detection of the radiolabel by qWBA, DESI-MSI however failed to detect the metabolite[153]. Drexler et al. compared the two techniques when analysing a proprietary drug in rat eye observing a good correlation between the generated images with the drug largely localised in the retina and uveal tract. MSI was used to confirm the absence of major metabolites contributing to the radiographic image[154]. More recently Goodwin et al. reported the comparison of a therapeutic cyclic peptide distribution in mouse kidney by MSI and qWBA, showing that the qWBA results were subject to a contribution from two labelled metabolites of the drug. Results were further complicated by isotopic overlay of one of the metabolites with the parent drug on a MALDI-ToF instrument. The MSI analysis was repeated using a high spectral resolution MALDI FT-ICR instrument which resolved the isotopic peaks by accurate mass[155].

1.8.2   Validation vs. LC-MS/MS

As highlighted in section 1.4 quantitative MSI methodology is an area of focus for the scientific community and as such extensive comparisons have been reported between qMSI and LC-MS/MS homogenisation methods. Table 3 in section 1.4.1 lists the various methods and drug compounds that have been validated by subsequent LC-MS/MS homogenate analysis. It should be highlighted that most of these methods have used tissue that is fairly homogeneous in nature such as liver as a direct comparison due to the loss of spatial information in the homogenate analysis. Comparison of MSI data in more complex tissue types with LC-MS/MS is much harder due to the potential localisation of drugs into different regions of the tissue. Validation in these complex tissues has been reported, Frank et al. used tissue microdissection to validate MALDI-MSI data mapping the protein expression difference in different regions of the rat brain[156]. Goodwin et al. also used tissue laser microdissection followed by LC-MS/MS to validate the distribution data for a compound generated by MSI in rat brain sections[111].

1.9   Application of MSI in Pharmaceutical Research and Development

Pharmaceutical Research and Development (R&D) is a lengthy, costly and competitive business. Potential new drugs can take as long as ten years to reach commercialisation, at a cost of billions of dollars, furthermore, attrition rates during the later stages of development increase the already high risk factors involved with taking a new compound into the clinic. Pharmaceutical companies have gone to great lengths to decrease these high failure rates, minimising risk in an effort to maximise reward

and bring life enhancing medicines to patients. Poor efficacy and toxicity are the main reasons for high attrition rates within R&D[157,158]. The industry has addressed this problem by adopting a strategy of early, accelerated compound optimisation with parallel generation of physicochemical and pharmacokinetic properties to design safer and more efficacious drug candidates that maximise therapeutic index whilst minimising any risk of toxicity.

Bioanalytical techniques such as LC-MS have kept pace with the need for higher throughput but are limited in value when trying to assess a drugs distribution *in vivo*. Traditionally drug distribution studies were performed during the later stages of development using radiolabelled compounds in low throughput techniques such as qWBA or homogenisation studies using long liquid chromatography gradients. MSI, whilst not replacing any of these established methods is increasingly being used to complement these approaches and provide timely and cost effective insights into the deposition and fate of new chemical entities. The application of the technique has been expanded further to encompass endogenous compound changes as markers for drug induced efficacy or toxicity and to bring insight into novel drug delivery technologies.

1.9.1   Drug distribution and efficacy

In order for a drug to exert a pharmacological response it needs to be present at the site of action in sufficient quantities and for the necessary time to elicit efficacy. If the drug concentrations are too high this can induce toxicity. Drug distribution studies are therefore integral to the pharmaceutical R&D pipeline. Troendle *et al.* were the first to demonstrate the applicability of MALDI-MS to drug compounds directly from tissue sections[159], successfully detecting the anti-tumour drug paclitaxel in ovarian cancer biopsies and the antipsychotic drug spiperone in incubated rat liver. Reyzer et al.

followed several years later with the first example of MALDI-MSI, reporting the distribution of 2 orally dosed anti-tumour drugs in rat brain sections[160] using targeted MS/MS on a triple quadrupole mass spectrometer. Early work in industry centered upon validation of the MALDI-MSI technique against labelled whole body analysis to establish the method as a viable unlabelled alternative or to complement qWBA data[125,161]. Khatib-Shahidi et al. successfully analysed olanzapine from rat whole body tissue sections[162], including the simultaneous elucidation of the distribution of several olanzapine metabolites. Tissue specific protein markers (*m/z* values) were used to highlight different histological features within both mouse and rat whole body sections and rat brain. A similar approach was used to highlight glioma tumour baring tissue in mouse brain, highlighting the potential MSI has within the field of pathology. Drug distribution from whole body tissue sections has subsequently been extensively reported for other medicines including β-peptide[163], vinblastine[164], terfenadine[128], raclopride[112,127] and reserpine[165].

MSI analysis of tissues (organs) dissected from animals post mortem has become much more popular than whole body tissue section analysis in the R&D industry, largely because of the costs related to sectioning whole animals and the logistical considerations involved in handling and analysing such large samples. The list of drug compounds studied and the diverse range of tissues that have been analysed using MSI is now extensive, a concise summary is shown in table 4.

Table 4: Summary of drugs studied using MSI (Updated and adapted from[165,166])

Drug	Met.	Tissue	Ionisation Method	Detection Mode	Mass Analyser	Ref.
3-Methoxysalicylamine	N	Kidney, liver (mouse)	MALDI	MS/MS	LTQ	[166]

Amphetamine, sibutramine & fluvoxamine	Y	Brain (rat)	DESI	MS, MS/MS	Orbitrap	[15]
Astemizole	N	Brain (rat)	MALDI	MS, MS/MS	QqToF	[167]
AQ4N	Y	Tumour (mouse)	MALDI	MS	QqToF	[168]
AZD2811	Y	Tumour (mouse)	DESI	MS	LTQ Orbitrap	[169]
AZD2820	Y	Kidney (mouse)	MALDI	MS	ToF/ToF, FTICR	[155]
AZD4017	N	Brain (rat)	LESA	SRM	QqQ	[170]
AZD8329	N	Brain (rat)	LESA	SRM	QqQ	[170]
AZx	N	Brain (rat)	MALDI, LESA	MS, SRM	QqToF, SRM	[170]
BMS-X-P	Y	Liver, heart, lung, spleen (rat)	MALDI	MS/MS	LTQ	[171]
Brimonidine	N	Eye (rabbit)	MALDI	MS	ToF/ToF	[172]
Chlorisondamine	N	Brain (rat)	MALDI	MS, MS/MS	ToF/ToF	[123]
Chloroquine	N	Eye (Rat), whole body (rat)	MALDI, LESA	MS/MS, SRM	QqToF, QqQ	[173,174]
Cimetidine	N	Lung (rat)	MALDI	MS	ToF/ToF	[77]
Clozapine	Y	Brain (rat), Lung, kidney, testis (rat)	MALDI, DESI, LESA	MS, MS/MS, SRM	ToF/ToF, QqToF, LTQ	[6,111,125,175]
Cobimetinib	N	Brain (mouse)	MALDI	MS	FTICR	[176]
Cocaine	N	Brain (rat), Hair (human)	MALDI	MS, MS/MS, SRM	ToF/ToF, QqQ	[123,177]
Dexamethazone	N	Eye (ovine)		MS	ToF	[178]
Ephedrine	N	Lung (rat)	MALDI	MS	ToF	[179]

Erlotinib	Y	Liver, spleen, muscle (rat), tumour (human)	MALDI, DESI, LESA	MS, MS/MS, SRM	QqToF, LTQ Orbitrap	[180,181]
Fosdevirine	Y	Brain (rabbit, guinea pig, monkey)	MALDI	MS	FTICR	[182]
Gefitinib	N	Tumour (human)	MALDI	MS, MS/MS	LTQ Orbitrap	[181]
Gentamycin	N	Kidney (mouse)	MALDI	MS	ToF/ToF	[149]
Glucocorticoid receptor agonists	N	Skin (porcine)	MALDI	MS/MS	ToF/ToF	[183]
Haloperidol	N	Brain (rat)	DESI, LESA	MS, SRM	LTQ Orbitrap	[6]
Ifosfamide & imatinib	N	Kidney (mouse)	MALDI	MS	LTQ Orbitrap	[184]
Imipramine	N	Lung (rat)	MALDI	MS	ToF/ToF	[77]
Ipratropium	N	Lung (human)	MALDI	MS, MS/MS	LTQ Orbitrap	[185]
Isoniazid	N	Lung (rabbit)	MALDI	MS/MS	LTQ	[84]
Ketoconazole	N	Skin (porcine)	MALDI	MS	QqToF	[186]
lapatinib	Y	Liver (dog)	MALDI	MS	FTICR	[187]
Lidocaine	Y	Skin (pig)	DESI	MS, MS/MS	LTQ Orbitrap	[188]
Loperamide	N	Brain (mouse)	MALDI	MS/MS	QqToF	[189]
Midazolam	N	Brain (rat)	LESA	SRM	QqQ	[6]
MK-0916	N	Brain (rat)	MALDI, LESA	MS, SRM	QqToF	[170]
Moxifloxacin	N	Lung (rabbit), liver, brain (rat)	MALDI, DESI, LESA	MS, SRM	QqQ	[6,32]
Nelfinavir	N	Cells	MALDI	MS	ToF/ToF	[190]

Octreotide	N	Liver, kidney	MALDI	MS	LTQ Orbitrap	[118]
Olanzapine	Y	Whole body, liver (rat)	MALDI, DESI, LESA	MS, SRM	QqToF	[17,162,191]
Oxaliplatin	Y	Kidney (rat)	MALDI	MS	ToF/ToF	[192]
Paclitaxel	N	Liver, tumour (rat)	MALDI	MS/MS	Ion Trap	[126,159]
Pictilisib & GNE-317	N	Brain (mouse)	MALDI	MS	FTICR	[193]
Pirfenidone	Y	Lung, kidney, liver (mouse)	MALDI	MS	FTICR	[194]
Polymyxin antibiotics	Y	Kidney (rat)	MALDI	MS, MS/MS	ToF/ToF	[195]
Promethazine	N	Brain (mouse)	MALDI	MS/MS	LTQ Orbitrap	[196]
Propranolol	N	Whole body (mouse)	MALDI, DESI	MS, SRM	QqQ	[153]
Raclopride	N	Whole body (mouse), brain, kidney (rat)	MALDI	MS/MS	LTQ, ToF/ToF	[112,197]
Reserpine	N	Whole body (rat)	MALDI	MS	LTQ Orbitrap	[165]
Rifampicin	N	Liver (rabbit)	MALDI	MS/MS	LTQ Orbitrap	[119]
S-777469	N	Whole body (mouse)	MALDI	MS	LTQ Orbitrap	[127]
Saquinavir	N	Cells	MALDI	MS	ToF, FTICR	[190]
SCH226374	N	Brain (mouse)	MALDI	SRM	QqToF	[160]
SCH23390	N	Brain (mouse, rat)	MALDI, LESA	SRM	ToF/ToF, QqToF FTICR	[112,170]
Sparfloxacin	N	Skin (mouse)	MALDI	MRM	QqQ	[198]

SR180711	N	Kidney (rat)	MALDI	MS, MS/MS	ToF/ToF	160
Terfenadine	Y	Whole body (rat, mouse), liver (rat)	MALDI, DESI, LESA	MS, SRM	QqToF	6,128
Tiotropium	N	Lung (rat, guinea pig)	MALDI	MS, MS/MS	ToF/ToF, LTQ Orbitrap	115,199, 200
Valiparib	N	Tumour (mouse)	MALDI	MS	LTQ Orbitrap	201
Vinblastine	N	Whole body (rat)	MALDI	IM-MS/MS	QqToF	164
β-peptide	N	Whole body (mouse), tumour (human)	MALDI	MS	ToF/ToF	163

Drug distribution elucidated by MALDI-MSI has been the most heavily reported MSI technique over the past decade with recent publications in various research areas. Bartelink et al. reported the analysis of the oncology drugs valiparib and carboplatin within tumours by MALDI-MSI and ICP-MS (non-imaging). Concluding that the heterogeneous distribution observed could lead to insufficient drug exposure to ensure efficacy in select cell populations[201]. Complementary techniques such as DESI and LESA-MSI are beginning to become more highly reported, notably Shariatgorji et al. recently reported some interesting results using DESI-MSI to image several different neurotransmitters and neuroactive drugs using chemical derivatisation to charge tag amine groups within the molecules to increase sensitivity and detection[15].

MSI is increasingly being used to assess efficacy biomarkers after treatment with novel pharmaceuticals. Atkinson et al. described the distribution of the oncology drug AQ4N with its active metabolite in solid tumour[168]. Drug and metabolite distribution were simultaneously related to the intratumoral distribution of ATP indicating that the

cytotoxic metabolite was not confined to the hypoxic tumour regions. More recently, Ait-Belkacem et al. have characterised endogenous metabolism of transfected murine tumour models expressing various levels of indoleamine-2,3-dioxygenase1 (IDO1)[202]. ID01 is a potential therapeutic target for cancer treatment, IDO1 inhibitors are being developed to stimulate antitumour immuno-oncology responses. MSI is used here, to evaluate the conversion rate of IDO1, a tryptophan-degrading enzyme, by following both tryptophan and kynurenine relative abundances within two tumour models (high and low expression). The over-expression of IDO1 in tumour induces tryptophan depletion and increased levels of kynurenine, the opposite was observed in the IDO1 low-expression model. These changes in the metabolites can affect the tissue at the cellular level by inhibiting NK and effector T-cell functions, activating regulatory T-cell phenotypes and M2-macrophages, generating tolerogenic dendritic cells. Thus, the kynurenine to tryptophan ratio was used as an indicator of IDO1 modulation and was linked to drug efficacy. Furthermore, a regional distribution of these metabolites throughout the tumour was used to describe different histological tissue (necrotic core, stroma or hypoxic tissues) by MSI. Finally, strong kynurenine accumulation and lower tryptophan levels were found to co-localise with IDO1 over-expression based on immunostaining showing a strong conversion rate of tryptophan. These local metabolite modulations were spatially correlated with drug distribution to explain mechanism of action and provide target engagement information.

1.9.2   Drug metabolism

The multiplex nature of MSI lends itself well to the analysis of both drug and metabolite distribution directly from the surface of tissue sections. Chen et al. reported the

analysis of terfenadine and its primary metabolite fexofenadine from mouse and rat whole body sections using MALDI-MSI[128]. This data was used to attribute the poor oral bioavailability of terfenadine to high first pass metabolism in the intestines and the liver prior to the drug reaching the systemic circulation. Similarly Goodwin et al. reported distribution data for drug candidate AZD2820 in mouse kidney using the multiplex nature of MALDI-MSI to show the distribution of a primary metabolite and highlight the screening power of MSI over conventional drug distribution techniques, in this case qWBA where the labelled nature of the analysis gave misleading representation of the AZD2820 distribution due to the presence of the radiolabel in the metabolite[155].

1.9.3   Toxicity studies

To date most MSI studies within the pharmaceutical industry have revolved around questions of efficacy, largely through drug and metabolite distribution data. The technique is however being increasingly used in toxicology studies where it is regularly included into study plans to assess things like blood brain barrier penetration, where brain exposure may be suspected to yield a toxic response. It is also being used in post study assessment to answer pathology driven hypotheses, for example, when pathological findings have suggested a toxicological response in tissue MSI can be used to highlight a co-localisation of drug or metabolite in the affected area.

Meistermann et al. used MALDI-MSI to investigate potential biomarkers of nephrotoxicity after administration of gemcitabine, a known nephrotoxicant to rats[149]. A spectral feature at 12,959 Da that strongly correlated with histopathology deduced alterations of the rat kidneys. The researchers were able to identify this spectral

feature as transthyretin (Ser(28)-Gln(146)) using other methods, demonstrating the emerging role of MSI in the discovery of toxicity biomarkers and in obtaining mechanistic insights concerning toxicity mechanisms.

Nilsson et al. published a paper assessing the nephrotoxicity of polymyxin antibiotics, highlighting the correlation between the toxicity of different polymyxin analogues and the degree of accumulation of such drugs in the renal cortex of rats compared to the medulla[195]. This gave valuable insight into the potential ways new, less toxic analogues could be designed to combat the growing need for new antibiotics caused by increasing antibiotic resistance.

Castellino et al. reported a study on fosdeverin, a HIV reverse transcriptase inhibitor that had shown adverse events in the clinic with 4 patients experiencing seizures after four weeks of treatment[182]. MSI was used to look into drug and metabolite distribution in rabbit, minipig and monkey brains highlighting inter-species variations in drug and metabolite distribution between humans, rabbit and minipig (which had high levels of a cysteine conjugate metabolite associated with the white matter of the brain) and in monkeys where the principle compound in brain was fosdeverin and this was associated mainly with grey brain matter. The authors were able to suggest several hypotheses for these different and novel distribution differences.

Drexler et al. published details of a pathology driven toxicity study looking at the appearance of a birefringent microcrystalline material that had been observed in formalin fixed rat tissue sections[171]. MSI was used to show that the composition of the crystals was made up of the active drug substance (after the administration of a pro-drug), MSI results were cross validated using several complementary techniques.

1.9.4 Drug delivery studies

Drug delivery is becoming an important consideration in the hunt for new medicines. Elegant drug delivery methods can be used to prolong exposure and smooth out so called C_{max} effects that can raise compound levels to potentially toxic levels, thus mitigating potential toxicity. Kreye et al. published a study using MSI to assess the release of theophylline and propranolol from slow release depot implants. MSI was used to show the temporal change in the structure of the implants and the release of the drugs into the external medium[203].

Zecchi et al. reported on the use of MALDI-MSI for the characterisation of two different routes of pulmonary drug administration of the anticholinergic drug tiotropium bromide[200]. The study found that the distribution of the drug in the lungs of guinea pigs varied considerably when administered by nebulised inhalation compared to intratracheal instillation at doses that induced significant anti-bronchoconstrictive activity.

The use of nanoparticles is becoming increasingly popular, particularly within the area of oncology. The nanoparticles usually consist of larger molecules, delivery vesicles or particles that surround or incorporate drug molecules and capitalise on the hypothesis that the larger particles can access 'leaky' tumour vasculature and subsequently tumour tissue but are restricted from entering normally vascularised tissue. Once inside the tumour the larger particles find it difficult to get out and be cleared due to compromised lymphatic drainage, a phenomenon known as the enhanced permeability and retention effect (EPR). Ashton et al. reported use of a 'accurin' based nanoparticle for the administration of AZD2811[169]. The accurin is made up of a polylactic acid/polyethylene glycol polymer which physically encapsulates the

drug molecules and a inert counter ion. Controlled release of the drug from the nanoparticle can be made faster or slower by using different counter ions. MALDI and DESI-MSI was used to map the distribution of the drug, a primary metabolite and a marker for the nanoparticle (L-poly lysine) in mouse tumour sections. Prolonged intra-tumoural exposure was shown with the drug being largely undetectable in the tissue at 24 hrs after a single IV administration, compared to high exposure at 6 days post accurin administration at the same dose level. Clinical translation of the EPR effect is the subject of on-going research but it is an area where MSI could have some significant impact due to its ability to acquire multiple molecular species in each mass spectrum and monitor drug abundance, released drug and any possible nanoparticle accumulation within the tumours.

1.9.5 Target engagement

Drug target engagement in cells or tissues is a key indicator of efficacy during drug development. Established techniques rely heavily on complex processing steps requiring many different reagents. MSI offers a label and reagent free method of monitoring target engagement *in situ.* Munteanu et al. reported a direct, quantitative approach using MALDI-MSI for measuring posttranslational modifications in cancer cells caused by histone deacetylase inhibitors in solid tumours[204]. The research showed a time-dependant decrease of nonacetylated histone H4 and a concomitant increase in acetylated H4 after administration of LBH-589 effectively monitoring drug induced mass shifts in protein ion intensities to quantify target engagement.

1.9.6 Clinical translation and emerging applications

To date most MSI analysis has been performed on tissues from preclinical models. However, for a compound to effectively transition to humans and become a new medicine requires clinical research. Late stage failures are what can make or break a company so as much translational data as possible can be of significant benefit. MS based tools are being developed for surgery, providing molecular information directly from the cut tissue (REIMS and iKnife)[205]. To perform MSI analysis from clinical trials will need analysis needle or punch biopsies, such small samples can now be analysed by high resolution imaging platforms.

The pharmaceutical industry is under increasing pressure to reduce the amount of animal experiments it performs during R&D and to have preclinical models that are more patient relevant. Advances in sample preparation techniques, instrument sensitivity and spatial resolution have enabled MSI to be applied to the analysis of 3D

and microphysiological systems (MPS). They are increasingly being employed within early drug discovery for efficacy and toxicity screening. Liu et al. reported on the application of MSI to a time dependant study of irinotecan in spheroids, showing for every treatment duration, an MSI image of the drug distribution several serial sections 120 µm apart[206]. Harvey et al. reported on the use of MALDI-MSI for the analysis of a 3D tissue engineered psoriatic skin model. MSI was used to to observe the spatial location of acetretin in 'Labskin™' living tissue equivalents, with the result that after 24 hours, the drug was located in the epidermis of psoriatic and nonpsoriatic skin models, but after 48 hours of treatment, it was detectable in the dermis[207].

1.10   Future perspectives

MSI has gained acceptance as an established tool within pharmaceutical R&D for the analysis of complex biological tissue samples. The multiplex nature of the technique makes it ideal for the simultaneous analysis of drug and metabolites *in situ* without the need for radio-labelled compounds that are needed in other, more traditional distribution studies. The combination of drug distribution images with endogenous lipid, peptide and protein detection makes the technique ideal for monitoring dose related changes in efficacy at the site of action or toxicity and can elucidate disease state progression. Advances in sample pre-treatment protocols, quantitative methodology and instrument hardware have created a suite of complementary, robust imaging techniques that can be used to explore various concepts within the drug discovery pipeline from early discovery through to the clinic.

There is however still progress to be made, in the areas of spatial resolution, where, as drug development targets and new modalities become more complex, the need to

move to nano-scale imaging in single cells will become an increasing requirement. Instrument sensitivity and speed also need to be developed to accommodate this new spatial paradigm and achieve real high throughput analysis.

Sample preparation techniques require further development to keep pace with the increased need for high throughput and address concerns over molecular post-mortem tissue degradation and its subsequent effect on the ionisation profile of analytes. For MALDI the identification of new matrices that cover a wider chemical scope and the development of on-tissue derivatisation techniques is another area of future expansion that should ease the burden away from instrument developers and improve the sensitivity of existing platforms and increase the application of MSI to ever wider areas of pharmaceutical research. Robust sample preparation protocols that can be applied in multiple R&D laboratories are needed to achieve the metrology and standards that will allow MSI data to be accepted in regulatory submissions. This work is being undertaken at various national measurement institutions across the world and progress in this area is essential as MSI moves to the clinic, where large multisite studies are performed as a matter of routine.

Higher throughput, higher spatial resolution and a subtle move towards increased use of 3D imaging bring problems of data storage. File sizes of 100GB+ are not uncommon, presenting researchers with data handling and backup issues that will need to be addressed by data reduction algorithms. Integration of MSI with multi modal high content imaging is an area that whilst being of benefit to the R&D business, could compound these data storage problems. Developments in artificial intelligence and machine learning will help to decrease this 'big' data burden, but these approaches are just beginning to emerge and are not yet widely adopted.

It is clear that MSI is a useful and important tissue imaging tool within pharmaceutical R&D. The technique has already made some impact in bringing new medicines to patients and looks set to build on this success and encompass even more areas of drug discovery for years to come.

2.0 AIMS AND OBJECTIVES OF THIS PROJECT

The aim of this project was to explore the use of mass spectrometry techniques to assess the biodistribution of drugs in tissues. To achieve this aim it was necessary to use and develop existing and emerging mass spectrometry imaging techniques and apply this state of the art technology to pharmaceutical R&D applications. The following objectives were investigated:

- Evaluate different surface sampling MS ionisation interfaces and assess advantages and disadvantages when applied to the analysis of drugs in pharmaceutical R&D.

- Apply MSI techniques to drug discovery projects to provide spatially resolved distribution information in early pharmacokinetic studies.

- Assess the advantages of spatially resolved analytical methodology against traditional 'gold standard' bioanalytical methods used to determine drug blood brain barrier penetration.

- Explore and develop the use of quantitative LESA-MSI, compare and contrast with other imaging platforms and traditional bioanalytical tissue analysis methodology.

- Apply quantitative MSI methods to drug discovery studies and aide development of robust pharmacokinetic/pharmacodynamic relationships based on target tissue concentration data.

3.0 MASS SPECTROMETRY IMAGING OF CASSETTE-DOSED DRUGS FOR HIGHER THROUGHPUT PHARMACOKINETIC AND BIODISTRIBUTION ANALYSIS

Swales, J. G.; Tucker, J. W.; Strittmatter, N.; Nilsson, A.; Cobice, D.; Clench, M. R.; Mackay, C. L.; Andren, P. E.; Takats, Z.; Webborn, P. J.; Goodwin, R. J., Mass spectrometry imaging of cassette-dosed drugs for higher throughput pharmacokinetic and biodistribution analysis. *Analytical Chemistry* 2014, *86* (16), 8473-80.

Author Contribution

JGS designed the cassette dosed studies, aided necropsy, performed all sample preparation and LESA and MALDI imaging experiments (with the exception of high spectral and spatial resolution imaging), interpreted results and prepared the manuscript for publication.

Mass Spectrometry Imaging of Cassette-Dosed Drugs for Higher Throughput Pharmacokinetic and Biodistribution Analysis

John G. Swales,*,[†,⊥] James W. Tucker,[†] Nicole Strittmatter,[‖] Anna Nilsson,[§] Diego Cobice,[‖] Malcolm R. Clench,[⊥] C. Logan Mackay,[‖] Per E. Andren,[§] Zoltán Takáts,[‖] Peter J. H. Webborn,[†] and Richard J. A. Goodwin[†]

[†]Drug Safety and Metabolism, Innovative Medicines, AstraZeneca R&D, Alderley Park, Macclesfield, Cheshire SK10 4TG, U.K.

[‡]SIRCAMS, School of Chemistry, University of Edinburgh, Edinburgh EH8 9YL, U.K.

[§]Biomolecular Imaging and Proteomics, National Center for Mass Spectrometry Imaging, Department of Pharmaceutical Biosciences, Uppsala University, Uppsala 751 05, Sweden

[‖]Department of Surgery and Cancer, Sir Alexander Fleming Building, Imperial College, London SW7 2AZ, U.K.

[⊥]Biomedical Research Centre, Sheffield Hallam University, Howard Street, Sheffield S1 1WB, U.K.

Ⓢ *Supporting Information*
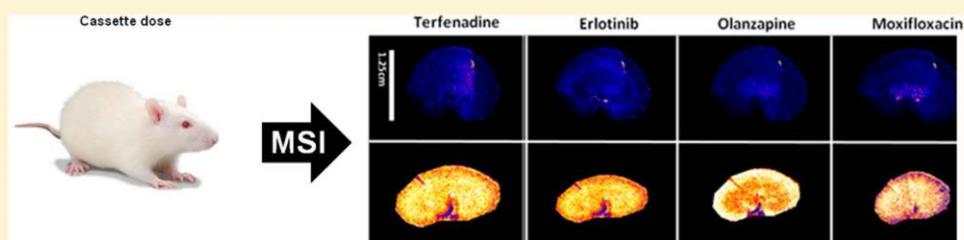
ABSTRACT: Cassette dosing of compounds for preclinical drug plasma pharmacokinetic analysis has been shown to be a powerful strategy within the pharmaceutical industry for increasing throughput while decreasing the number of animals used. Presented here for the first time is data on the application of a cassette dosing strategy for label-free tissue distribution studies. The aim of the study was to image the spatial distribution of eight nonproprietary drugs (haloperidol, bufuralol, midazolam, clozapine, terfenadine, erlotinib, olanzapine, and moxifloxacin) in multiple tissues after oral and intravenous cassette dosing (four compounds per dose route). An array of mass spectrometry imaging technologies, including matrix-assisted laser desorption ionization mass spectrometry imaging (MALDI MSI), liquid extraction surface analysis tandem mass spectrometry (LESA-MS/MS), and desorption electrospray ionization mass spectrometry (DESI-MS) was used. Tissue analysis following intravenous and oral administration of discretely and cassette-dosed compounds demonstrated similar relative abundances across a range of tissues indicating that a cassette dosing approach was applicable. MALDI MSI was unsuccessful in detecting all of the target compounds; therefore, DESI MSI, a complementary mass spectrometry imaging technique, was used to detect additional target compounds. In addition, by adapting technology used for tissue profiling (LESA-MS/MS) low spatial resolution mass spectrometry imaging (∼1 mm) was possible for all targets across all tissues. This study exemplifies the power of multiplatform MSI analysis within a pharmaceutical research and development (R&D) environment. Furthermore, we have illustrated that the cassette dosing approach can be readily applied to provide combined, label-free pharmacokinetic and drug distribution data at an early stage of the drug discovery/development process while minimizing animal usage.

The development of mass spectrometric analytical technologies has enabled pharmaceutical research and development to employ an increasingly wide array of high-throughput screening modalities. Compound optimization with early, parallel elucidation of the physiochemical and pharmacokinetic properties enables a broader choice of compound leads from which candidate drugs can be selected and has also been shown to reduce compound attrition in development.[1] The simultaneous dosing of drugs during in vivo research is typically termed cassette dosing (though also referred to as *N*-in-one dosing). Cassette dosing was first employed by pharmaceutical companies toward the end of the 1990s, when

simultaneous measurements of five compounds were made during the development of potential therapeutics for the treatment of benign prostatic hyperplasia.[2] Cassette dosing and analysis has been shown to be applicable for both orally[3] and intravenously[4] administered drugs. Factors that need to be considered when devising a cassette dosing experiment include mass spectrometry instrumentation and liquid chromatography (LC) requirements (positive or negative mode ionization),

8473

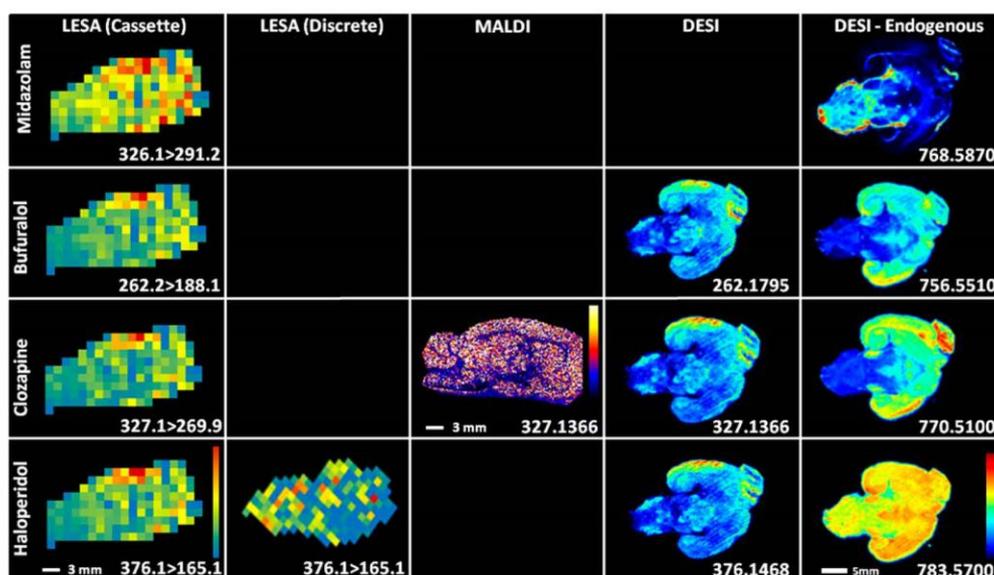dx.doi.org/10.1021/ac502217r | *Anal. Chem.* 2014, 86, 8473−8480

Figure 1. Images of intravenously dosed compounds detected using LESA-MS/MS, MALDI-MS, and DESI-MS after cassette dosing or discrete dosing (haloperidol), highlighting the value of using orthogonal analytical techniques to cover a wider chemical space than that covered by MALDI-MS alone.

whether drugs or their metabolites are likely to have common structures or fragmentation patterns, whether compounds require specific formulation (solubility at specific pH), and careful attention should be given to the dose levels selected. While such factors can be mitigated for by the selection of appropriate combinations of compounds to be analyzed, there remains a risk of drug–drug interactions during in vivo administration. This topic is extensively discussed in several reviews on cassette dosing.[5−7] Interactions mainly arise around competition at clearance pathways. Other reported interactions including heteroactivation of clearance pathways, which is the activation of a metabolic enzyme by a second drug acting through an allosteric mechanism (acting on a site other than the active site). There is also the chance of pharmacological and toxicological effects on organ blood flows and clearances.[7] However, during early drug discovery, the advantage of parallel preliminary experiments means that the risk of erroneous results from drug–drug interactions is outweighed by the saving in reduced time and cost, as noncassette experiments will always be performed on compounds that are to be progressed later in the discovery pipeline.

Traditionally discovery phase pharmacokinetic analysis has been performed using sensitive triple quadrupole mass spectrometers, usually in combination with rapid chromatography systems and operated with automated or semiautomated optimization software.[8] This generic approach enables rapid quantification of chemically diverse compounds from biofluids or tissue homogenates. While these methods are ideally suited for deriving pharmacokinetic parameters from homogeneous biofluids, they are less suitable to analysis of heterogeneous tissue samples. Furthermore, any tissue information from homogenates can be misleading due to factors such as residual blood concentration or dilution. Compound biodistribution information is usually collected at a later stage in a compound's life cycle using techniques like quantitative whole body autoradiography (qWBA).[9] Such analysis retains distribution information lost during homogenization but has major limitations such as the need for a radiolabeled compound,

rendering the technique impractical for discovery use. Label-based techniques are also limited in their inability to distinguish a parent compound from any metabolites that still contain the label, hence producing an ambiguous representation of a compound's distribution.

Mass spectrometry imaging (MSI),[10,11] regarded as collection of multiple mass spectra by rastering across a tissue section in two dimensions, and mass spectrometry profiling (MSP),[12−15] generally regarded as collection of mass spectra at discrete points on a tissue section, have recently emerged as technologies that have the capability to obtain label-free compound biodistribution, relative abundance, and quantitation data by analyzing tissue sections directly.

Such methods enable the simultaneous analysis of drugs, metabolites, endogenous small molecules, lipids, and peptides directly from tissue sections. Several comprehensive reviews describe methodologies[16−18] utilizing a range of sample ionization methods. Matrix-assisted laser desorption ionization (MALDI) is arguably the most effective for pharmaceutical research and is most commonly employed for MSI. However, alternative ionization methods such as desorption electrospray ionization (DESI) are amenable for use in MSI.[25] Techniques like liquid extraction surface analysis (LESA) can be used to increase the sensitivity of tissue analysis when target compounds cannot be detected by other MSI ionization methods, but their use to date has been restricted to low spatial tissue profiling at only a few sampling positions across a tissue section.[13] While the origins of LESA and DESI can both be traced back to electrospray ionization, they exhibit different but complementary strengths and weaknesses. LESA can have high sensitivity when used in selected reaction monitoring mode on a triple quadrupole MS but lacks the high spatial resolution that DESI is capable of providing. DESI, in contrast, can supply structure-rich mass spectrometry (MS) images (Figure 1, DESI endogenous masses, showing multiplex analysis within the cassette-dosed sections) at high spatial resolution ($\sim$50 μm)[25] but has less apparent sensitivity due to the decrease in sampling area.

The utility of MSI is determined by the ability to detect the target compound at the level present in the sample and is determined by a number of factors such as the ionization efficiency and localized suppression caused by salts and endogenous compounds within the tissues. There is also a risk that the mass of the target compound is masked in the mass spectrum by endogenous compounds or MALDI matrix adduct signal. Therefore, "up-front" MSI ionization assessments are routinely performed to detect target compound in tissue samples before undertaking extensive studies. The risk of failing to detect a target in a sample can be further mitigated by using the orthogonal MSI techniques previously alluded to, such as LESA and DESI, which are becoming increasingly popular as imaging tools. These ionization techniques are essentially based on generic nanoelectrospray ionization and can be used to cover a much wider chemical space than MALDI which is limited by MALDI matrix selection. These ambient ionization techniques are often combined with triple quadrupole, ion trap, or time-of-flight mass spectrometers offering increased sensitivity at the cost of lower spatial resolution.

In a pharmacokinetic study multiple biofluid samples can be taken at required time points post dose; however, samples for MSI require the termination of the subject animal and the dissection and sectioning of a target organ. This means that a greater number of animals are required to generate corresponding time course MSI data. Effective cassette-dosed MSI experiments would be advantageous with a reduction in both the analytical turnaround time but also the animal handling and husbandry costs. Any significant reduction in the number of animals is advantageous, above and beyond cost savings and analysis time, as it is in keeping with industry-wide aims to reduce, reuse, and refine experimental animal numbers, the so-called "3-Rs".

The research presented here outlines a novel strategy of mass spectrometry tissue imaging and profiling in routine intravenous and orally cassette-dosed pharmacokinetic studies. MSI analysis was not adversely affected by cassette dosing, and the tissue distribution data corresponds with the plasma pharmacokinetic (PK) analysis and highlights the advantage of gaining important pharmacokinetic and distribution data from the same animals at an early phase of drug discovery. Demonstrated for the first time is enhanced tissue profiling technology (LESA) for low spatial resolution imaging. Furthermore, such analysis is combined with near cellular resolution MSI (~20 μm) and demonstrates that a suite of instrumentation enables detection of all target compounds, and therefore, a multiplatform MSI strategy is required for effective pharmaceutical research and development (R&D).

■ MATERIALS AND METHODS

Materials and Reagents. Analytical grade acetonitrile, methanol, and formic acid were obtained from Fisher Scientific (Loughborough, Leicestershire, U.K.). 2-Methylbutane was obtained from Sigma-Aldrich (Poole, Dorset, U.K.). Test compounds were obtained in house from AstraZeneca compound management group (Macclesfield, Cheshire, U.K.) with the exception of moxifloxacin which was purchased from Sigma-Aldrich (Poole, Dorset, U.K.). MALDI-MS grade α-cyano-4-hydroxycinnamic acid (CHCA) and 2,5-dihydroxybenzoic acid (DHB) were purchased from Sigma-Aldrich (Poole, Dorset, U.K.).

Animals. Adult male Hans Wistar rats (approximate weight 260 g) were obtained from Charles River Laboratories (Margate, Kent, U.K.) and were acclimatized on site for a minimum of 3 days prior to dosing. Compounds administered by oral gavage and intravenous bolus injection (via the tail vein) were formulated in 5% dimethyl sulfoxide/95% (30% w/v Captisol in water). Control animals were dosed with vehicle via the same administration route in each arm of the study.

Dosing and Scheduling. An initial pilot study using intravenous administration consisted of the following: one animal was dosed with vehicle, one animal was dosed discretely with haloperidol (2 mg/kg), and two animals were cassette-dosed (2 mg/kg/compound, haloperidol, bufuralol, midazolam, and clozapine). All intravenously dosed animals were euthanized at 15 min post dose.

A more extensive study using oral administration consisted of the following: one animal was dosed with vehicle, two animals were dosed discretely with moxifloxacin (25 mg/kg), two animals were dosed discretely with olanzapine (10 mg/kg), and three animals were cassette-dosed (moxifloxacin, olanzapine, erlotinib, and terfenadine at 25, 10, 10, and 25 mg/kg, respectively). Blood samples were taken at 0.5, 1, 2, 3, 4, and 5 h post dose via the tail vein (0.2 mL) and 6 h via cardiac puncture (0.5 mL); the blood was spun at 4500g for 2 min to yield plasma (approximately 0.1 mL) which was subsequently stored at −20 °C prior to analysis. Animals were euthanized at either 2 or 6 h post dose.

All tissue dissection was performed by trained AstraZeneca staff (project license 40/3484, procedure number 10). Tissues (brain, kidneys, lungs, and liver) were snap-frozen in 2-methylbutane on dry ice, subsequent transfer of tissues was done on dry ice, and samples were stored at −80 °C until tissue processing.

Tissue Processing. Tissue sections were cut at a thickness of 14 μm and thaw-mounted onto indium tin oxide (ITO)-coated MALDI target slides (Bruker Daltonics, Bremen, Germany) or standard glass microscope slides (VWR, Leicestershire, U.K.). Sections were taken at approximately equal depth from all organs to allow visualization of similar structures between samples. Organ tissue sections from cassette-dosed, discrete-dosed, and vehicle control animals were mounted adjacent on the same slides to minimize variability caused through variations in matrix application or when analyzing separate MALDI targets. Tissue sections were analyzed randomly and nonsequentially to limit the risk of any observed variation in relative abundance being as a result in loss of analyzer sensitivity during the course of the analysis. Mounted tissue sections were stored at −80 °C until required.

MALDI Matrix Application. Thaw-mounted tissue sections were dried in a stream of nitrogen when removed from −80 °C storage. Optical images were taken using a standard flat bed scanner (Seiko Epson, Negano, Japan) prior to MALDI matrix application. Matrix coating was applied as previously described for the analysis of small molecules using a pneumatic TLC sprayer (Sigma-Aldrich).[19] Either 15 mL of CHCA (10 mg/mL, 50/50 v/v acetonitrile/water, 0.1% TFA) or DHB (70 mg/mL, 50/50 v/v acetonitrile/water, 0.1% TFA) was applied. Following matrix application all subsequent transportation was performed with samples sealed in container to limit effects of light and humidity on sample and matrix. For high spatial resolution, tissue sections were transferred from −80 °C to a desiccator and dried for about 30 min prior to matrix coating. An optical image of the slide was acquired using a flatbed scanner (Epson perfection V500). The tissue was coated with DHB at a lower concentration of 35 mg/mL (50/50 v/v

methanol/water, 0.2% TFA) to reflect the more direct application of matrix and to prevent system blockages when using the TM-Sprayer tissue MALDI sample preparation system (HTX Technologies, LCC, Carrboro, NC, U.S.A.). A flow rate of 80 μL/min, nitrogen pressure 8 psi, and a spray nozzle temperature of 95 °C were used for two passes and 90 °C for a subsequent four passes of the tissue.

MALDI Mass Spectrometry Imaging. MALDI MSI was initially performed using a MALDI q-TOF MS (MALDI SYNAPT G2 HDMS, Waters Corporation, U.K.). The region of interest selected for imaging was defined using HDI Imaging software (version 1.2, Waters Corporation, U.K.), where the spatial resolution was also set (100 μm). Positive ion data was acquired with the mass spectrometer set to sensitivity mode over the range of m/z 100–1200 with 300 laser shots per raster position using a 1 kHz laser. Optimization of the mass spectrometer was achieved by tuning acquisition settings while collecting data from a manually deposited control spot of the target compounds (0.5 μL of drug standard solution at approximately 2 μM manually spotted onto the ITO target with equal volume of matrix in solution). Raw data was converted to image files via processing through Mass Lynx (version 4.1, Waters Corporation, U.K.), then viewed in HDI Imaging software (version 1.2, Waters Corporation, U.K.). Data was normalized by total ion current, and subsequent image analysis was performed. Mass filter windows were selected with a precision of $\pm$0.04 Da.

High mass resolution data were acquired on a 12 T SolariX FTICR (Bruker Daltonics, Billerica, MA) running SolariX control v1.5.0 build 103. Ions were excited (frequency chirp 48–500 kHz at 100 steps of 25 μs) for 0.8 s to yield broadband 2 Mword time-domain data. Each mass analysis was the sum of 400 random laser sample positions across tissue. Fast Fourier transforms and subsequent analyses were performed using DataAnalysis v 4.1 build 362.7 and Fleximaging v4.0 build 32 (Bruker Daltonics, Billerica, MA).

High spatial resolution MSI experiments were carried out in positive reflectron mode over a mass range of m/z 150–900 using the UltrafleXtreme MALDI-TOF/TOF MS (Bruker Daltonics) equipped with a 2 kHz, smartbeam-II Nd:YAG laser. Data was collected at a spatial resolution of 15 μm, summing up 500 laser shots/raster position. FlexImaging 3.0 (Bruker Daltonics) was used for data analysis, normalization, and molecular image extraction typically using mass selection window of $\pm$0.05 Da.

DESI Mass Spectrometry Imaging. DESI MSI analysis was performed using an Exactive mass spectrometer (Thermo Fisher Scientific Inc., Bremen, Germany) operated in positive ion mode. The mass spectrometer was equipped with a custom-built automated DESI ion source. The mass resolution used for all measurements was set to 100 000. Mass spectra were collected in the mass range of m/z = 150–1300. Methanol/water (95:5 v/v) was used as the electrospray solvent at a flow rate of 2.5 μL/min. Nebulizing nitrogen was used as gas at a pressure of 10 bar. The height distance between the DESI sprayer and the sample surface was set to 2 mm with the distance between the sprayer and the inlet capillary set to 14 mm. The distance between the sample surface and the inlet capillary of the mass spectrometer was <1 mm. The angle between the sprayer tip and the sample surface was set at 80°. For line scan experiments, the parameters described above were used with a scan speed of 150 μm/s. Imaging experiments were conducted using 150 μm spatial resolution. Image analysis

consisted of individual horizontal line scans combined into imzML format using the imzML converter V.1.1.4.5 (www.maldi-msi.org). All images were created using 0.01 Da bin size and were normalized to the total ion count (TIC) to compensate for signal instabilities.

LESA Mass Spectrometry Imaging. LESA MSI was performed using LESA-MS/MS on a Triversa Nanomate chip-based electrospray ionization system (Advion, Ithaca, NY, U.S.A.) coupled to a QTRAP 5500 (AB Sciex, Framingham, MA, U.S.A.) mass spectrometer that was operated in positive ion multiple reaction monitoring (MRM) mode. The LESA sampling method consisted of aspiration of a 0.9 μL volume of extraction solution (acetonitrile/water/formic acid 60/40/0.1 v/v/v). An amount of 0.5 μL of the solution was then dispensed at a height of 0.4 mm above the tissue with a 1 s postdispense delay time; a liquid microjunction between the pipette tip and the sample was maintained throughout the procedure. An amount of 1.1 μL of sample was reaspirated into the pipet tip prior to infusion via the Nanomate chip for tandem mass spectrometry (MS/MS) analysis. Relative abundance was determined between samples by comparison of MRM transition intensity at m/z 326 > 291.2, 262.2 > 188.1, 327.1 > 269.9, and 376.1 > 165.1 for midazolam, bufuralol, clozapine, and haloperidol (intravenously dosed cassette), respectively, and 402.1 > 261.1, 313.1 > 256.1, 394.1 > 278.0, and 472.2 > 436.2 for moxifloxacin, olanzapine, erlotinib, and terfenadine (orally dosed cassette). LESA-MS/MS data was processed using a purpose-built software package capable of extracting relative abundance values from Analyst 6.1 (ABSciex, Framingham, MA, U.S.A.).

LESA-MS/MS images were created using in-house-developed software capable of color grading ion intensities acquired from each individual LESA spot in a heat map configuration.

PK Bioanalysis. Details of the preparation of bioanalytical stock solutions and the bioanalytical method used can be found in the Supporting Information.

■ RESULTS AND DISCUSSION

Obtaining knowledge of the abundance and spatial distribution of compounds in target tissue can be extremely valuable in drug discovery or during a toxicological investigation. An understanding of the distribution profile of candidate drugs can be fed back into project design/make/test cycles, allowing researchers to refine the properties of chemical series early in the drug discovery process. In order to use such distribution information effectively the analysis techniques need to be high throughput while not compromising data quality. This study explores cassette dosing as a viable method of increasing throughput and decreasing the numbers of animals used in distribution studies using mass spectrometry imaging. Data quality was validated by comparing compounds dosed using the cassette approach with compounds that are dosed orally and intravenously as discrete formulations.

Technical replicates were not performed due to instrument time constraints, number of samples involved, and the cost of LESA consumables (specifically nanoESI emitters). However, reproducibility of MSI strategies have previously been reported and therefore were not considered to be required for these experiments where relative abundances were measured. If absolute quantitation was performed we would recommend technical replicate analysis to be performed.

Test Substance Selection. Four compounds were selected for a pilot intravenous cassette dosing experiment. Haloperidol,
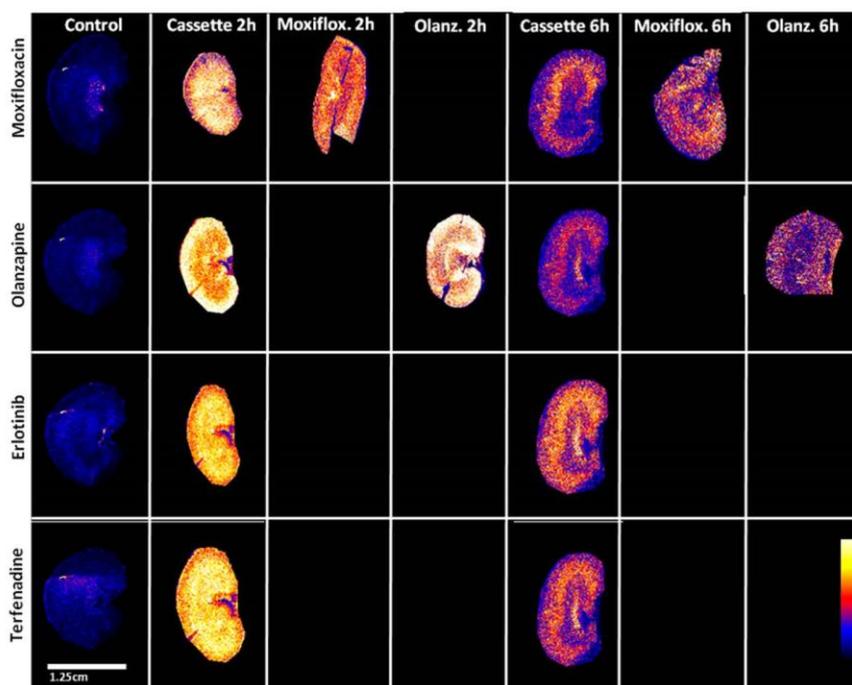
Figure 2. MSI abundance distributions of cassette- and discrete-dosed compounds in rat kidney sections (14 μm) at 2 and 6 h post dose. Moxifloxacin and olanzapine distributions are comparable at the two time points validating the cassette approach.

a dopamine D_2 antagonist, bufuralol, a β-adrenoceptor antagonist, and midazolam, a GABA antagonist, were chosen at random; no data about prior MSI analysis has been published to date. Clozapine, a serotonin antagonist that has been used in several in-house studies and is known to be detectable by MALDI MSI, was added to the intravenous cassette to mitigate the risk of failing to detect all compounds in the pilot study by our primary analytical technique.

A further four compounds were selected for a more extensive oral cassette dosing experiment. Terfenadine, an H_1 receptor antagonist, has been analyzed by MSI following a 50 mg/kg dose (single oral dose) using a hybrid quadrupole−time-of-flight (QqTOF, QStar Pulsar, Applied Biosystems)[20] and at the same dose by LESA profiling (QTRAP 5500, AB Sciex).[13] Erlotinib, a tyrosine kinase inhibitor, was detected using a hybrid quadrupole−time-of-flight (QqTOF, QStar XL, AB/MDS Sciex))[21] following 5 mg/kg oral dose. Olanzapine, a dopamine D_2 antagonist, was orally dosed at 8 mg/kg and detected using a MALDI time-of-flight (Autoflex, Bruker).[22] The final compound in the cassette was moxifloxacin, a DNA gyrase inhibitor, detected on a FlashQuant QTRAP (AB Sciex) following oral dose at 25 mg/kg.[23]

Intravenous (iv) Dosing. An initial intravenously dosed pilot study consisting of cassette-dosed, discrete-dosed, and vehicle-dosed animals was performed in order to confirm the proof of principle that cassette dosing and discrete dosing show a similar relationship in terms of relative distribution across different tissues. Animals were euthanized at 15 min post dose, with brain, kidney, liver, and lung samples dissected and snap-frozen in 2-methylbutane postmortem.

Distribution of Intravenously Dosed Compounds by MALDI MSI. Brain, kidney, liver, and lung sections (14 μm) were thaw-mounted onto ITO-coated microscope slides. Sections were arranged, as stated in the Materials and Methods

section, to minimize intra-analysis variability caused by matrix applications and interanalysis variability. Typically three brain sections representing cassette-dosed, discrete-dosed, and control were mounted on the same slide. Positive ion MALDI MSI (MALDI Synapt Q-TOF, Waters, Manchester, U.K.) was employed to analyze brain and liver sections. DHB and CHCA were used as standard MALDI matrixes with limited success. Haloperidol, bufuralol, and midazolam were not detected with either matrix from either tissue type even though initial ionization testing in the absence of tissue had been positive using both matrixes (data not shown). This poor response could be due to various factors such as ionization suppression from endogenous components and salts in the tissue and could be rectified by using an alternative MALDI matrix, solvent system, or by carefully optimized slide washing of the tissue prior to matrix application[24] and analysis. Clozapine was detected on both tissue types using CHCA as the MALDI matrix; the relative distribution of clozapine at 15 min post dose in a sagittal brain section can be seen in Figure 1, normalized by total ion count, at a spatial resolution of 100 μm.

Additional MSI Analysis by LESA-MS/MS and DESI-MS. The failure of MALDI MSI to detect several of the intravenously dosed compounds presented an opportunity to highlight the value of orthogonal analysis by other techniques. Figure 1 shows images of intravenously dosed sagittal brain sections analyzed by LESA-MS/MS (1 mm spatial resolution) and coronal brain sections analyzed by DESI-MS (150 μm spatial resolution). LESA-MS/MS detected all of the compounds in the sagittal brain sections. Relative distribution of the compounds was largely around the frontal cortex with little distribution into the rear left and right hemispheres of the cerebrum. Cassette-dosed and discrete-dosed comparisons of haloperidol in the brain sections by LESA-MS/MS (Figure 1) highlighted some differences in distribution. This is due to the
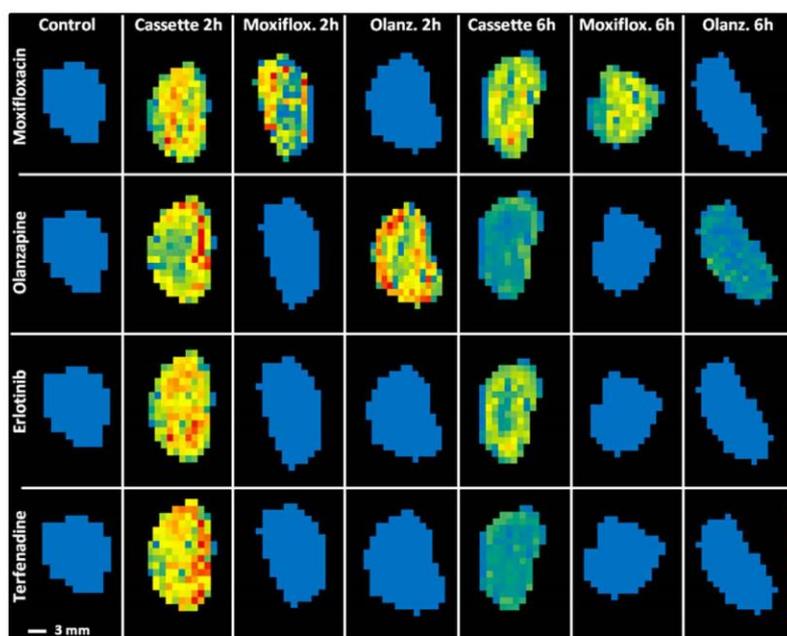
Figure 3. LESA-MS/MS abundance distributions of cassette- and discrete-dosed compounds in rat kidney sections (14 μm) at 2 and 6 h post dose. This data mirrors the MALDI MSI data showing comparable distributions of moxifloxacin and olanzapine dosed discretely and by the cassette approach.

in-house imaging program applying a rainbow scale to a narrow drug intensity window across the two sections; the actual distribution was relatively homogeneous throughout the tissue. Coronal brain tissue sections (14 μm) were thaw-mounted onto standard glass slides for accurate mass DESI-MS analysis. Due to the requirement to place DESI-MS samples onto nonconductive glass slides, additional tissue sections were cut by cryostat and thaw-mounted. It was necessary to use a brain from a different animal (dosed and sacrificed under same conditions) as the first brain fractured during the remounting process. While this prevents intersample consistency it does allow the coronal DESI analysis to show symmetry in detected analytes and endogenous compounds. Detection of haloperidol, bufuralol, and clozapine at (mass $\pm$ ppm) 376.1468 $\pm$ 1.6217, 262.1795 $\pm$ 2.4945, and 327.1366 $\pm$ 1.5254 Da, respectively, was achieved (Figure 1). Midazolam could not be detected with sufficient mass accuracy (326.0850 Da) from the tissue sections using DESI-MS.

Oral (po) Dosing. A larger, more comprehensive study was designed to compare cassette dosing to discrete dosing after oral administration. Plasma analysis by LC−MS/MS revealed that cassette- and discrete-dosed animals were exposed to the test substances in all instances. Comparative plasma concentrations post dose for moxifloxacin and olanzapine were equivalent in cassette-dosed versus discrete-dosed animals (Figure S-1, Supporting Information), indicating that plasma exposures were not adversely affected by drug−drug interactions. PK parameters for each compound are listed in Table S-1, Supporting Information. The parameters exhibit reproducibility between orally administered cassette- and discrete-dosed moxifloxacin and olanzapine and provide an initial indication that the cassette dosing approach is valid.

Distribution of Orally Dosed Compounds by MALDI MSI. Brain, kidney, liver, and lung tissue sections (14 μm) were thaw-mounted onto ITO-coated microscope slides and were arranged in a similar order as the intravenously dosed sections to maintain a consistent approach; where possible five sections were mounted per slide, representing cassette dose 2 and 6 h, discrete dose 2 and 6 h, and control tissue. The mass spectrometer source was rigorously cleaned after every two analytical runs to limit the risk of any observed variation in relative abundance being as a result in loss of analyzer sensitivity during the course of the analysis. Positive ion MALDI MSI (MALDI Synapt Q-TOF, Waters, Manchester, U.K.) was employed to analyze the kidney sections and produced high-quality MS images (Figure 2), normalized by total ion count, at a spatial resolution of 100 μm and signal thresholding consistent across samples. The spatial distribution and relative abundance of the test substances at the 2 h time point were homogeneous throughout the kidney tissue. Moxifloxacin and olanzapine distributions were relatively consistent between cassette- and discrete-dosed animals, with some minor differences which could be attributed to pharmacokinetic interanimal variability (supported by the differences in plasma PK levels, Supporting Information Table S-1) or the depth at which the section was cut from the kidney sample. At the 6 h time point the relative abundance of the test substances in the cassette-dosed kidneys was approximately 6-fold lower in abundance than the 2 h time point for moxifloxacin. A reduction was also detected for olanzapine (30-fold lower), erlotinib (8-fold reduced), and terfenadine (3-fold diminished). This drop in relative abundance reflects the decrease in concentrations observed in the plasma samples between the two time points but was not directly comparable in terms of the drop in response in tissue versus the drop in concentration in plasma. Erlotinib and terfenadine were distributed in both the cortex and medulla of the kidney, with greater intensity in the medullary region,

77

whereas moxifloxacin and olanzapine were more localized in the medulla of the kidney. The consistent relative abundance between the images for moxifloxacin and olanzapine at each time point for cassette and discrete dosing provides further validation of the cassette dosing approach. Liver and brain sections were also analyzed by MALDI MSI to confirm detection of the test substances in the various tissue types (data not shown).

Analysis of Orally Dosed Tissues by LESA-MS/MS. An advantage of tissue sectioning is that, from each sample, multiple, nearly identical tissue sections can be taken, allowing analysis such as LESA-MS/MS and DESI-MS to be performed in addition to MALDI MSI. LESA-MS/MS is based upon nanoelectrospray ionization, a proven, robust technique that is capable of ionizing a wide variety of different chemical species. The combination of the ionization technique with sensitive tandem mass spectrometry offers a complementary method of analysis to MALDI MSI. MALDI by contrast is a much more complex process, subject to subtle changes in ablation, ionization, and sensitivity due to matrix choice, matrix crystal size, preparation conditions, and endogenous interferences from material in the tissue such as salts. These limitations of the technique lead to a lower than ideal success rate when working in a high-throughput environment. LESA-MS/MS and other direct ionization techniques such as DESI-MS provide a way of bridging that gap, enabling MSI scientists to pass on meaningful distribution data to project teams. Kidney sections were analyzed by LESA-MS/MS (QTRAP 5500, ABSciex, Framingham, MA, U.S.A.) to generate low spatial resolution (1 mm) mass spectrometry images. Figure 3 displays the images from the LESA-MS/MS analysis of the orally cassette-dosed and discrete-dosed sections. The images are generated using in-house-developed software that creates a heat map of the mean ion intensity data from each LESA extraction (~125 extractions per kidney section). The LESA imaging data correlate well with the observations of the MALDI MSI data, showing a clear difference in the relative abundance of the test substances at 2 and 6 h post dose and good reproducibility in terms of spatial distribution between cassette- and discrete-dosed compounds.

High-Resolution MSI. Lung sections were analyzed by high mass resolution MS (12 T SolariX FTICR, Bruker Daltonics, Billerica, MA, U.S.A.) for confirmation of the presence of the test substances. Sample spectra are shown in Figure S-2, Supporting Information; the presence of moxifloxacin, olanzapine, erlotinib, and terfenadine at m/z 402.1824, 313.1481, 394.1761, and 472.3210 is confirmed by accurate mass and comparison of each compound with a vehicle-dosed sample.

High spatial resolution MSI is a powerful tool that allows near-cellular resolution. The higher spatial resolution images can be used to identify regions of tissue structure within organ tissue sections. Figure 4 shows a high spatial resolution image (20 μm, UltrafleXtreme MALDI-TOF/TOF MS, Bruker Daltonics) of dosed lung section. Olanzapine (m/z 313), represented in green, is distributed throughout the lung tissue, while a blood vessel can be clearly seen in the optical image and is reflected in the MSI image as an area of high heme abundance (m/z 616). High spatial resolution MSI can highlight distribution of test substances into localized areas of tissue to demonstrate drug presence at the site of action and could be expanded further to confirm target engagement via changes in endogenous disease markers.
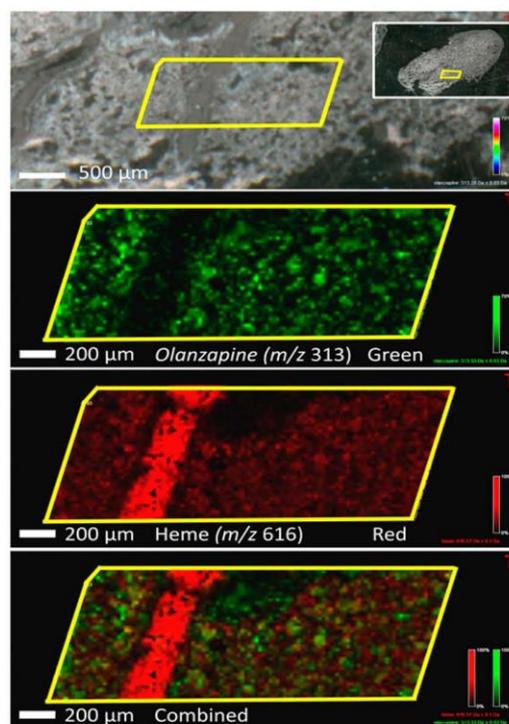

Figure 4. High spatial resolution MSI (15 μm) of orally cassette-dosed lung tissue showing an optical image describing the region of interest and MSI images of olanzapine (green) and heme (red). A blood vessel can be clearly seen with the compound being homogeneously distributed over the rest of the tissue, highlighting the power of high-resolution MSI.

■ CONCLUSIONS

Cassette dosing is a widely adopted practice within pharmaceutical discovery research for plasma PK analysis. Here we have demonstrated for the first time its utility in PK tissue distribution studies using mass spectrometry imaging techniques. Cassette dosing fundamentally increases throughput, in this case by 4-fold, greatly reducing what has traditionally been an analytical bottleneck. The combination of cassette-dosed PK and drug distribution studies has many advantages; ethically the technique reduces the number of animals used, typically by around 75%; the combination also leads to a wealth of pharmacokinetic and distribution data being available at a much earlier stage of drug discovery and can lead to a much greater confidence that compounds are present at the pharmacological site of action. It is also possible to measure and monitor compound abundance target tissue in response to dose or time.

Mass spectrometry imaging covers a variety of relatively new and exciting technologies that can be used to study the regional abundance of xenobiotics within tissues, while also simultaneously measuring endogenous molecules. A single technique is yet to emerge that can successfully analyze the full scope of chemistries encountered in drug discovery, at sufficient sensitivity and with high spatial resolution. MALDI MSI was successfully used to analyze orally cassette-dosed tissue sections at 100 μm and at higher spatial resolution (15 μm). LESA-MS/MS was validated against the MALDI MSI data. The success of MALDI MSI to analyze the compounds in the oral cassette-dosed study was contrasted against an intravenously dosed

cassette study in which the technique had less success. LESA-MS/MS and DESI-MS were used to profile the relative distribution of the intravenously dosed compounds, at lower spatial resolution, but with a higher success rate.

The cassette dosing strategy has been shown to be a successful approach to obtain early, combined pharmacokinetic and distribution data. Mass spectrometric imaging techniques have an increasingly important role to play in pharmaceutical R&D, with techniques being developed to provide more quantitative data and the expansion of MALDI MSI, in particular, into areas of targeted and untargeted metabolomics.

■ ASSOCIATED CONTENT

Ⓢ Supporting Information

Additional information as noted in text. This material is available free of charge via the Internet at http://pubs.acs.org.

■ AUTHOR INFORMATION

Corresponding Author

*E-mail: john.swales@astrazeneca.com. Phone: +44 0 7818 523 771.

Notes

The authors declare no competing financial interest.

■ REFERENCES

(1) Bass, A. S.; Cartwright, M. E.; Mahon, C.; Morrison, R.; Snyder, R.; McNamara, P.; Bradley, P.; Zhou, Y.; Hunter, J. *J. Pharmacol. Toxicol. Methods* **2009**, *60*, 69−78.

(2) Berman, J.; Halm, K.; Adkison, K.; Shaffer, J. *J. Med. Chem.* **1997**, *40*, 827−829.

(3) Alien, M. C.; Shah, T. S.; Day, W. W. *Pharm. Res.* **1998**, *15*, 93−97.

(4) Olah, T. V.; McLoughlin, D. A.; Gilbert, J. D. *Rapid Commun. Mass Spectrom.* **1997**, *11*, 17−23.

(5) Frick, L. W.; Adkison, K. K.; Wells-Knecht, K. J.; Woollard, P.; Higton, D. M. *Pharm. Sci. Technol. Today* **1998**, *1*, 12−18.

(6) Manitpisitkul, P.; White, R. E. *Drug Discovery Today* **2004**, *9*, 652−658.

(7) White, R. E.; Manitpisitkul, P. *Drug Metab. Dispos.* **2001**, *29*, 957−966.

(8) Swales, J. G.; Wilkinson, G.; Gallagher, R.; Hammond, C.; O'Donnell, C.; Peter, R. *Int. J. High Throughput Screening* **2010**, *1*, 1−14.

(9) Madden, S.; Patterson, A.; Stevenson, K. *Drug Metab. Rev.* **2012**, *44*, 63−63.

(10) Stoeckli, M.; Chaurand, P.; Hallahan, D. E.; Caprioli, R. M. *Nat. Med.* **2001**, *7*, 493−496.

(11) Solon, E. G.; Schweitzer, A.; Stoeckli, M.; Prideaux, B. *AAPS J.* **2010**, *12*, 11−26.

(12) Stegemann, C.; Drozdov, I.; Shalhoub, J.; Humphries, J.; Ladroue, C.; Didangelos, A.; Baumert, M.; Allen, M.; Davies, A. H.; Monaco, C. *Circ.: Cardiovasc. Genet.* **2011**, *4*, 232−242.

(13) Eikel, D.; Vavrek, M.; Smith, S.; Bason, C.; Yeh, S.; Korfmacher, W. A.; Henion, J. D. *Rapid Commun. Mass Spectrom.* **2011**, *25*, 3587−3596.

(14) Parson, W. B.; Koeniger, S. L.; Johnson, R. W.; Erickson, J.; Tian, Y.; Stedman, C.; Schwartz, A.; Tarcsa, E.; Cole, R.; Van Berkel, G. J. *J. Mass Spectrom.* **2012**, *47*, 1420−1428.

(15) Blatherwick, E. Q.; Van Berkel, G. J.; Pickup, K.; Johansson, M. K.; Beaudoin, M.; Cole, R. O.; Day, J. M.; Iverson, S.; Wilson, I. D.; Scrivens, J. H. *Xenobiotica* **2011**, *41*, 720−734.

(16) Goodwin, R. J.; Pitt, A. R. *Bioanalysis* **2010**, *2*, 279−293.

(17) Goodwin, R. J. *J. Proteomics* **2012**, *75*, 4893−4911.

(18) Sugiura, Y.; Setou, M. *J. Neuroimmune Pharmacol.* **2010**, *5*, 31−43.

(19) Goodwin, R. J.; Dungworth, J. C.; Cobb, S. R.; Pitt, A. R. *Proteomics* **2008**, *8*, 3801−3808.

(20) Hsieh, Y.; Chen, J.; Knemeyer, I.; Crossman, L.; Korfmacher, W. A. *Drug Metab. Lett.* **2008**, *2*, 1−4.

(21) Signor, L.; Varesio, E.; Staack, R. F.; Starke, V.; Richter, W. F.; Hopfgartner, G. *J. Mass Spectrom.* **2007**, *42*, 900−909.

(22) Hamm, G.; Bonnel, D.; Legouffe, R.; Pamelard, F.; Delbos, J.; Bouzom, F.; Stauber, J. *J. Proteomics* **2012**, *75*, 4952−4961.

(23) Prideaux, B.; Dartois, V.; Staab, D.; Weiner, D. M.; Goh, A.; Via, L. E.; Barry, C. E., III; Stoeckli, M. *Anal. Chem.* **2011**, *83*, 2112−2118.

(24) Shariatgorji, M.; Källback, P.; Gustavsson, L.; Schintu, N.; Svenningsson, P.; Goodwin, R. J.; Andren, P. E. *Anal. Chem.* **2012**, *84*, 4603−4607.

(25) Campbell, D. I.; Ferreira, C. R.; Eberlin, L. S.; Cooks, R. G. *Anal. Bioanal. Chem.* **2012**, *404*, 389−398.

4.0 <u>**MAPPING DRUG DISTRIBUTION IN BRAIN TISSUE USING LIQUID EXTRACTION SURFACE ANALYSIS MASS SPECTROMETRY IMAGING**</u>

Swales, J. G.; Tucker, J. W.; Spreadborough, M. J.; Iverson, S. L.; Clench, M. R.; Webborn, P. J.; Goodwin, R. J., Mapping drug distribution in brain tissue using liquid extraction surface analysis mass spectrometry imaging. *Analytical Chemistry* **2015,** *87* (19), 10146-52.

Author Contribution

JGS designed the blood brain barrier studies, aided necropsy, performed all sample preparation and LESA and MALDI imaging experiments, processed imaging data, interpreted results and prepared the manuscript for publication.

Mapping Drug Distribution in Brain Tissue Using Liquid Extraction Surface Analysis Mass Spectrometry Imaging

John G. Swales,*[†,‡] James W. Tucker,[†] Michael J. Spreadborough,[†] Suzanne L. Iverson,[†] Malcolm R. Clench,[‡] Peter J. H. Webborn,[†] and Richard J. A. Goodwin[†]

[†]Drug Safety and Metabolism, AstraZeneca R&D, Cambridge Science Park, Milton Road, Cambridge CB4 0WG, U.K.
[‡]Biomedical Research Centre, Sheffield Hallam University, Howard Street, Sheffield, South Yorkshire S1 1WB, U.K.

ABSTRACT: Liquid extraction surface analysis mass spectrometry (LESA-MS) is a surface sampling technique that incorporates liquid extraction from the surface of tissue sections with nanoelectrospray mass spectrometry. Traditional tissue analysis techniques usually require homogenization of the sample prior to analysis via high-performance liquid chromatography mass spectrometry (HPLC–MS), but an intrinsic weakness of this is a loss of all spatial information and the inability of the technique to distinguish between actual tissue penetration and response caused by residual blood contamination. LESA-MS, in contrast, has the ability to spatially resolve drug distributions and has historically been used to profile discrete spots on the surface of tissue sections. Here, we use the technique as a mass spectrometry imaging (MSI) tool, extracting points at 1 mm spatial resolution across tissue sections to build an image of xenobiotic and endogenous compound distribution to assess drug blood–brain barrier penetration into brain tissue. A selection of penetrant and "nonpenetrant" drugs were dosed to rats via oral and intravenous administration. Whole brains were snap-frozen at necropsy and were subsequently sectioned prior to analysis by matrix-assisted laser desorption ionization mass spectrometry imaging (MALDI-MSI) and LESA-MSI. MALDI-MSI, as expected, was shown to effectively map the distribution of brain penetrative compounds but lacked sufficient sensitivity when compounds were marginally penetrative. LESA-MSI was used to effectively map the distribution of these poorly penetrative compounds, highlighting its value as a complementary technique to MALDI-MSI. The technique also showed benefits when compared to traditional homogenization, particularly for drugs that were considered nonpenetrant by homogenization but were shown to have a measurable penetration using LESA-MSI.
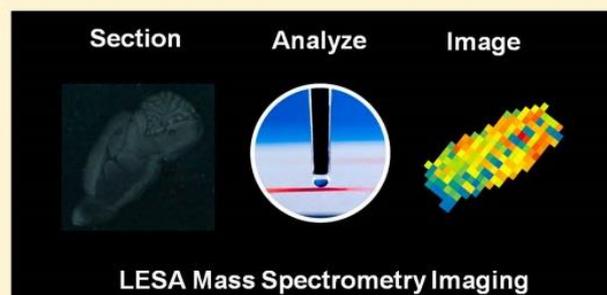
How a drug distributes in the body and its effects on safety and efficacy is an important consideration in the development of novel medicines. Traditional analytical methods such as homogenization[1] and quantitative whole-body autoradiography (QWBA)[2] have been widely used, but have significant drawbacks. Homogenization methods result in the loss of all spatial information from a tissue sample, usually providing quantitative (in terms of amount per gram of tissue) confirmation of compound presence in the tissue of interest. This concentration can be misleading in highly perfused organs due to residual blood in the sample which may contain high drug levels and distort measurements. Furthermore, the need to make the tissue sample amenable to liquid chromatography (LC) methods usually requires a significant dilution step that, in the case of poorly distributed compounds, can result in overdilution, to the extent that such compounds are undetectable by the analytical technique of choice.

QWBA is a sensitive, robust analytical technique that provides absolute quantitative data and retains meaningful spatial distribution information.[3] The technique has several drawbacks, the most significant of which stem from the need for a radiolabeled compound. Synthesis of radiolabeled

compounds is expensive and can take significant time. This makes the technique unsuitable for early discovery phase studies where many compounds may be under investigation at any one time. The requirement for a radiolabeled drug also leads to the inability of the technique to distinguish between parent compound and any metabolites that contain the radiolabel leading to an overestimation of the drugs biodistribution; there is also the potential to miss any metabolites that do not contain the radiolabel but that may be significant in terms of being active against the chosen target or be a cause of toxicity.

Mass spectrometry imaging (MSI) is a term used to describe a number of complementary imaging technologies based on the use of different surface sampling and different ionization techniques. These include matrix-assisted laser desorption ionization imaging (MALDI-MSI),[4] secondary ion mass spectrometry imaging (SIMS-MSI),[5] desorption electrospray ionization mass spectrometry imaging (DESI-MSI),[6] and laser

ablation electrospray ionization imaging (LAESI-MSI),[7] with MALDI-MSI being arguably the most effective technique for pharmaceutical research and development.[8−11] Each technique has its own strengths and weaknesses determined by the ability to detect target analytes at the appropriate level present in tissues; this in turn is determined by a number of factors such as localized signal suppression caused by endogenous compounds or salts present within the tissues, compound ionization efficiencies, and the presence of isobaric endogenous compounds or, in the case of MALDI, matrix adducts. Failure to analyze a target compound by a chosen MSI technique can often be mitigated by employing a complementary MSI technique such as those already mentioned.

A new addition to the range of MSI techniques is liquid extraction surface analysis mass spectrometry (LESA-MS), which is capable of obtaining spatially resolved analyte information from a tissue section via a liquid extraction from the surface of the tissue followed by nanoelectrospray ionization.[12,13] Until recently LESA-MS was used largely in a tissue profiling capacity,[14] analyzing discrete spots at points on a tissue section yielding qualitative data roughly equivalent to homogenization; however, recent developments have meant the technique can now be used to generate two-dimensional (2D) images of the analyte of interest by sampling at multiple points across tissues. The relatively low spatial resolution of LESA-MS (1 mm) compared with, for instance, MALDI-MS, which is capable of resolution down to ∼10 μm, means a vastly greater amount of sample is available for ionization and subsequent detection (10 000× more sensitivity based on area); thus, the technique is highly sensitive especially when combined with triple quadrupole mass spectrometers which offer selectivity and specificity when used in selected reaction monitoring mode.

Many therapeutic agents rely on passage across the blood−brain barrier (BBB) to reach a pharmacological target.[15] Treatments for indications such as Alzheimer's disease,[16] Parkinson's disease,[17] cancer,[18] diabetes,[19] obesity,[20] and central neuropathic pain[21] rely on transit across the BBB and distribution into brain tissue to have efficacy. The reverse can be said for drugs that induce an unwanted toxicological response in the central nervous system where significant BBB exclusion may be required.[22]

Traditionally, penetration across the BBB into brain tissue can be difficult to accurately measure using conventional tissue analysis methods such as LC−MS/MS, largely because they are based on tissue homogenization.[23] This is particularly true if a drug is poorly penetrative due to the inevitable presence of residual blood in the brain. Liu et al. have shown that MALDI-MSI techniques[24] have the ability to mitigate this problem by spatially resolving compound distribution across brain tissue sections and by offering the potential to acquire data over a wide mass range to capture information on different analytes. By performing this "multiplex" analysis[25] compound distribution can be correlated against endogenous markers such as heme as a surrogate for blood, to separate actual drug penetration into parenchyma from signal derived from residual blood contamination.

The data presented here aims to show for the first time that LESA-MSI has intrinsic advantages over traditional tissue homogenization techniques by spatially resolving the distribution of drugs and an endogenous marker for blood, in this case heme, to establish BBB penetration. The research novelly expands on this concept to show that the technique can be used

to profile poorly penetrative compounds, which analysis by homogenization has concluded are nonpenetrative and any compound detected is due to residual blood contamination. Furthermore, we demonstrate that, by sacrificing spatial resolution to achieve higher sensitivity, LESA-MSI can be used to profile compounds that our primary analytical technique MALDI-MSI has failed to detect.

■ MATERIAL AND METHODS

Materials and Reagents. Analytical grade acetonitrile, methanol, and formic acid were obtained from Fisher Scientific (Loughborough, Leicestershire, U.K.). 2-Methylbutane was obtained from Sigma-Aldrich (Poole, Dorset, U.K.). Test compounds were obtained in house from AstraZeneca compound management group (Macclesfield, Cheshire, U.K.) with the exception of SCH-23390 which was purchased from Sigma-Aldrich (Poole, Dorset, U.K.) and AZx which was obtained from AstraZeneca compound management group (Mölndal, Gothenburg, Sweden).

Animals. Adult male Hans Wistar rats (approximate weight 260 g) were obtained from Charles River Laboratories (Margate, Kent, U.K.) and were acclimatized on site for a minimum of 3 days prior to dosing. Compounds administered by oral gavage and intravenous bolus injection (via the tail vein) were formulated in 5% dimethyl sulfoxide (DMSO)/95% (30% w/v Captisol in water). Control animals were dosed with vehicle via the same administration route in each arm of the study.

The study was reviewed by the Institutional Animal Welfare and Ethical Review Body and was conducted in accordance with the animal care and ethics described in "Guidance on the Operations of the Animals (Scientific Procedures) Act 1986" issued by the U.K. Home Office.

Dosing and Scheduling. The study consisted of seven individual animals (project license 40/3484, procedure number 10). One animal was dosed intravenously with vehicle and was terminated at 30 min post dose. Two animals were dosed intravenously with a cassette containing AZD8329 and SCH23390, each dosed at 5 mg/kg and terminated at either 1 or 30 min post dose. Four animals were dosed orally with a cassette containing AZD4017 and MK-0916, each dosed at 50 mg/kg and terminated at either 2 h ($n = 2$) or 6 h ($n = 2$) post dose.

All tissue dissection was performed by trained AstraZeneca staff. Brain samples were harvested at termination and snap-frozen in 2-methylbutane on dry ice; subsequent transfer of tissues was done on dry ice, and samples were stored at −80 °C until tissue processing. Terminal plasma samples were stored at −20 °C prior to analysis.

Tissue Processing. Sagittal tissue sections were cut at a thickness of 14 μm and thaw-mounted onto indium−tin oxide (ITO)-coated MALDI target slides (Bruker Daltonics, Bremen, Germany) Sections were taken at approximately equal depth from all whole brain samples. Tissue sections from dosed and vehicle control animals were mounted adjacent on the same slides to minimize intra-animal variability caused by changes in mass spectrometer response throughout the analytical run. Mounted tissue sections were stored at −80 °C until required.

LESA Mass Spectrometry Imaging. LESA MSI was performed using LESA-MS/MS on a Triversa Nanomate chip-based electrospray ionization system (Advion, Ithaca, NY, U.S.A.) coupled to a QTRAP 5500 (AB Sciex, Framingham, MA, U.S.A.) mass spectrometer operated in positive ion MRM

mode. The LESA sampling method consisted of aspiration of a 0.9 μL volume of extraction solution (acetonitrile/water/formic Acid 60/40/0.1 v/v/v). An amount of 0.5 μL of the solution was then dispensed at a height of 0.4 mm above the tissue with a 1 s post dispense delay time; a liquid microjunction between the pipet tip and the sample was maintained throughout the procedure. An amount of 1.1 μL of sample was reaspirated into the pipet tip prior to infusion via the nanomate chip for MS/MS analysis. Relative abundance was determined between samples by comparison of MRM transition intensity at m/z 420.2 > 320.9 and 332.1 > 286.1 for AZD4017 and MK-0916 (orally dosed cassette) and 422.2 > 148.1 and 288.1 > 90.9 for AZD8329 and SCH23390 (intravenously dosed cassette). LESA-MS/MS data was processed using a purpose-built software package capable of extracting relative abundance values from Analyst 6.1 (AB Sciex, Framingham, MA, U.S.A.).

LESA-MS/MS images were created using in-house developed software capable of color grading ion intensities acquired from each individual LESA spot in a heat map configuration.

MALDI Matrix Application. Thaw-mounted tissue sections were dried in a stream of nitrogen when removed from −80 °C storage. Optical images were taken using a standard flat-bed scanner (Seiko Epson, Negano, Japan) prior to MALDI matrix application. Matrix coating was applied as previously described for the analysis of small molecules using a pneumatic TLC sprayer (Sigma-Aldrich).[26] Either 15 mL of α-cyano-4-hydroxycinnamic acid (CHCA) (10 mg/mL, 50/50 v/v acetonitrile/water, 0.1% TFA) or 2,5-dihydroxybenzoic acid (DHB) (70 mg/mL, 50/50 v/v acetonitrile/water, 0.1% TFA) was applied. Following matrix application all subsequent transportation was performed with samples sealed in a container to limit effects of light and humidity on sample and matrix.

MALDI Mass Spectrometry Imaging. MALDI-MSI was performed using a MALDI q-TOF MS (MALDI SYNAPT G2 HDMS, Waters Corporation, U.K.). The region of interest selected for imaging was defined using HDI Imaging software (version 1.2, Waters Corporation, U.K.), where the spatial resolution was also set (100 μm). Positive ion data was acquired with the mass spectrometer set to sensitivity mode over the range of m/z 100−1200 with 300 laser shots per raster position using a 1 kHz laser. Optimization of the mass spectrometer was achieved by tuning acquisition settings while collecting data from a manually deposited control spot of the target compounds (0.5 μL of drug standard solution at approximately 2 μM manually spotted onto the ITO target with equal volume of matrix in solution. Raw data was converted to image files via processing through Mass Lynx (version 4.1, Waters Corporation, U.K.), then viewed in HDI Imaging software (version 1.2, Waters Corporation, U.K.). Data was normalized by total ion current, and subsequent image analysis was performed. Mass filter windows were selected with a precision of ±0.04 Da.

Preparation of Brain Homogenates. Brain homogenates were prepared by adding deionized water to one cerebral hemisphere at a 3:1 v/w ratio in a Precellys CK28 7 mL tissue homogenizing tube (KT03961-11302.7) and subjecting to rapid multidirectional motion using a Precellys Evolution homogenizer (Bertin Technologies, Montigney-le-Bretonneux, FR). Following homogenization, identical protocols were used for plasma and brain analysis.

Preparation of Calibration Standards and Quality Controls. Calibration (Cal) (0.300−300 nmol/L) and quality

control (QC) (0.900, 12, 240 nmol/L) samples were prepared by serial dilution of separate 2 mM DMSO stock solutions in either control plasma or control brain homogenate. Cal samples were prepared fresh on the day of analysis; QC samples were prepared in advance and stored at −20 °C alongside homogenized test samples whereby being subjected to the same freeze/thaw cycle.

Bioanalytical Method. On the day of analysis 30 μL of test, Cal, or QC sample was subjected to protein precipitation with 90 μL of acetonitrile containing 1 μg/mL of the assay internal standard, rosuvastatin. Following mixing and centrifugation 50 μL of the resulting supernatant was transferred to the well of a 96 deep well plate containing 150 μL of 0.1% v/v formic acid (aq).

Amounts of 10 μL of the resulting extracts were injected onto a gradient UHPLC system (Acquity, Waters, Milford, U.S.A.) comprising 0.1% v/v formic acid (aq) as mobile phase A, 0.1% v/v formic acid in acetonitrile as mobile phase B and an Acquity BEH C18 1.7 μM 2.1 mm × 50 mm i.d. column (Waters) as the stationary phase. Detection was performed using an API5000 (Applied Biosystems Sciex, Framingham, U.S.A.) mass spectrometer operating in multiple reaction monitoring mode (MRM) with an electrospray ionization source (ESI). The mass transitions monitored for compounds dosed orally were m/z 420.2 > 320.9 and 332.1 > 286.1 for AZD4017 and MK-0916. The mass transitions monitored for compounds dosed intravenously were m/z 422.1 > 148.1 and 288.1 > 90.9 for AZD8329 and SCH23390. The internal standard, rosuvastatin, was measured using a transition of 482.2 > 269.4.

Analyte/internal standard peak area ratios were calculated and the calibration data fitted using a linear regression with a 1/$X2$ weighted fit. Test and QC sample concentrations were back-calculated from the fitted line. Analytical batches was considered acceptable if 75% of the calibration levels fell within 15% of their nominal concentrations and a minimum of four out of six of the back-calculated QC samples fell within 15% of their nominal concentrations.

■ RESULTS AND DISCUSSION

Selection of Compounds. Compounds (Figure 1) were selected based upon historical rat brain homogenate concentration data. In these historical data AZD4017 and AZD8329 had a brain/plasma concentration ratio of 0.01 and 0.02, respectively (Table 1), at 10 min post dose. This value is extremely low and is indicative of compounds that are poorly penetrative, the measured concentration in brain (0.07 and 0.10 μM for AZD4017 and AZD8329, respectively) being attributed to residual blood contamination in the tissue.

MK-0916 and SCH23390 had a brain/plasma concentration ratio of 0.8 and >1.0, respectively (Table 1), at 10 min post dose, indicating that the compounds are brain penetrative. Correspondingly high concentrations were observed in the brain homogenates (9.1 and 1.5 μM for MK-0916 and SCH23390, respectively).

Oral and intravenous cassette doses each containing a brain penetrative and a brain nonpenetrative compound (based on homogenization data) were dosed to cover the extreme ranges likely to be encountered in pharmaceutical research and to highlight the advantages that LESA-MSI could bring over conventional homogenization methods.

Oral Study. MK-0916 and AZD4017 were dosed orally in the same cassette as examples of brain penetrative and
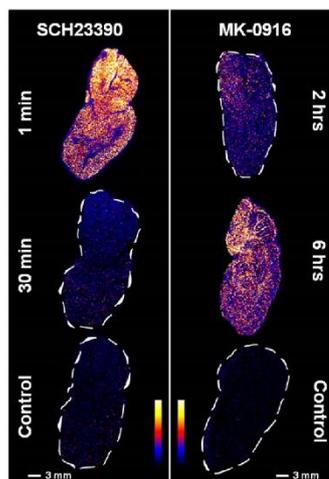
Figure 1. MALDI-MSI images of SCH23390 and MK-0916 distribution in brain tissue at different time points. SCH23390 intensity was high in the 1 min post dose sample but indistinguishable from the response given in control in the 30 min sample. MK-0916 signal intensity was higher in the 6 h sample than in the 2 h sample reflecting the pharmacokinetics of the drug.

nonpenetrative compounds. Initial analysis by our primary imaging technique, MALDI-MSI (Figure 1), showed high exposure to MK-0916 (Figure 1), the compound was homogeneously distributed across the 2 h brain section. There was a clear differentiation in signal intensities between the 2 h section and the 6 h section, with the 2 h section giving a mean signal intensity across the tissue around 40% lower than the mean signal intensity observed in the 6 h section. This was consistent with previously acquired plasma pharmacokinetic data (data not shown) which showed a T_{max} of between 3 and 6 h for MK-0916. Signal intensity in the 6 h section showed some localization of the drug (at 100 μm spatial resolution) in the pons and medulla oblongata regions of the brain, with

homogeneous distribution throughout the remainder of the tissue.

AZD4017 in the brain tissue was undetected by MALDI-MSI despite having given a good response off-tissue during ionization testing using a variety of different matrixes and mass spectrometer modes (MS and MS/MS). Various unsuccessful homogeneous coatings were attempted, including wetter coatings which would closer simulate manual matrix spotting used during tissue profiling experiments.[27] However, the target compound could still not be detected. This could be due to various reasons such as poor on-tissue analyte extraction during MALDI matrix application or ion suppression caused by endogenous compounds and salts in the tissue but was attributed to the technique having insufficient sensitivity to detect the low levels of the drug that were in the samples. The failure of MALDI-MSI to detect the drug provided an opportunity to analyze the orally dosed sections using LESA-MSI and to examine usefulness of the increased sensitivity at the expense of decreased spatial resolution.

LESA-MSI was performed on adjacent tissue sections to those used for MALDI-MSI at a spatial resolution of 1000 μm. MK-0916 exposure in both the 2 h (Figure 2e) and 6 h (Figure 2f) sections reflected the observations in the MALDI analysis with clear differentiation between the time points, the 6 h sample giving a significantly higher mean signal intensity than the 2 h sample. Initial assessment of the 6 h image with the pixel color applied on a linear scale failed to reveal any localization of MK-0916; this was dissimilar to the MALDI-MSI analysis which showed increased signal intensity in the lower rear area of the brain. It was hypothesized that this was due to the homogeneous high signal intensity across the tissue section. The LESA-MSI data was subsequently reprocessed using a logarithmic scale, allowing greater differentiation between the high signal intensity pixels throughout the tissue section and revealing the localization of the drug in the pons and medulla oblongata regions of the brain that were visible in the MALDI-MSI analysis.

Table 1. Table Showing the Structures, Transitions, and Homogenate-Derived Brain/Plasma Ratios of Compounds Used in the Studies Showing a Clear Difference in the Brain Penetration Profiles of the Drugs

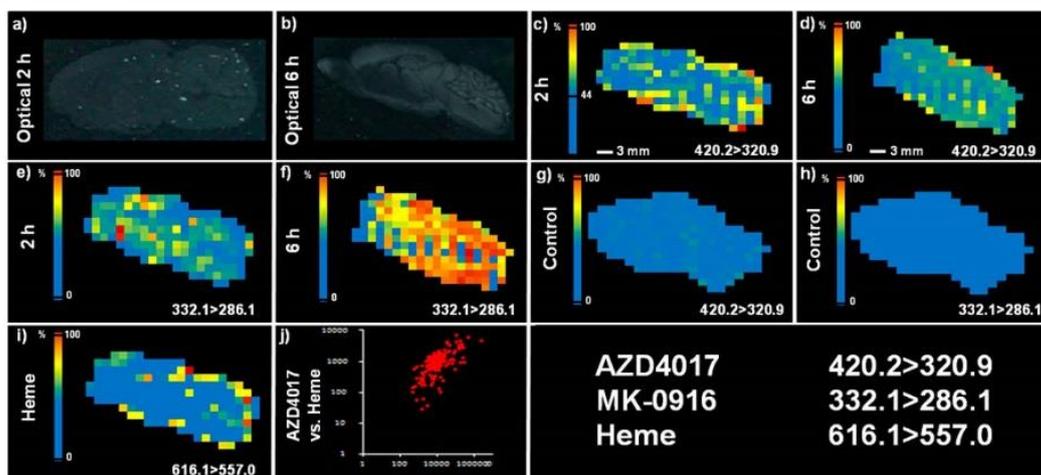| Compound	Structure	Parent	Product	Plasma Conc (μM)	Brain Conc (μM)	Brain:Plasma Ratio	Penetrative
MK-0916		332.1	286.1	11.7	9.1	0.8	Yes
AZD4017		420.2	320.9	5.2	0.1	0.01	No
SCH23390		288.1	90.9	1.0	1.5	1.5	Yes
AZD8329		422.1	147.1	4.8	0.1	0.02	No
AZx		426.2	127.2	7.0	0.1	0.01	No

Figure 2. LESA-MSI images of brain tissue sections showing the distribution after oral dosing of AZD4017 (thresholded to 44% to better display the compounds distribution in tissue) at (c) 2 h and (d) 6 h with a corresponding image (g) in control tissue at 2 h post dose. MK-0916 distribution can be seen at (e) 2 h, and (f) 6 h post dose, with a corresponding image in control tissue (h) at 2 h post dose. Heme distribution (i) is displayed in the 2 h dosed tissues. Panel j shows the correlation of AZD4017 vs heme. Panels a and b show representative optical images of the tissue sections prior to analysis.
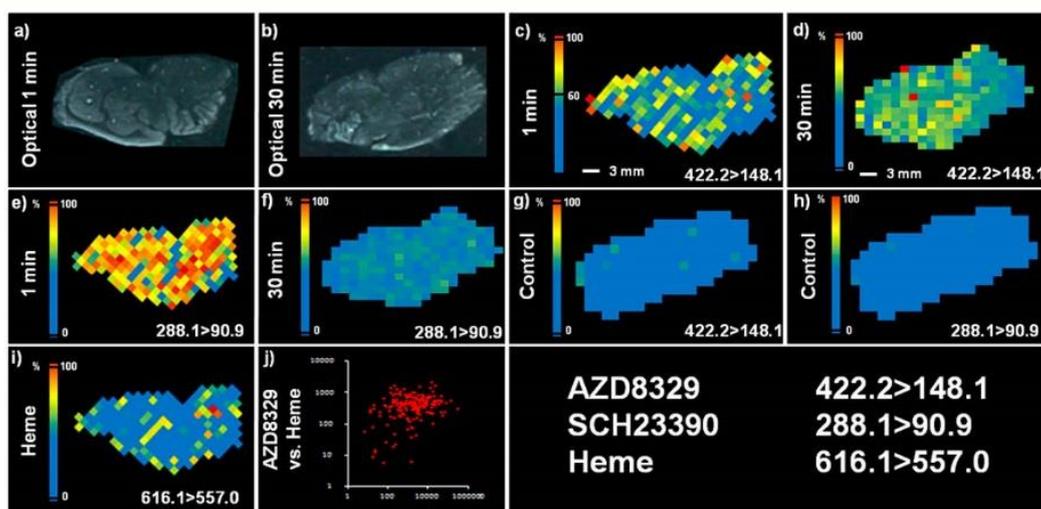

Figure 3. LESA-MSI images of brain tissue sections showing the distribution after intravenous dosing of AZD8329 (thresholded to 60% to better display the compounds distribution in tissue) at (c) 1 min and (d) 30 min with a corresponding image (g) in control tissue at 30 min post dose. SCH23390 distribution can be seen at (e) 1 min and (f) 30 min post dose, with a corresponding image in control tissue (h) at 30 min post dose. Heme distribution (i) is displayed in the 1 min dosed tissues. The correlation of AZD8329 vs heme (j) is presented. Panels a and b show representative optical images of the tissue sections prior to analysis. All images are configured to ensure brain slices are displayed in the same orientation.

AZD4017 signal intensity in the same cassette-dosed brain sections was much lower than those observed for MK-0916. Although AZD4017 signal intensity was markedly higher than the intensity observed in vehicle-dosed sections, it was difficult to visually distinguish between penetration of compound into brain tissue (Figure 2c) and the response attributed to residual blood contamination (Figure 2i). One of the advantages of using LESA-MSI is that it can be used in a multiplex mode, where many different mass transitions are tuned into the mass spectrometer and can be used in any subsequent data acquisition. The mass transition for heme (m/z 616.1 > 557.0) was acquired alongside the MK-0916 and AZD4017 as a surrogate marker for residual blood (Figure 2i), essentially giving an analyte signal intensity and a heme signal intensity in

each pixel of the images. Using these data it is possible to plot AZD4017 and heme signal intensities against each other and to visualize the correlation between the two (Figure 2j). The analysis gave a correlation coefficient R of 0.6869 suggesting that there is a relationship between AZD4017 and heme, although subsequent examination of the images shows the compound is homogeneously distributed throughout the brain tissue at both the 2 and 6 h time point in areas where there is little or no heme, inferring that the compound is poorly penetrant. This result would be at odds with the homogenization data which concluded that the compound was "nonpenetrant" and highlights the benefits a sensitive and multiplex technique such as LESA-MSI can bring to the analysis of marginally penetrative compounds.

Intravenously Study. SCH23390 and AZD8329 were dosed intravenously in the same cassette as examples of brain penetrative and nonpenetrative compounds. Brain sections after intravenous dosing showed high exposure of SCH23390 (Figure 1) when analyzed by MALDI-MSI. The compound was distributed throughout the tissue sections with greater signal intensity being observed in the rear portion of the brain (cerebellum and pons/medulla oblongata regions). A clear differentiation was observed between the 1 and 30 min brain sections with the 1 min sample giving a mean signal intensity across the tissue of around 10-fold greater than the mean intensity observed across the 30 min section. This result was expected due to the rapid elimination half-life of the compound (25 min in rat). On further examination, the MALDI-MSI data at 30 min post dose was similar to the result observed in vehicle-dosed tissue, indicating that the technique was not sensitive enough to detect the compound at these levels.

AZD8329, a compound with a similar chemical structure to AZD4017 (Table 1) dosed in the oral study, was undetected in brain tissue at 1 and 30 min post dose by MALDI-MSI. Various different MALDI matrixes and mass spectrometer modes were explored. Failure to detect the compound could be due to levels of AZD8329 in the brain tissue being below the limit of detection of the MALDI-MSI technique. This presented another opportunity to analyze the samples using LESA-MSI and to examine the use of improved sensitivity at the expense of spatial resolution.

LESA-MSI detected both SCH23390 and AZD8329 in the brain samples. SCH23390 gave a strong signal in the 1 min time point (Figure 3e) with the compound exhibiting a homogeneous distribution across the tissue section. SCH23390 was also detected at much lower levels in the 30 min sample (Figure 3f) than those observed at 1 min with clear differentiation from the response observed in the control. Similarly AZD8329 was detected at low levels in both the 1 min (Figure 3c) and 30 min (Figure 3d) samples; once again this response was clearly greater than the response observed in vehicle-dosed control sections (4-fold greater), again highlighting the sensitivity of LESA-MSI. The signal intensity was consistent and homogeneous across the two time points indicating that the compound is poorly penetrant. This was in line with data generated in previous intravenous experiments (data not shown) that observed a small change in systemic plasma concentration between the 1 and 30 min time points ($n = 4$).

A plot of the AZD8329 and heme signal intensities showed a relatively poor correlation, with a correlation coefficient of $R = 0.0200$. This lack of correlation combined with the homogeneous distribution observed when the image threshold is set to 100% indicates that AZD8329 penetrates into brain tissue at low levels and that the response is not linked to residual blood contamination, a result that was missed by tissue homogenization.

Application in AZ Drug Projects. After the initial LESA-MSI brain penetration experiments the technique was applied to live AstraZeneca (AZ) projects. AZx (Table 1) is a compound that is currently of interest within the cardiovascular and metabolic diseases therapeutic area within AZ. The compound is a triazine analogue with a logD of 2.1. The compound has a brain/plasma ratio of 0.01 based on concentrations of 0.1 and 7 μM in brain homogenate and plasma, respectively. This brain/plasma ratio is very low and indicative of a poorly penetrative compound, the response

being attributed to residual blood contamination in the brain homogenate. LESA-MSI analysis (Figure 4e) revealed local-
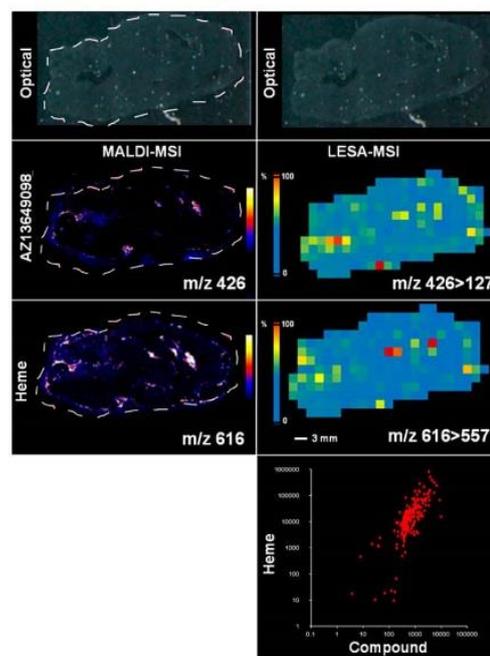

Figure 4. Figure showing the distribution of AZx and heme in rat brain tissue sections analyzed by MALDI-MSI (b and c) and LESA-MSI (e and f). The similarities between the distribution from the two different techniques can be clearly seen. The LESA-MSI data shows a clear correlation (g) between AZx signal intensity and heme intensity.

ization of AZx at various hot spots across the sagittal brain section. The compound distribution correlated well with heme (Figure 4f), giving a correlation coefficient of $R = 0.7681$, indicating the compound had a reasonably strong relationship with the residual blood in the section (Figure 4g). In addition to this the compound was not detected in areas of the brain tissue which did not contain heme indicating that the compound has very poor brain penetration.

Adjacent tissue sections were subsequently analyzed using MALDI-MSI analysis (Figure 4b) to further validate the LESA-MSI technique. Co-localization of AZx with heme (Figure 4c) was confirmed at 100 μm spatial resolution. This result was interesting as it implies that LESA-MSI could be used to highlight localization of drug in tissue even at 1 mm spatial resolution.

■ CONCLUSIONS

Liquid extraction surface analysis has traditionally been used for profiling of discrete points across tissue sections. Here we have demonstrated that the technique is applicable to low-resolution mass spectrometry imaging to highlight compound distribution in tissue sections.

The work presented here has shown that LESA-MSI has many advantages over traditional methods of analysis such as tissue homogenization. The multiplex nature of mass spectrometry allows simultaneous capture of many different mass transitions, e.g., drug and heme, which when coupled with the spatial resolution that is inherent in LESA allows distinction between real compound penetration and that which would

normally be attributed to residual blood contamination. LESA-MSI has also been shown to be highly sensitive and has the ability to cover a wide chemical scope due to being built around electrospray ionization, positioning it as a complementary technique to MALDI-MSI, offering lower spatial resolution results where MALDI, our primary analytical technique, cannot deliver the sensitivity needed or where excessive matrix identification may lead to long delays.

While we have shown that LESA-MSI is good at distinguishing brain penetrative compounds and distinguishing between penetration and residual blood contamination, a disadvantage of the technique and indeed all mass spectrometry imaging based techniques is that the conclusion can never be made that a compound is completely nonpenetrative. Even at the highest spatial resolution MSI could not confirm penetration of drug into the cells surrounding the brain vasculature. Furthermore, all techniques have a limit of detection; just because a compound is undetected does not mean there is no compound present. MSI techniques can, however, provide some reassurance that brain penetration is minimal. Another important consideration for the scientist is that mass spectrometry imaging techniques highlight regions of total drug concentration and do not differentiate between protein-bound drug and free drug which is needed to have a pharmacological effect.

It is believed that LESA-MSI techniques can be further developed in terms of higher spatial resolution, absolute quantitation, and the ability to capitalize on the multiplex approach of mass spectrometry to encompass simultaneous measurement of endogenous small molecule and neuropeptide changes in the brain post drug administration as an indication of efficacy and target engagement.

■ AUTHOR INFORMATION

Corresponding Author

*E-mail: john.swales@astrazeneca.com. Phone: +44 0 1223 223417.

Notes

The authors declare no competing financial interest.

■ REFERENCES

(1) Rönquist-Nii, Y.; Edlund, P. O. *J. Pharm. Biomed. Anal.* **2005**, *37*, 341–350.

(2) McNally, W.; Roth, M.; Young, R.; Bockbrader, H.; Chang, T. *Pharm. Res.* **1989**, *6*, 924–932.

(3) Solon, E.; Balani, S.; Lee, F. *Curr. Drug Metab.* **2002**, *3*, 451–462.

(4) Caprioli, R. M.; Farmer, T. B.; Gile, J. *Anal. Chem.* **1997**, *69*, 4751–4760.

(5) Todd, P. J.; Schaaff, T. G.; Chaurand, P.; Caprioli, R. M. *J. Mass Spectrom.* **2001**, *36*, 355–369.

(6) Takáts, Z.; Wiseman, J. M.; Gologan, B.; Cooks, R. G. *Science* **2004**, *306*, 471–473.

(7) Nemes, P.; Vertes, A. *Anal. Chem.* **2007**, *79*, 8098–8106.

(8) Bunch, J.; Clench, M. R.; Richards, D. S. *Rapid Commun. Mass Spectrom.* **2004**, *18*, 3051–3060.

(9) Hsieh, Y.; Chen, J.; Korfmacher, W. A. *J. Pharmacol. Toxicol. Methods* **2007**, *55*, 193–200.

(10) Nilsson, A.; Fehniger, T. E.; Gustavsson, L.; Andersson, M.; Kenne, K.; Marko-Varga, G.; Andrén, P. E. *PLoS One* **2010**, *5*, e11411.

(11) Stoeckli, M.; Staab, D.; Schweitzer, A. *Int. J. Mass Spectrom.* **2007**, *260*, 195–202.

(12) Eikel, D.; Vavrek, M.; Smith, S.; Bason, C.; Yeh, S.; Korfmacher, W. A.; Henion, J. D. *Rapid Commun. Mass Spectrom.* **2011**, *25*, 3587–3596.

(13) Kertesz, V.; Van Berkel, G. J. *J. Mass Spectrom.* **2010**, *45*, 252–260.

(14) Edwards, R. L.; Creese, A. J.; Baumert, M.; Griffiths, P.; Bunch, J.; Cooper, H. J. *Anal. Chem.* **2011**, *83*, 2265–2270.

(15) Alavijeh, M. S.; Chishty, M.; Qaiser, M. Z.; Palmer, A. M. *NeuroRx* **2005**, *2*, 554–571.

(16) Subaiea, G. M.; Alansi, B. H.; Serra, D. A.; Alwan, M.; Zawia, N. H. *Curr. Alzheimer Res.* **2011**, *8*, 860–867.

(17) Dietz, G. P.; Valbuena, P. C.; Dietz, B.; Meuer, K.; Müller, P.; Weishaupt, J. H.; Bähr, M. *Brain Res.* **2006**, *1082*, 61–66.

(18) Juillerat-Jeanneret, L. *Drug Discovery Today* **2008**, *13*, 1099–1106.

(19) Goldberg, F. W.; Dossetter, A. G.; Scott, J. S.; Robb, G. R.; Boyd, S.; Groombridge, S. D.; Kemmitt, P. D.; Sjögren, T.; Gutierrez, P. M.; deSchoolmeester, J.; Swales, J. G.; Turnbull, A. V.; Wild, M. J. *J. Med. Chem.* **2014**, *57*, 970–986.

(20) Moran, T. H.; Dailey, M. J. *Endocrinology* **2009**, *150*, 2526–2530.

(21) Ledeboer, A.; Hutchinson, M. R.; Watkins, L. R.; Johnson, K. W. *Expert Opin. Invest. Drugs* **2007**, *16*, 935–950.

(22) Receveur, J.-M.; Murray, A.; Linget, J.-M.; Nørregaard, P. K.; Cooper, M.; Bjurling, E.; Nielsen, P. A.; Högberg, T. *Bioorg. Med. Chem. Lett.* **2010**, *20*, 453–457.

(23) Ooie, T.; Terasaki, T.; Suzuki, H.; Sugiyama, Y. *J. Pharmacol. Exp. Ther.* **1997**, *283*, 293–304.

(24) Liu, X.; Ide, J. L.; Norton, I.; Marchionni, M. A.; Ebling, M. C.; Wang, L. Y.; Davis, E.; Sauvageot, C. M.; Kesari, S.; Kellersberger, K. A.; Easterling, M. L.; Santagata, S.; Stuart, D. D.; Alberta, J.; Agar, J. N.; Stiles, C. D.; Agar, N. Y. R. *Sci. Rep.* **2013**, *3*, 2859.

(25) Swales, J. G.; Tucker, J. W.; Strittmatter, N.; Nilsson, A.; Cobice, D.; Clench, M. R.; Mackay, C. L.; Andren, P. E.; Takáts, Z.; Webborn, P. J.; Goodwin, R. J. A. *Anal. Chem.* **2014**, *86*, 8473–8480.

(26) Goodwin, R. J.; Dungworth, J. C.; Cobb, S. R.; Pitt, A. R. *Proteomics* **2008**, *8*, 3801–3808.

(27) Caldwell, R. L.; Caprioli, R. M. *Mol. Cell. Proteomics* **2005**, *4*, 394–401.

5.0 SPATIAL QUANTITATION OF DRUGS IN TISSUES USING LIQUID EXTRACTION SURFACE ANALYSIS MASS SPECTROMETRY IMAGING

Swales, J. G.; Strittmatter, N.; Tucker, J. W.; Clench, M. R.; Webborn, P. J.; Goodwin, R. J., Spatial quantitation of drugs in tissues using liquid extraction surface analysis mass spectrometry Imaging. *Scientific reports* **2016, *6*, 37648.**

Author Contribution

JGS designed the quantitation studies, aided necropsy, performed all method development and proof of concept, sample preparation, performed all LESA and DESI qMSI imaging experiments, performed all homogenisation analysis, processed all data, interpreted results and prepared the manuscript for publication.

SCIENTIFIC REP⚙RTS

Spatial Quantitation of Drugs in tissues using Liquid Extraction Surface Analysis Mass Spectrometry Imaging

John G. Swales[1,2], Nicole Strittmatter[1], James W. Tucker[1], Malcolm R. Clench[2], Peter J. H. Webborn[1] & Richard J. A. Goodwin[1]

Liquid extraction surface analysis mass spectrometry imaging (LESA-MSI) has been shown to be an effective tissue profiling and imaging technique, producing robust and reliable qualitative distribution images of an analyte or analytes in tissue sections. Here, we expand the use of LESA-MSI beyond qualitative analysis to a quantitative analytical technique by employing a mimetic tissue model previously shown to be applicable for MALDI-MSI quantitation. Liver homogenate was used to generate a viable and molecularly relevant control matrix for spiked drug standards which can be frozen, sectioned and subsequently analyzed for the generation of calibration curves to quantify unknown tissue section samples. The effects of extraction solvent composition, tissue thickness and solvent/ tissue contact time were explored prior to any quantitative studies in order to optimize the LESA-MSI method across several different chemical entities. The use of a internal standard to normalize regional differences in ionization response across tissue sections was also investigated. Data are presented comparing quantitative results generated by LESA-MSI to LC-MS/MS. Subsequent analysis of adjacent tissue sections using DESI-MSI is also reported.

A drugs distribution and the relationship with efficacy and safety are important considerations during drug development. It is crucial that a compound is present in sufficient quantity at the site of action to deliver efficacy. Equally, excessive abundance of the drug in tissues may lead to unwanted toxicological findings rendering the drug unsafe.

Drug distribution has historically been assessed in various ways. Tissue homogenization techniques, coupled to liquid chromatography and mass spectrometry have been the mainstay to quantify drugs in tissues[1]. However, this approach results in the loss of all spatial information from the sample and merely provides an average concentration within the tissue. There is also a risk of variation caused by residual blood contamination.

Mapping and quantifying the distribution of compounds *in vivo* was historically performed using radiolabeled compounds in techniques such as quantitative whole body autoradiography (QWBA)[2,3]. The technique is reliable, sensitive, quantitative and retains meaningful spatial information. However, the necessity for a radiolabeled compound is a major drawback that can lead to significant 'synthesis' delays. Furthermore, quantitation of the parent drug can be misrepresented due to drug metabolites that still include the radiolabel.

Mass spectrometry imaging (MSI) is a complementary, viable, multiplex and label free way of elucidating the distribution of drugs and endogenous metabolites directly from the surface of tissue sections[4]. MSI is a term used to describe a group of complementary surface sampling technologies based on different mass spectrometry ionization methods. The most commonly used are matrix assisted laser desorption ionization (MALDI-MSI)[5–7], secondary ion mass spectrometry (SIMS-MSI)[8], desorption electrospray ionization (DESI-MSI)[9,10] and nano-electrospray ionization based liquid microjunction techniques such as liquid extraction surface analysis (LESA-MSI)[11,12]. Each technique has innate advantages and disadvantages in sensitivity, speed and spatial resolution.

[1]Drug Safety & Metabolism, AstraZeneca R&D, Cambridge Science Park, Cambridge, CB4 0WG, UK. [2]Biomolecular Sciences Research Centre, Sheffield Hallam University, Howard Street, Sheffield S1 1WB, UK. Correspondence and requests for materials should be addressed to J.G.S. (email: john.swales@astrazeneca.com)

MALDI-MSI and more recently DESI-MSI have been gaining popularity within the pharmaceutical industry as scientifically and economically feasible technology platforms to assess drug distribution. MALDI-MSI is capable of delivering images at low micron spatial resolution[13], a drawback however is that it is not easily applicable to all analytes often requiring lengthy matrix optimization or on-tissue chemical derivatization to ensure detection[14]. DESI-MSI is an electrospray ionization based technique and thus has a much wider chemical scope. Spatial resolution is more limited than MALDI-MSI, typically around 50–100 μm. SIMS-MSI is again limited in chemical scope, high energy ionization and the technique being combined with low spectral resolution mass analyzers make it unsuitable for the analysis of medium and high size molecules. SIMS-MSI is capable of nanometer spatial resolution, however the technique has not been widely adopted within the pharmaceutical industry, primarily due to high set up costs and the availability of the technique within academia as a fee for service answer to bespoke distribution questions. LESA-MSI is a surface sampling technique that has been shown to be widely applicable and sensitive but can deliver only low spatial resolution images (typically 1000 μm)[11]. The technique can be combined with Orbitrap or time of flight mass spectrometers for effective use as a profiling tool[15] but has also been used effectively with high sensitivity triple quadrupole mass spectrometers operated in selected reaction monitoring mode for mass spectrometry imaging[16].

All of the above techniques provide relatively fast and reliable qualitative localization information that can be used to show drug distribution to target tissues or drug accumulation in tissues where a toxic effect has been observed. However this data is of a qualitative nature only and as such is often hard to put into context and difficult to draw meaningful conclusions from without a quantitative determination of the drug levels within the tissues. Quantitative MSI methods for drugs have been widely reported, most prevalently for MALDI-MSI[17]. Groseclose and Castellino published a report based on the use of tissue mimetics for the quantitation of drug compounds in liver tissue sections using MALDI-MSI[18]. Likewise, Nilsson *et al.* published MALDI-MSI data showing the quantitation of tiotropium in rat lung tissue utilizing calibration standard spotting on control tissue[19]. Other reported techniques employ the use of internal standards to normalize differences in ionization efficiency across tissue sections[20,21]. Quantitative methods have also been published for nano-DESI-MSI[22] based on similar techniques as those employed in MALDI-MSI.

The research presented here details a quantitative LESA-MSI method using tissue mimetics for the quantitation of various drugs in tissue sections. Details of method optimization are reported. The quantitative LESA-MSI method was directly compared to results obtained by traditional LC-MS/MS tissue homogenization analysis and to results generated by DESI-MSI analysis.

Methods

Materials and reagents. Analytical grade acetonitrile, methanol and formic acid were obtained from Fisher Scientific (Loughborough, Leicestershire, UK). 2-methylbutane was obtained from Sigma-Aldrich (Poole, Dorset, UK). Test compounds were obtained in house from AstraZeneca compound management group (Macclesfield, Cheshire, UK) with the exception of moxifloxacin and SCH-23390 which were purchased from Sigma-Aldrich (Poole, Dorset, UK) and clozapine-d4 which was purchased from Qmx Laboratories (Thaxted, Essex, UK).

Animals. Adult male Hans Wistar rats (approximate weight 260 g) were obtained from Charles River Laboratories (Margate, Kent, UK) and were acclimatized on site for a minimum of 3 days prior to dosing. Compounds were administered by oral gavage and were formulated in 5% dimethylsulfoxide/95% (30% w/v Captisol in water). Control animals were dosed with vehicle via the same administration route.

The study was performed under project license 40/3484, procedure number 10 and was reviewed and approved by the Institutional Animal Welfare and Ethical Review Body within AstraZeneca and was conducted in accordance with the animal care and ethics described in "Guidance on the Operations of the Animals (Scientific Procedures) Act 1986" issued by the UK Home Office.

Dosing and scheduling. Liver samples were taken from 1 animal dosed with vehicle, 2 animals dosed discretely with olanzapine (10 mg/kg), and 2 cassette dosed animals (Moxifloxacin, olanzapine, erlotinib and terfenadine at 25, 10, 10 and 25 mg/kg respectively). Animals were euthanized at either 2 or 6 hrs post dose.

All tissue dissection was performed by trained AstraZeneca staff. Liver samples were harvested at termination and snap-frozen in 2-methylbutane on dry-ice, subsequent transfer of tissues was done on dry-ice and samples were stored at −80 °C until tissue processing.

Tissue processing. Tissue sections were cryosectioned at a thickness of 14 μm and thaw mounted onto indium tin oxide (ITO) coated MALDI target slides (Bruker Daltonics, Bremen, Germany) for LESA analysis (ITO slides are not essential for LESA analysis but are used as standard within our laboratories to allow sections to be analyzed by either LESA or MALDI) and Superfrost slides (Fisher Scientific) for DESI analysis. Sections were taken at approximately equal depth from all samples. Mimetic calibration standards were thaw mounted onto the slide prior to the dosed unknowns in a semi random order to mitigate the risk of bias caused by duration on slide (mounting order - blank, 1, 20, 0.1, 5, 50, 0.5, 10, 100 nmol/g). Tissue sections from dosed and control animals were randomly thaw-mounted on the same slides (order cassette 2 h, discrete 2 h, control, cassette 6 h, discrete 6 h). Mounted tissue sections, were stored at −80 °C until analysis.

Preparation of liver mimetics. Liver mimetics were prepared by homogenizing control liver tissue using a Fisher Powergen 500 homogenizer for a minimum of 30 s at room temperature. Each 250 μL of liver homogenate was pipetted into 9 separate molds (prepared from the bottom end of a 2 mL plastic Pasteur pipette bulb) and subsequently weighed. Appropriate volumes of compound solution (containing olanzapine, moxifloxacin, erlotinib and terfenadine) were spiked into the homogenate (assuming 1 mL of standard equivalent to 1 g of tissue and

not accounting for density differences) to form liver homogenate calibration standards at 0, 0.1, 0.5, 1, 5, 10, 20, 50 and 100 nmol/g. The homogenates were then frozen at −80 °C for a minimum of 1 h prior to cryosectioning.

LESA Optimization experiments. *Extraction solvent composition.* Three solvents were used (acetonitrile (ACN), methanol (MeOH) and isopropyl alcohol (IPA)) at 4 different compositions in water (solvent content 50, 60, 70 and 80%), each extraction solvent contained 0.1% formic acid to promote positive ionization and aide conductivity in the nanospray interface. Mimetic liver tissue containing four analytes (clozapine, albendazole, tamoxifen and astemizole) spiked at a concentration of 50 nmol/g and covering a LogD (pH 7.4) range between 2.9 and 4.09 was sectioned at a thickness of 14 μm and subsequently thaw mounted onto microscope slides. Ten LESA extractions were performed at random points across the tissue with mean signal intensity used to compare the different solvents and solvent compositions.

Tissue thickness. The effect of tissue thickness was assessed using mimetic liver tissue spiked with clozapine, albendazole, tamoxifen and astemizole at a concentration of 50 nmol/g and sectioned at 12, 25 and 50 μm thickness. Ten extractions were performed at random points across the tissue with mean signal intensity used to compare the differences between the sections.

Solvent dwell time. The effects of solvent dwell time on signal intensity were explored using mimetic liver tissue sections cut at 12, 25 and 50 μm thickness and spiked with 50 nmol/g of SCH-23390. Ten extractions were performed at random points across the tissue with mean signal intensity used to compare the differences between the sections.

Effects of internal standard. The effect of spraying a non-deuterated internal standard and a deuterated internal standard (IS) over the tissue to normalize differences in ionization response across different tissue areas was explored. A mimetic liver tissue calibration curve was constructed containing clozapine, albendazole, tamoxifen and astemizole (in cassette) at the following concentration levels 0, 0.1, 0.5, 1, 5, 10, 20, 50 and 100 nmol/g. A compound taken from the AstraZeneca compound collection that is routinely used as an internal standard in LC-MS/MS analysis was used as an non-deuterated IS (an acidic quinoline tetrazole, LogD 2.67, RMM 407.5), clozapine-d4 was used as a deuterated IS. The internal standard was sprayed over the tissue sections using a TMsprayer (HTx Technologies, Chapel Hill, North Carolina, USA). An additional experiment was performed with the clozapine-d4 spiked at 1 uM in the LESA extraction solvent. Ten LESA extractions were performed at random points across each calibration standard and the signal intensity was used to calculated a mean value and coefficient of variation for each calibration point in the presence and absence of the internal standard.

Optimized LESA quantitative mass spectrometry imaging. LESA MSI was performed using LESA-MS/MS on a Triversa Nanomate chip based electrospray ionization system (Advion, Ithaca, NY, USA) coupled to a QTRAP 5500 (AB Sciex, Framingham, MA, USA) mass spectrometer operated in positive ion MRM mode. The LESA sampling method consisted of aspiration of a 0.9 μL volume of extraction solution (Acetonitrile/water/Formic Acid 60/40/0.1 v/v/v). 0.5 μL of the solution was then dispensed at a height of 0.4 mm above the tissue with a 3 s post dispense delay time, a liquid micro junction between the pipette tip and the sample was maintained throughout the procedure. 1.1 μL of sample was re-aspirated into the pipette tip prior to infusion via the nanomate chip for MS/MS analysis. Relative abundance was determined between samples by comparison of MRM transition intensity at m/z 326.9 > 269.8, 266.1 > 234.3, 372.0 > 71.9 and 459.1 > 218.0 for clozapine, albendazole, tamoxifen and astemizole and 472.3 > 436.2, 313.1 > 256.1, 402.2 > 358.1 and 394.2 > 278.0 for terfenadine, olanzapine, moxifloxacin and erlotinib respectively. LESA-MS/MS data was processed using a purpose built software package capable of extracting relative abundance values from Analyst 6.1 (ABSciex, Framingham, MA, USA).

LESA-MS/MS images were created using in-house developed software capable of colour grading ion intensities acquired from each individual LESA spot in a heat map configuration fixing the colour scale at maximum for the highest intensity response in the spot and scaling the colour intensity down accordingly relative to the maximum.

Analysis of liver homogenates by LC-MS/MS. Experimental procedures for the preparation of liver homogenates, calibration standards and quality controls and general LC-MS/MS methodologies can be found in the supplementary information.

DESI mass spectrometry imaging. DESI MSI analysis was performed using a Q-Exactive mass spectrometer (Thermo Fisher Scientific Inc., Bremen, Germany) operated in positive ion mode. The mass spectrometer was equipped with an automated Prosolia 2D DESI source (Indianapolis, IN, USA). Mass spectra were collected in the mass range of m/z 200–600 at a mass resolution of 140,000 (at m/z 200). Methanol/water (95:5 v/v) was used as the electrospray solvent held at 4.5 kV spray voltage and delivered at a flow-rate of 1.5 μL/min by a Dionex Ultimate 3000 nanoLC pump (Thermo Fisher Scientific). Nitrogen was used as nebulising gas at a pressure of 7 bars. The height distance between the DESI sprayer and the sample surface was set to 1.5 mm with the distance between the sprayer and the inlet capillary set to 7 mm. The distance between the sample surface and the inlet capillary of the mass spectrometer was <1 mm. The angle between the sprayer tip and the sample surface was set at 750°. Spatial resolution for the imaging experiment was set to 125 μm with 173.61 μm/s scan speed at an injection time of 150 ms per spectrum. Individual horizontal line scans were combined into imzML format using the imzML converter V.1.1.4.5 (www.maldi-msi.org). Data visualization and region of interest extraction was performed using MSiReader v0.05[23]. Intensity data was extracted for each pixel within a region of interest and
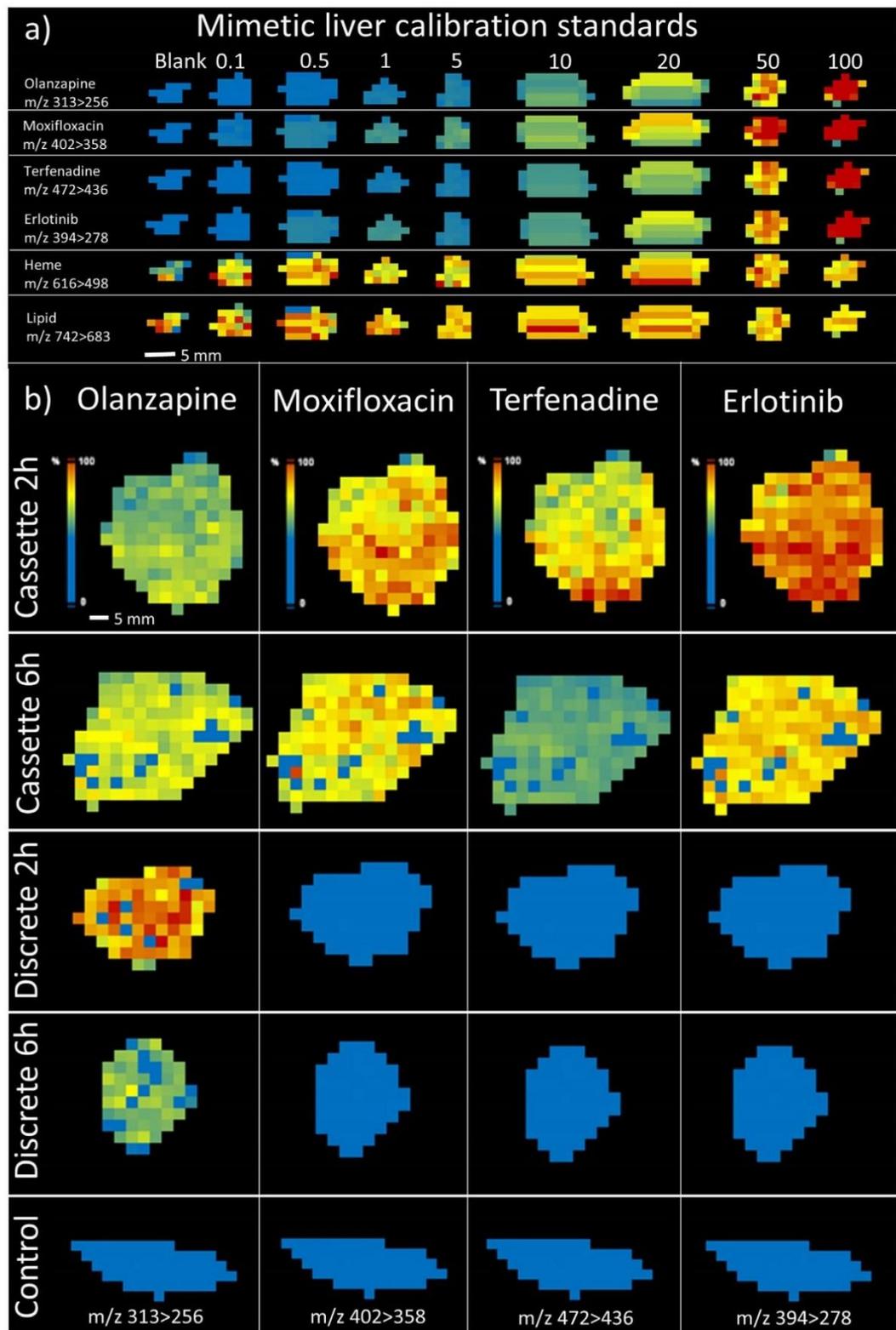
Figure 1. (a) LESA-MSI images of olanzapine, moxifloxacin, terfenadine and erlotinib in mimetic liver calibration standards showing the increasing intensity throughout the calibration range. Heme and a generic lipid marker are included to show the contrast between a spiked and endogenous response (b) LESA-MSI images of dosed rat liver tissue sections showing the distribution of olanazapine, moxifloxacin, terfenadine and erlotinib at 2 and 6 h post dose.
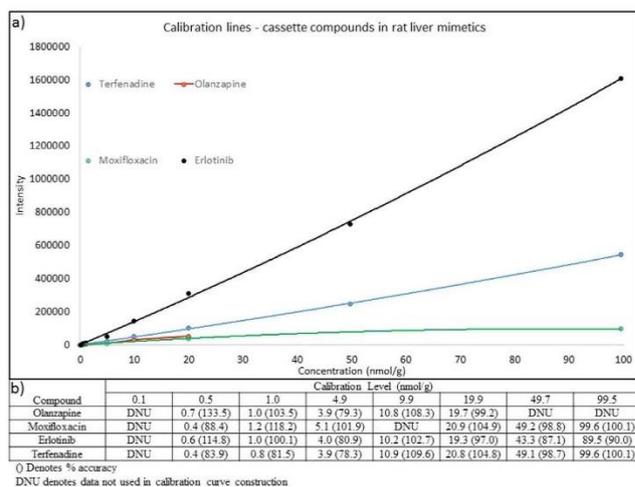
Figure 2. (**a**) Calibration curves of Olanzapine, moxifloxacin, terfenadine and erlotinib in rat liver mimetic tissue standards analyzed by LESA-MSI. (**b**) Back calculated concentrations of each calibration standard used in the construction of the calibration lines with corresponding accuracy values in parenthesis.

	Timepoint (h)											
	Cassette 2 h			Cassette 6 h			Discrete 2 h			Discrete 6 h		
Compound	LESA	Homog.	DESI	LESA	Homog.	DESI	LESA	Homog.	DESI	LESA	Homog.	DESI
Olanzapine	9.3	10.2	14.4	12.5	18.6	19.6	25.8	19.6	38.1	8.3	10.0	6.2
Moxifloxacin	15.6	14.6	10.8	12.0	12.5	16.4	—	—	—	—	—	—
Erlotinib	38.4	28.5	26.9	26.6	25.2	19.8	—	—	—	—	—	—
Terfenadine	11.9	9.0	12.0	4.0	4.7	2.8	—	—	—	—	—	—

Table 1. Comparison of back calculated concentrations (nmol/g) for compounds analyzed by LESA-MSI, homoginization and DESI-MSI.

subsequently averaged using Microsoft Excel. All images were created using 0.01 Da bin size and linear interpolation (order 1).

Results and Discussion

Prior to any quantitative LESA analysis a study was undertaken to optimize the method used in previously reported work from our laboratory[11]. The optimization experiments consisted of comparison of different extraction solvent systems, the effects of different tissue section thickness, the length of time the extraction solvent is in contact with the tissue (solvent dwell time) and the effects of using an internal standard on the analytical performance.

LESA Optimization. The solvent systems tested gave varying results. Isopropyl alcohol (SI Fig. 1a) and methanol (SI Fig. 1b) based systems gave fairly low signal intensities across all of the different solvent compositions with isopropyl alcohol mixed at 60% IPA and methanol mixed at 70% MeOH giving the best results for all of the compounds tested. 70% MeOH gave signal intensities roughly 1.5-fold higher than those observed at 60% IPA. Extractions that used 70 and 80% IPA resulted in unreliable extractions 6 out of 10 times (60%), this was due to loss of the liquid junction between the tissue and the pipette tip caused by the low surface tension in high organic content solvent systems. A greater number (8/10) of extractions failed at 80% MeOH, although at all other composition ratios the number of failed extractions was less than 2/10.

Acetonitrile based solvents systems (SI Fig. 1c) gave results with higher signal intensities. Extraction failure rates at 70 and 80% ACN were 5/10 and 6/10 respectively. Failure rates at 50 and 60% ACN were zero with 60% ACN giving the highest mean signal intensity across all of the compounds and solvent compositions tested combined with a consistently good extraction. Thus, 60% ACN with 0.1% formic acid was used as a standard extraction system in all subsequent experiments.

Liver mimetic tissue sections cut at 12, 25 and 50 μm thickness were analyzed. The effect on signal intensity was negligible across the different tissue thickness and for each of the four compounds analyzed (SI Fig. 2). Extraction failure across each of the different sections was 3/10. It was decided to use 12 μm tissue thickness for any subsequent analysis as this is the standard used for MALDI and DESI analysis within our laboratories.

Different solvent dwell times (time solvent/tissue liquid junction is maintained) were evaluated. This showed a gradual increase for the analyte SCH-23390 when moving from 1 s to 3 s dwell time (SI Fig. 3) but the signal intensity subsequently dropped moving from the 3 s dwell time to 4 s and 5 s dwell time. Extraction failure was
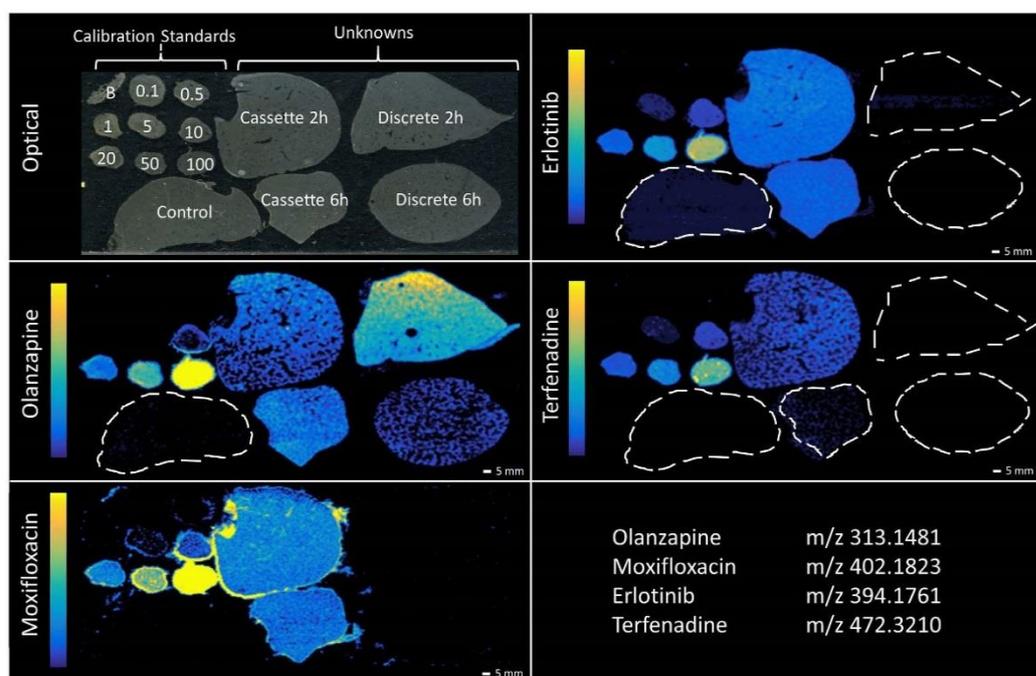
Figure 3. DESI-MSI images of olanzapine, moxifloxacin, erlotinib and terfenadine in rat liver mimetic calibration standards and rat liver 'unknown' samples. Poor detection of moxifloxacin, manifested in the compound being detected in all samples and highlighting the halo effect around the top liver mimetic tissue section.

≤1/10 across all of the dwell times in the experiment. Increasing variability with increasing dwell time resulted from the instability of the liquid junction over time for some extractions. A dwell time of 3 s was used as standard for all subsequent experiments.

Effects of using an Internal Standard. The effects of using an internal standard to normalize different ionization suppression effects across tissue has been widely reported in MALDI imaging[24,25]. Here the most commonly used approaches were reproduced using LESA-MSI and experiments were conducted in the presence of a non-deuterated IS (standard AZ internal standard used for plasma analysis) and deuterated IS (clozapine-d4), both applied over the tissue at a constant concentration. A further experiment explored the use of the deuterated internal standard spiked into the LESA extraction solution.

When a non-deuterated IS was used the co-efficient of variation across all of the compounds at each calibration point ranged between 19.5–42.5% compared to 8.6–41.8% when no IS was used indicting greater variability when the IS was present. The differences were even more apparent when each calibration level and each compound was compared directly (SI Table 1) with the IS showing a greater co-efficient of variation at all points (with the exception of Albendazole 5 nmol/g level, 26.8% no IS vs. 24.4% with IS).

The experiment was repeated using clozapine-d4 as the IS. This had a similar result showing a clozapine co-efficient of variation range of 19.3–44.0% in the absence of IS and 17.1–64.1% in the presence of the clozapine-d4 IS. When each individual calibration point is compared (SI Table 2) the variation in the presence of the clozapine-d4 is more variable at all of the calibration points with the exception of the 5 nmol/g standard, indicating the deuterated standard made the variation worse.

As an alternative to spraying the IS over the tissue sections, spiking the IS into the LESA extraction solvent was attempted. This experiment resulted in a co-efficient of variation range of 12.8–46.3 with no IS compared to 13.0–41.1% in the presence of clozapine-d4 (SI Table 3). When individual points were compared the data with the clozapine-d4 spiked into the extraction solvent was less variable at all of the points except the 0.1 and 0.5 nmol/g calibration standards which gave 12.6% no IS vs. 19.7% with IS and 40.3% no IS vs. 41.1% with IS. This result would indicate that the presence of the deuterated internal standard decreases the variation observed in the experiment and we would recommend using this approach where a deuterated internal standard is available. Deuterated standards are not usually available in the early discovery phase of pharmaceutical development and as we intended to develop a widely applicable approach it was decided to progress the quantitation experiments without an internal standard.

Quantitative LESA experiments. The objective of this study was to establish a robust and reproducible method for quantitative LESA-MSI analysis. The mimetic tissue model lends itself well to LESA-MSI analysis, offering a large enough sample area to accommodate the lower spatial resolution of the LESA technique, something that cannot easily be achieved using conventional standard spotting techniques used in higher spatial
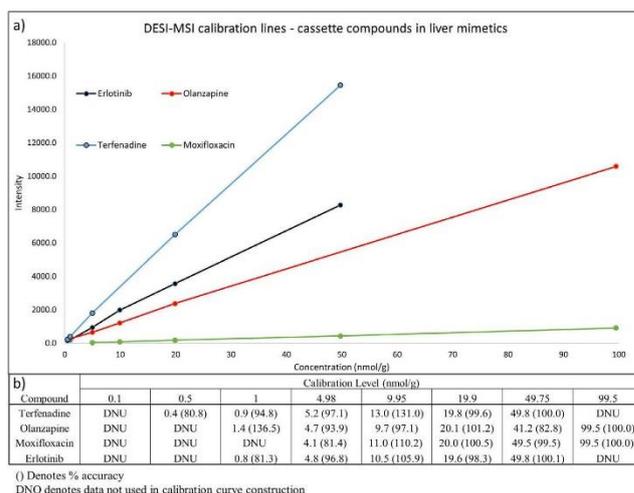
Figure 4. Calibration curves of Olanzapine, moxifloxacin, terfenadine and erlotinib in rat liver mimetic tissue standards analyzed by DESI-MSI. (b) Back calculated concentrations of each calibration standard used in the construction of the calibration lines with corresponding accuracy values in parenthesis.

resolution MALDI analysis. The mimetic tissue model utilizes un-diluted homogenized tissue in the preparation of the mimetics, presenting a control matrix for spiked standards. Here we report data to support the use of mimetic tissues for quantitative LESA-MSI and compare and contrast the results to data generated by classical tissue homogenization and analysis by LC-MS/MS and to quantitative DESI-MSI.

Quantitation of dosed rat tissues. Quantitation of olanzapine, moxifloxacin, erlotinib and terfenadine was performed on liver sections were animals had been cassette dosed at 10, 25, 10, 25 mg/kg of the compounds respectively. Liver samples were collected from rats at 2 and 6 h post dose. 2 and 6 h liver sections from rats dosed discretely with olanzapine at 10 mg/kg were also tested. Residual liver tissue was sent for homogenization analysis by LC-MS/MS. Images of the mimetic liver calibration standard sections and dosed liver sections are presented in Fig. 1. The analytes were distributed continuously but at a range of abundances throughout the liver mimetics and the dosed samples. Tissue homogeneity was visually assessed via microscope after sectioning.

The calibration curves derived from the mimetic liver calibration standards are summarized in Fig. 2a. The linearity of the response for all four analytes was acceptable with R^2 values equal to 0.9933, 0.9998, 0.9994 and 0.9996 for olanzapine, moxifloxacin, erlotinib and terfenadine respectively. Back calculated concentrations for all of the calibration standards used to construct the calibration curves are reported in Fig. 2b. Accuracy of the calibration standards for each compound ranged between 79.3–133.5%, 88.4–118.2%, 80.9–114.8% and 78.3–109.6% for olanzapine, moxifloxacin, erlotinib and terfenadine respectively. The LESA extraction failure rate (measured by monitoring nanospray ion current) for the experiment was ≤5%. Failed extractions were repeated at the end of the analytical run to complete the data set.

Comparison with homogenate LC-MS/MS data. Mean intensity of each analyte in each section was calculated from all of the sampling points across the entire tissue area. This mean intensity was used to back calculate the concentration in the unknown samples from the mimetic calibration curves, giving a mean concentration across the entire tissue of interest. This value provided a direct comparison to the concentration data generated by LC-MS/MS analysis (Table 1). The concentrations observed in the unknown samples for each analyte were within the calibration range used and the correlation between the concentration data derived from LESA-MSI and LC-MS/MS was similar for each of the analytes. The percentage difference between the LESA and the LC-MS/MS results for olanzapine, moxifloxacin, erlotinib and terfenadine ranged from 9.1–32.8, 3.8–7.0, 5.6–35.1 and 14.0–32.3% respectively across the different time points and dosing regimens.

Comparison with DESI-MSI data. LESA-MSI and DESI-MSI are both spray based analytical techniques and as such should show similar results. DESI-MSI is being increasingly used within academia and industry as a reliable and robust imaging technique[26]. Quantitative DESI-MSI has still to be extensively compared to other techniques such as LC-MS/MS and MALDI-MSI but several groups have reported positive quantitative measurements[22]. Adjacent sections to those run by LESA-MSI were used to repeat the analysis using DESI-MSI analysis (Fig. 3). DESI-MSI was sensitive across the calibration range used, giving a limit of quantitation (LOQ) of 1.0 nmol/g for olanzapine, erlotinib and terfenadine and 4.98 nmol/g for moxifloxacin. This compared to a LOQ of 0.5 nmol/g for all analytes by LESA-MSI analysis. To our knowledge this is the first time a comparison between the two techniques has been performed, the differences however could be caused by the use of different mass analyzers. DESI-MSI also operates at higher spatial resolution than LESA-MSI so could be inherently more sensitive when compared directly.

The calibration curves derived from the DESI-MSI analysis of the mimetic liver calibration standards are summarized in Fig. 4a. The linearity of the response for all four analytes was good with R^2 values equal to 0.9999, 0.9998, 0.9997 and 1.0000 for olanzapine, moxifloxacin, erlotinib and terfenadine respectively. Back calculated concentrations for all of the calibration standards used to construct the calibration curves are reported in Fig. 4b. Accuracy of the calibration standards for each compound was 82.8–136.5%, 81.4–110.2%, 81.3–105.9% and 80.8–131.0% for olanzapine, moxifloxacin, erlotinib and terfenadine respectively. Moxifloxacin sensitivity was relatively low compared to the other analytes, this can be clearly observed in Fig. 4a by the low intensity calibration curve for the compound. Sensitivity for each compound was variable between LESA-MSI and DESI-MSI with erlotinib giving the highest sensitivity in LESA-MSI but terfenadine being more sensitive in DESI-MSI. This could be due to extraction efficiency of the different compounds in the different extraction solvent systems being used in the two techniques.

The concentrations observed in the dosed samples for each analyte were within the calibration range used (Table 1). The correlation between the concentration data derived from LESA-MSI and DESI-MSI was comparable for each of the analytes. The percentage difference (using DESI-MSI as the standard) between the LESA and the DESI-MSI results for olanzapine, moxifloxacin, erlotinib and terfenadine ranged from 33.8–36.2, 26.8–44.4, 34.3–42.7 and 0.8–42.8% respectively across the different time points and dosing regimens.

DESI-MSI also correlated well with the LC-MS/MS results giving a percentage difference (using the LC-MS/MS data as standard) of 5.4–41.2%, 26.0–31.2%, 5.6–21.4% and 33.3–40.4% for olanzapine, moxifloxacin, erlotinib and terfenadine respectively.

These results were thought to be a reasonable difference when quantifying drugs in tissues using different analytical techniques.

Conclusion

Liquid extraction surface analysis has been demonstrated to be a reliable low resolution mass spectrometry imaging technique to qualitatively image compound distribution in tissue sections. Qualitative images highlight the distribution of drugs in tissue, but often images can be misleading due to the scaling methods and any thresholding used in the visualization of the images[27]. Quantitative measurements give a definitive answer as to the drug concentration within a particular tissue. LESA-MSI has many advantages over traditional homogenization analysis such as speed of analysis, increased sample stability, low sample use allowing further analysis by other techniques and arguably the largest benefit, spatial resolution. If compound levels are located in a specific sub-compartment of an organ this information is lost with homogenization and the concentration is diluted as an average of all of the tissue sampled. Here we have shown that a mimetic tissue model lends itself well to quantitative LESA-MSI, having many advantages over more traditional quantitative mass spectrometry imaging methods. Indeed, mimetics were used as a basis for LESA method optimization in the work presented here, providing some fundamental changes that improved the sensitivity, reproducibility and robustness of the technique and ultimately a better platform on which to perform quantitative LESA analysis. The mimetic tissue can be used to make reasonably large tissue sections which makes it ideal for lower resolution imaging platforms such as LESA-MSI.

The tissue mimetic model however is not without its drawbacks. It is labor intensive when compared to simpler standard spotting techniques, uses quite high quantities of control tissue and its application to more structurally diverse tissue types such as brain has not yet been demonstrated.

LESA-MSI is often employed when other MSI techniques have failed to detect analytes of interest, due to the techniques greater sensitivity resulting from the larger sampling area. It can also be used when profiling, rather than imaging, drug distribution in large tissues from higher animals (e.g. dog liver). Typically in pharmaceutical R&D the different MSI platforms (LESA, MALDI, DESI-MSI) are used in combination, complementing data from standard bioanalysis with information from other multimodal analysis.

Quantitative LESA-MSI is not limited to detection of drugs in tissues, work is ongoing to expand the use of the mimetic model to quantitation of endogenous small molecules and small peptides as markers for drug induced efficacy in our projects using stable labelled standards.

References

1. Rönquist-Nii, Y. & Edlund, P. O. Determination of corticosteroids in tissue samples by liquid chromatography–tandem mass spectrometry. *J. Pharm. Biomed. Anal.* **37**, 341–350 (2005).
2. Solon, E., Balani, S. & Lee, F. Whole-body autoradiography in drug discovery. *Curr Drug Metab.* **3**, 451–462 (2002).
3. McNally, W., Roth, M., Young, R., Bockbrader, H. & Chang, T. Quantitative whole-body autoradiographic determination of tacrine tissue distribution in rats following intravenous or oral dose. *Pharm. Res.* **6**, 924–932 (1989).
4. Reyzer, M. L., Hsieh, Y., Ng, K., Korfmacher, W. A. & Caprioli, R. M. Direct analysis of drug candidates in tissue by matrix-assisted laser desorption/ionization mass spectrometry. *J Mass Spectrom* **38**, 1081–1092 (2003).
5. Bunch, J., Clench, M. R. & Richards, D. S. Determination of pharmaceutical compounds in skin by imaging matrix-assisted laser desorption/ionisation mass spectrometry. *Rapid Comm. Mass Spectrom.* **18**, 3051–3060 (2004).
6. Hsieh, Y. *et al.* Matrix-assisted laser desorption/ionization imaging mass spectrometry for direct measurement of clozapine in rat brain tissue. *Rapid Comm. Mass Spectrom.* **20**, 965–972 (2006).
7. Prideaux, B. & Stoeckli, M. Mass spectrometry imaging for drug distribution studies. *J. proteomics* **75**, 4999–5013 (2012).
8. Todd, P. J., Schaaff, T. G., Chaurand, P. & Caprioli, R. M. Organic ion imaging of biological tissue with secondary ion mass spectrometry and matrix-assisted laser desorption/ionization. *J Mass Spectrom* **36**, 355–369 (2001).
9. Takáts, Z., Wiseman, J. M., Gologan, B. & Cooks, R. G. Mass Spectrometry Sampling Under Ambient Conditions with Desorption Electrospray Ionization. *Science* **306**, 471–473 (2004).
10. Wiseman, J. M. *et al.* Desorption electrospray ionization mass spectrometry: Imaging drugs and metabolites in tissues. *Proceedings of the National Academy of Sciences* **105**, 18120–18125 (2008).
11. Swales, J. G. *et al.* Mapping Drug Distribution in Brain Tissue Using Liquid Extraction Surface Analysis Mass Spectrometry Imaging. *Anal. Chem.* **87**, 10146–10152 (2015).
12. Eikel, D. *et al.* Liquid extraction surface analysis mass spectrometry (LESA-MS) as a novel profiling tool for drug distribution and metabolism analysis: the terfenadine example. *Rapid Commun. Mass Spectrom.* **25**, 3587–3596 (2011).

13. Nilsson, A. *et al.* Investigating Nephrotoxicity of Polymyxin Derivatives by Mapping Renal Distribution Using Mass Spectrometry Imaging. *Chemical Research in Toxicology* **28**, 1823–1830 (2015).
14. Cobice, D. F. *et al.* Mass spectrometry imaging for dissecting steroid intracrinology within target tissues. *Anal. Chem.* **85**, 11576–11584 (2013).
15. Edwards, R. L. *et al.* Hemoglobin variant analysis via direct surface sampling of dried blood spots coupled with high-resolution mass spectrometry. *Anal. Chem.* **83**, 2265–2270 (2011).
16. Swales, J. G. *et al.* Mass Spectrometry Imaging of Cassette-Dosed Drugs for Higher Throughput Pharmacokinetic and Biodistribution Analysis. *Anal. Chem.* **86**, 8473–8480 (2014).
17. Hamm, G. *et al.* Quantitative mass spectrometry imaging of propranolol and olanzapine using tissue extinction calculation as normalization factor. *Journal of proteomics* **75**, 4952–4961 (2012).
18. Groseclose, M. R. & Castellino, S. A mimetic tissue model for the quantification of drug distributions by MALDI imaging mass spectrometry. *Analytical chemistry* **85**, 10099–10106 (2013).
19. Nilsson, A. *et al.* Fine mapping the spatial distribution and concentration of unlabeled drugs within tissue micro-compartments using imaging mass spectrometry. *PloS one* **5**, e11411 (2010).
20. Wilkinson, W., Gusev, A., Proctor, A., Houalla, M. & Hercules, D. Selection of internal standards for quantitative analysis by matrix-assisted laser desorption-ionization (MALDI) time-of-flight mass spectrometry. *Fresenius' Journal of Analytical Chemistry* **357**, 241–248 (1997).
21. Pirman, D. A., Reich, R. F., Kiss, A., Heeren, R. M. A. & Yost, R. A. Quantitative MALDI Tandem Mass Spectrometric Imaging of Cocaine from Brain Tissue with a Deuterated Internal Standard. *Anal. Chem.* **85**, 1081–1089 (2012).
22. Bergman, H. M., Lundin, E., Andersson, M. & Lanekoff, I. Quantitative mass spectrometry imaging of small-molecule neurotransmitters in rat brain tissue sections using nanospray desorption electrospray ionization. *Analyst* **141**, 3686–3695 (2016).
23. Robichaud, G., Garrard, K. P., Barry, J. A. & Muddiman, D. C. MSiReader: an open-source interface to view and analyze high resolving power MS imaging files on Matlab platform. *J. Am. Soc. Mass Spectrom.* **24**, 718–721 (2013).
24. Pirman, D. A., Kiss, A., Heeren, R. M. & Yost, R. A. Identifying tissue-specific signal variation in MALDI mass spectrometric imaging by use of an internal standard. *Anal. Chem.* **85**, 1090–1096 (2013).
25. Kallback, P., Shariatgorji, M., Nilsson, A. & Andren, P. E. Novel mass spectrometry imaging software assisting labeled normalization and quantitation of drugs and neuropeptides directly in tissue sections. *J. Proteomics* **75**, 4941–4951 (2012).
26. Wiseman, J. M., Ifa, D. R., Song, Q. & Cooks, R. G. Tissue imaging at atmospheric pressure using desorption electrospray ionization (DESI) mass spectrometry. *Angew Chem Int Ed Engl* **45**, 7188–7192 (2006).
27. Race, A. & Bunch, J. Optimisation of colour schemes to accurately display mass spectrometry imaging data based on human colour perception. *Anal. Bioanal. Chem*, **407**, 2047–2054 (2015).

Author Contributions

J.G.S., P.J.H.W. and R.J.A.G. designed the experiments. J.G.S. and N.S. performed all of the imaging experiments. J.T. designed the LESA imaging software. M.R.C. provided academic supervision and review of the final manuscript. J.G.S. wrote the manuscript with feedback from all authors.

Additional Information

97

6.0   QUANTITATION OF ENDOGENOUS METABOLITES IN MOUSE TUMORS USING MASS SPECTROMETRY IMAGING

Swales J. G., Dexter A., Hamm G., Nilsson A., Strittmatter N., Michopoulos F. N., Hardy C., Morentin-Gutierrez P., Mellor M., Andren P. E., Clench M. R., Bunch J., Critchlow S., Goodwin R. J. A., Quantitation of endogenous metabolites in mouse tumors using mass spectrometry imaging; Analytical Chemistry 2018, 90, 6051-6058.

Author Contribution

JGS performed all method development and proof of concept experiments, designed and analysed the stability studies, performed all sample preparation and lactate MALDI imaging experiments, processed all imaging data, interpreted results and prepared the manuscript for publication.

Quantitation of Endogenous Metabolites in Mouse Tumors Using Mass-Spectrometry Imaging

John G. Swales,*,[†,§] Alex Dexter,[∥] Gregory Hamm,[†] Anna Nilsson,[⊥] Nicole Strittmatter,[†] Filippos Michopoulos,[‡] Christopher Hardy,[†] Pablo Morentin-Gutierrez,[‡] Martine Mellor,[‡] Per E. Andren,[⊥] Malcolm R. Clench,[§] Josephine Bunch,[∥] Susan E. Critchlow,[‡] and Richard J. A. Goodwin[†]

[†]Pathology, Drug Safety & Metabolism, IMED Biotech Unit, AstraZeneca, Darwin Building, Cambridge Science Park, Milton Road, Cambridge, Cambridgeshire CB4 0WG, U.K.

[‡]Bioscience, Oncology, IMED Biotech Unit, AstraZeneca, Cambridge CB4 0WG, U.K.

[§]Centre for Mass Spectrometry Imaging, Biomolecular Research Centre, Sheffield Hallam University, Sheffield S1 1WB, U.K.

[∥]National Centre of Excellence in Mass Spectrometry Imaging (NiCE-MSI), National Physical Laboratory, Teddington TW11 0LW, U.K.

[⊥]Biomolecular Mass Spectrometry Imaging, National Resource for MSI, Science for Life Laboratory, Department of Pharmaceutical Biosciences, Uppsala University, Uppsala 752 37, Sweden

S Supporting Information

ABSTRACT: Described is a quantitative-mass-spectrometry-imaging (qMSI) methodology for the analysis of lactate and glutamate distributions in order to delineate heterogeneity among mouse tumor models used to support drug-discovery efficacy testing. We evaluate and report on preanalysis-stabilization methods aimed at improving the reproducibility and efficiency of quantitative assessments of endogenous molecules in tissues. Stability experiments demonstrate that optimum stabilization protocols consist of frozen-tissue embedding, post-tissue-sectioning desiccation, and storage at −80 °C of tissue sections sealed in vacuum-tight containers.

Optimized stabilization protocols are used in combination with qMSI methodology for the absolute quantitation of lactate and glutamate in tumors, incorporating the use of two different stable-isotope-labeled versions of each analyte and spectral-clustering performed on each tissue section using *k*-means clustering to allow region-specific, pixel-by-pixel quantitation. Region-specific qMSI was used to screen different tumor models and identify a phenotype that has low lactate heterogeneity, which will enable accurate measurements of lactate modulation in future drug-discovery studies. We conclude that using optimized qMSI protocols, it is possible to quantify endogenous metabolites within tumors, and region-specific quantitation can provide valuable insight into tissue heterogeneity and the tumor microenvironment.
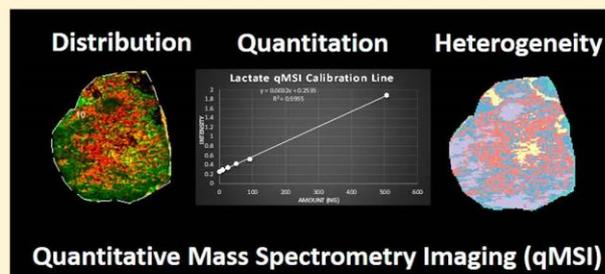
Oncology is a key, highly competitive pharmaceutical research area. The complex nature of cancer has prompted research into many therapeutic pathways targeting changes in cancer-cell growth, division, proliferation, and death.

A common difference between tumor cells and normally differentiated cells is changed cellular metabolism. Otto Warburg documented the well-characterized metabolic shifts of cancer cells toward aerobic glycolysis, higher energy production, and increased lactate production.[1] More recently, Vander Heiden et al. have hypothesized that adaptations to metabolic pathways in tumor cells drive cellular proliferation, facilitating the uptake of nutrients and their incorporation into the constituents needed for the generation of new cells.[2] Metabolic features of the Warburg effect, that most tumors rely on glucose and glutamine catabolism to produce ATP and the

building blocks necessary to sustain rapid cell growth, are a hallmark of cancer.[3]

Effective analytical methodologies that enable the quantitative evaluation of tumor metabolism are therefore critical for understanding the impact of therapeutic agents on tumor lactate levels in the tumor microenvironment. Given the complex and heterogenic tumor architecture, spatial evaluation of tumor lactate levels can provide valuable information for better understanding both the endogenous distribution of tumor lactate and also the effects on endogenous levels from drug dosing in animal-model efficacy testing. This under-

standing can then enable reliable pharmacokinetic–pharmaco-dynamic (PK–PD) understandings of the modulation of tumor lactate levels and how they correlate with overall effects on tumor growth.

To date, bioanalytical techniques such as LC-MS have kept pace with the need for higher-throughput measurements[4] but are limited in value when trying to assess drug distribution in vivo. Traditionally, drug-distribution studies have been performed during the later stages of development using radio-labeled compounds and low-throughput techniques, such as qWBA,[5] or homogenization[6] studies using LC-MS with long liquid-chromatography gradients. Mass-spectrometry imaging (MSI) is a group of label-free, multiplex analytical techniques that map the molecular distribution of endogenous compounds, drugs,[7] lipids,[8] proteins,[9] peptides,[10] and drug-delivery systems[11] in biological tissues. MSI techniques are all based on different mass-spectrometry surface-sampling ion sources, of which matrix-assisted-laser-desorption-ionization (MALDI)[12] has arguably had the most widespread use within the pharmaceutical industry. MALDI-MSI is being rapidly joined by other MSI techniques, such as desorption-electro-spray-ionization mass-spectrometry imaging (DESI)[13] and liquid-extraction-surface-analysis mass-spectrometry imaging (LESA),[14] that bring complementary properties such as expanded chemical scopes and increased sensitivities, usually at the expense of decreased spatial resolution. Although it is not replacing traditional bioanalysis, MSI is increasingly being used alongside these techniques, providing timely and cost-effective insights into the deposition and fates of new chemical entities.[15] Applications of MSI within the drug-discovery industry are well documented.[16] Although several groups have reported the successful imaging of low-mass endogenous metabolites in tumors,[17] the data has largely been qualitative in nature. In order to expand the applicability of MALDI-MSI into the pharmacodynamic testing of compound efficacies, robust quantitative-MSI (qMSI) methods are needed that can spatially resolve regions of high abundance in tumor architectures, which are often complex, and can provide assurance that modulation in endogenous-metabolite levels is not the result of poor postcollection sample storage or processing.

Here, we describe a mass-spectrometry-imaging method-ology using a standard "spotting" technique combined with a stable-labeled normalization that has previously been reported as being suitable for quantitative-MSI analysis.[18,19] Data is presented for the absolute quantitation of two key endogenous metabolites involved in tumor-cell energy production (i.e., glycolysis and the TCA cycle), lactate and glutamate. We also present region-specific-quantitation postspectral clustering to highlight the heterogeneity of each tumor model. The techniques developed were used to screen several mouse tumor models to identify a suitable phenotype for reliably monitoring lactate changes after drug administration in efficacy studies.

■ EXPERIMENTAL SECTION

Materials and Reagents. Analytical-grade acetonitrile, methanol, and formic acid were obtained from Fisher Scientific (Loughborough, Leicestershire, U.K.). 2-Methylbutane, gelatin, lactate-^{13}C3, lactate-^{13}C1, glutamate-D5, 1,5-diaminonaphtha-lene, and 9-aminoacridine were purchased from Sigma-Aldrich (Poole, Dorset, U.K.). Glutamate-D3 was purchased from QMX Laboratories (Thaxted, Essex, U.K.).

Endogenous-Metabolite Stability in Mouse-Tumor Sections. Duplicate control tumor sections of 10 μm taken from an NCI-H358 tumor model were cut (Leica CM3050S cryomicrotome, Leica Biosystems, Nussloch, Germany) and mounted onto glass microscope slides over a 24 h time course (0, 1, 2, 4, 6, 12, and 24 h). Between time points, the sections were stored under one of three different conditions: (1) they were left in the cryostat and thaw-mounted at −16 °C; (2) they were thaw-mounted, desiccated in N$_2$, vacuum-packed, and stored at ambient temperature; or (3) they were thaw-mounted, desiccated in N$_2$, vacuum-packed, and stored at −80 °C. A "fresh" tumor section from the same biological sample as the stability sections (stored at −80 °C prior to mounting) was thaw-mounted and desiccated on each slide immediately prior to analysis. This was done as a quality-control measure to ensure there was a section unaffected by the storage conditions in each batch, as the analysis was performed over the course of several days.

Animal Studies. All in vivo studies were conducted in accordance with U.K. Home Office legislation; the Animal Scientific Procedures Act, 1986; and the AstraZeneca Global Bioethics Policy. All experimental work is outlined in home office cancer-therapy licenses, which have gone through the AstraZeneca Ethical Review Process.

Initial qMSI Proof-of-Principle Study. Female athymic mice from an NCI-H358 tumor model were orally dosed with the vehicle (HPMC/Tween). Five animals were sacrificed at 0.5, 2, 6, and 24 h after the dose to mimic the typical design of efficacy studies and to monitor lactate changes throughout the study duration. All the tumors were resected at necropsy and snap-frozen in liquid N$_2$. The tumors were stored at −80 °C prior to cryo-sectioning and subsequent analysis by MALDI-MSI to assess the performance of the analytical method and the variability of the animal model.

Screening Mouse Tumor Models. Four different tumor models were screened for lactate and glutamate concentrations and distributions. The four models tested were NCI-H358 (n = 5 animals), a female athymic human-xenograft model; MC38 (n = 4 animals); B16.F10.AP3 (n = 4 animals); and an MC38 variant (n = 5 animals). All the syngeneic mouse tumor models were grown in female C57/Bl6. All the tumors were resected at necropsy and snap-frozen in liquid N$_2$. The tumors were stored at −80 °C prior to cryo-sectioning and subsequent analysis by MALDI-MSI.

Tissue Embedding. The tissue-embedding methodology can be found in the Supporting Information.

Tissue Sectioning. Details of the methodology used in the cryo-sectioning of the tissues can be found in the Supporting Information.

Lactate-Calibration-Standard Preparation. Three stock solutions of sodium L-lactate-^{13}C3 (Sigma-Aldrich, 485926-500MG) were prepared daily as needed at concentrations of 500, 5000, and 50 000 μM in 50/50 (v/v) methanol/water. A sample of blank 50/50 (v/v) methanol/water was also retained.

Calibration spots for quantitation were added to the control tissue sections on each day of analysis using a Preddator robotic liquid handler (Redd and Whyte, London, U.K.) at amounts equal to 0, 10, 25, 50, 100, 250, and 500 ng of lactate on-tissue. The liquid handler dispensed 50 nL droplets of the standards, over-spotting in a total of four cycles to reach the required on-tissue amounts of the analyte. The spots were allowed to dry at room temperature prior to matrix addition.
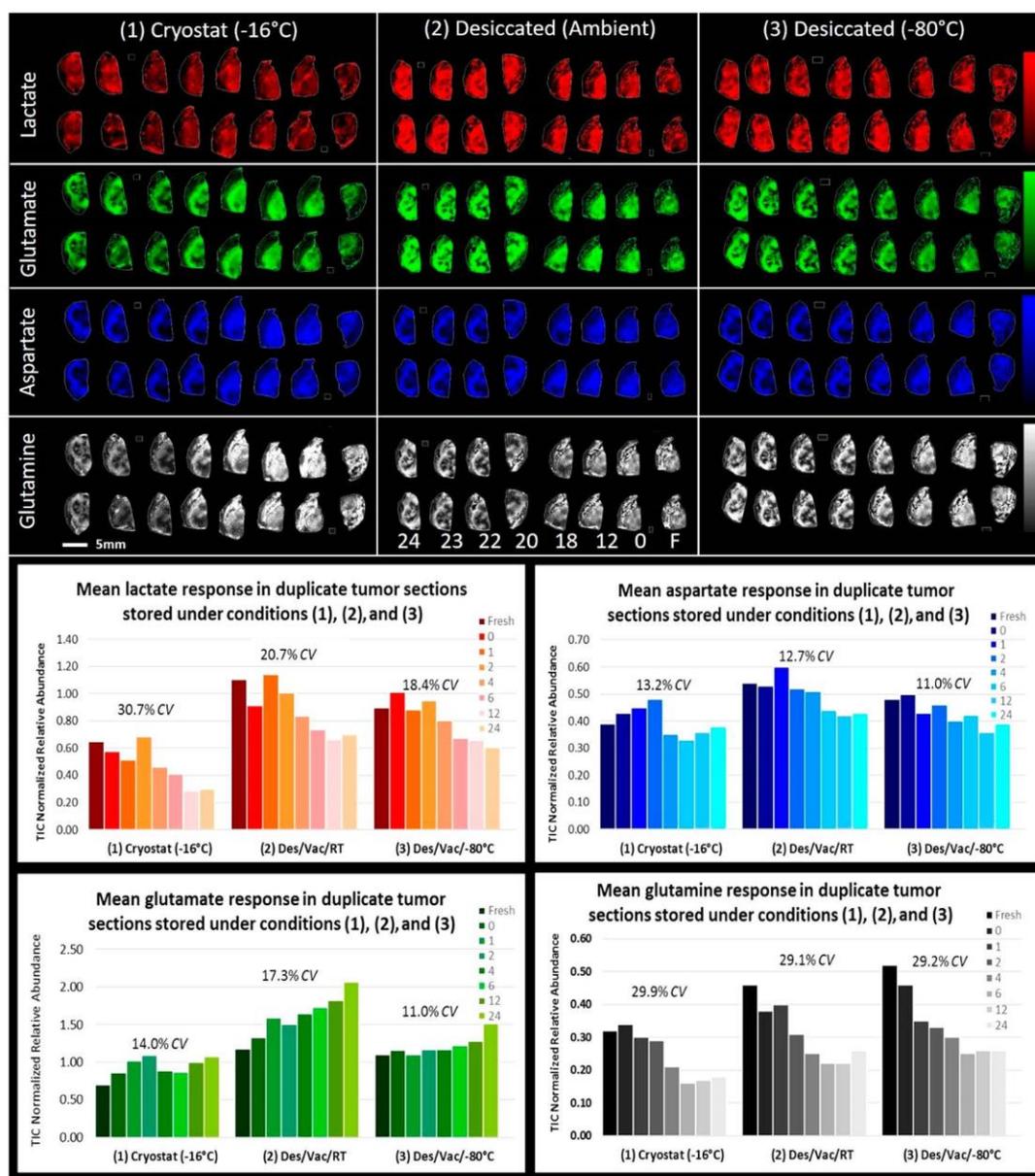
100

Figure 1. Stability of lactate, aspartate, glutamate, and glutamine in control serial adjacent tumor sections under different postsectioning storage conditions. The bar charts show the relative abundances and coefficients of variation (C_v) of the endogenous metabolites in the tumor tissues under the different storage conditions over time (in hours). The images and relative abundances were generated from the TIC-normalized MALDI-MSI raw data. All analyte images are scaled between 0−100%.

Glutamate-Calibration-Standard Preparation. Stock solutions of D3-glutamate and D5-glutamate (100 mM) were prepared daily in 0.1 M HCl. The D5-glutamate standards were prepared as 2, 0.67, 0.22, 0.074, and 0.025 mM dilutions in 50/50 (v/v) ethanol/water. The standards (0.1 μL) and a blank sample (0.1 μL; 50/50, v/v, ethanol/water) were manually applied via a pipet to the control tissue. D3-Glutamate was used as an internal standard. The stock solution (50 μL) was added to 5.95 mL of 50/50 (v/v) methanol/water and sprayed onto the tissue before the matrix application using a TM-sprayer (HTX technologies, Chapel Hill, NC) with the following parameters: six passes were completed at 90 °C with a flow of

50/50 (v/v) methanol/water at a flow rate of 0.07 mL/min and nebulized with nitrogen at 6 psi.

MALDI-Matrix Application. Vacuum-packed, thaw-mounted tissue sections were allowed to reach room temperature after their removal from the −80 °C storage prior to the breaking of the vacuum seals. Optical images were taken using a standard flat-bed scanner (Seiko Epson, Nagano, Japan) prior to the MALDI-matrix application. The matrix coating was applied in eight passes using a TM-sprayer (HTX technologies, Chapel Hill, NC) set at 75 °C with a backup flow of 50% (v/v) methanol/water at a flow rate of 0.08 mL/min and nebulized with nitrogen at 8 psi (lactate) or 6 psi (glutamate). For lactate quantitation, 1,5-diaminonaphthalene (10 mg/mL; 50/50, v/v,

acetonitrile/water) containing 100 μL of a sodium L-lactate-^{13}C1 solution (Sigma-Aldrich, Loughborough, Leicestershire, U.K.) was used (^{13}C1 was not used in the proof-of-principle study), and for glutamate quantitation, 9-aminoacridine (5 mg/mL, 70/30, v/v, acetonitrile/water) was applied under the same conditions as those for the internal standard (D3-glutamate).

MALDI qMSI. MALDI-MSI experiments were carried out in negative-reflectron mode over a mass range of m/z 60 to 1000 using a MALDI rapifleX tissuetyper (lactate) or an ultrafleXtreme (glutamate) MALDI-TOF/TOF MS (Bruker Daltonics, Bremen, Germany) equipped with a 10 kHz Smartbeam 3D and a 2 kHz smartbeam-II Nd:YAG laser, respectively. The data collection on the rapifleX was at a spatial resolution of 50 μm, and 500 laser shots were summed per raster position. The data collection on the ultrafleXtreme was at a spatial resolution of 80 μm, and 300 laser shots were summed per raster position.

FlexImaging 5.0 (Bruker Daltonics, Bremen, Germany) software was used for the initial data analysis. Normalization, molecular-image extraction, and regions of interest for lactate quantitation were defined in SCiLS Lab 2017b (Bruker Daltonics, Bremen, Germany) software typically using a mass-selection window of $\pm$0.05 Da. Glutamate quantitation was performed using msIQuant software.[20] Endogenous lactate, lactate-^{13}C1 (for normalization), and lactate-^{13}C3 were detected at m/z 89.1, 90.1, and 92.1, respectively.

Spectral-Clustering Analysis. The raw data were converted to imzML and imported into MatLab (version R2017a and statistics toolbox, Math-Works, Inc., Natick, MA) using SpectralAnalysis version 1.01.[21] Briefly, a mean spectrum was generated for each data set and was peak-picked using SpectralAnalysis gradient peak-picking. These peaks were then extracted into a datacube by integrating the area under each peak. The data were then normalized to that of the lactate-^{13}C or glutamate peak (nominally m/z 90.0 and 149.0). These lactate and glutamate concentrations were then quantified using the calibration curves generated from the spots applied to separate tissue sections. Clustering was then performed on each of the individual tissue sections using k-means clustering with k = 2–5 (k = 4 shown) and the cosine distance metric.[22] Box plots of lactate and glutamate concentrations were generated using the "boxplot" MatLab function. In the box plots, the central lines show the median concentrations, the boxes represent the 25–75% interquartile ranges of the data, and each of the whiskers represents one additional interquartile range. Any points outside these ranges are considered outliers and are marked with red crosses.

The overlap between the lactate and glutamate concentrations in the different clusters was calculated using the Bhattacharyya coefficient.[23] This was performed for each pair of clusters to give an overall measure of the heterogeneity of these metabolites' concentrations in the different tumor models.

Homogenization and Quantitation of Lactate Levels by LC-MS. Details of the homogenization and LC-MS methods can be found in the Supporting Information.

■ RESULTS AND DISCUSSION

Endogenous-Metabolite-Stability Experiment. Previous in-house experience of endogenous-metabolite analysis using DESI-MSI had indicated degradation of endogenous lactate within rat kidney tissue during sample preparation (data not reported). This ex-vivo change in endogenous small-molecule levels was found to be related to the amount of time

the tissues spent in the −20 °C environment of the cryomicrotome during the sectioning process and appeared to stabilize during analysis when the sample was removed from the freezer and effectively kept in a desiccated, nitrogen-rich environment on the DESI stage. Prior to embarking on a quantitative study of lactate and glutamate concentrations in different tumor models, it was thus necessary to establish a protocol to stabilize the samples or make sure that any degradation of the endogenous compounds within the tissues was as uniform as possible. The experimental methodology is presented in the Experimental Section, but in summary, tumor sections were taken over a time course spanning 24 h in total, and the resulting sections were stored between time points in one of three different conditions: (1) they were left in the cryostat and thaw-mounted at −16 °C; (2) they were thaw-mounted, desiccated in N_2, vacuum-packed, and stored at room temperature; or (3) they were thaw-mounted, desiccated in N_2, vacuum-packed, and stored at −80 °C. Sections from each time point were analyzed in duplicate using MALDI-MSI, and a fresh section was added to each slide immediately before analysis to give a baseline relative abundance of lactate (lac), glutamate (glu), aspartate (asp), or glutamine (gln) for comparison. The MALDI-MSI images and relative abundances derived from the analysis can be seen in Figure 1. The data was normalized using total ion currents. Sections stored under condition (1) exhibited degradation of the relative abundances of lac, asp, and gln over the time course. The glu relative abundance increased upon storage compared with the levels in the fresh tissue section (possibly as a product of the gln degradation) but remained stable during the storage period. Sections stored under condition (2) also showed decreasing lac, asp, and gln relative abundances over the storage period. The levels of glu again trended to increase over the storage period under the same conditions. Sections stored under condition (3) had lac levels more stable than those observed in the samples under conditions (1) and (2), with coefficient of variation (C_v) values of 18.4, 30.7, and 20.7%, respectively. Glu, asp, and gln levels were also found to be more stable under condition (3), with corresponding improvements in their C_v values versus the values from the other storage conditions. These results highlighted the need for −80 °C storage, even over a short period of time. Interpreting the results further, it was clear that immediate desiccation after sectioning followed by vacuum-packing and storing at −80 °C was needed to minimize the degradation of the endogenous metabolites in the tissues. However, even with this safeguard, instability could still occur, as multiple sections are cut one at a time onto the same microscope slide within the cryostat. To minimize the amount of time the sections were kept in the cryostat chamber, multiple tissues were embedded in gelatin and sectioned simultaneously, with a single cut of the microtome blade. This significantly reduced the amount of variability in the time the sections spent at temperatures higher than −20 °C, while also reducing the overall sample preparation time (from 6 h to <1 h). The embedding, thaw-mounting, desiccating, vacuum-packing, and storing at −80 °C protocol was thus adopted for all subsequent analyses.

Preliminary qMSI Proof of Principle. In order to test the hypothesis that it was possible to quantify and map the spatial distribution of lactate in a tumor tissue using qMSI, an initial study was performed using samples from an NCI-H358 human-xenograft mouse tumor model. MALDI-qMSI was used to map and quantify the lactate distribution within the tumor tissue

(Figure 2). A second, different stable-labeled version of lactate proved difficult to source at the time of this experiment;
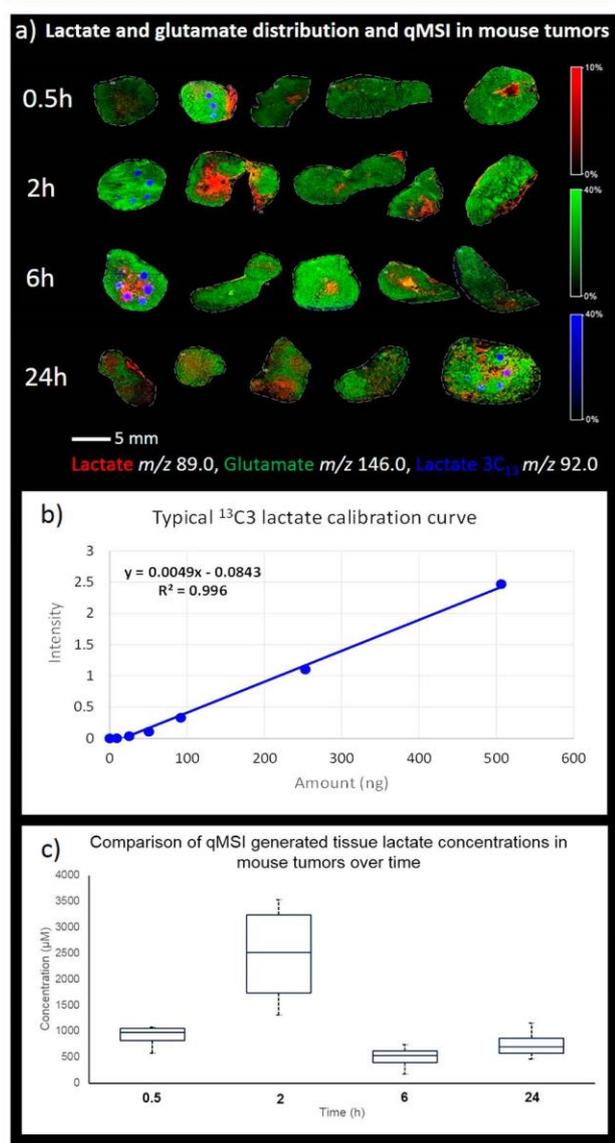

b) Typical $^{13}C_3$ lactate calibration curve

$y = 0.0049x - 0.0843$
$R^2 = 0.996$

c) Comparison of qMSI generated tissue lactate concentrations in mouse tumors over time

Figure 2. (a) Lactate and glutamate distribution in an NCI-H358 tumor model generated using quantitative mass-spectrometry imaging. The images are scaled between 0–10% (lactate) and 0–40% (glutamate), and the data was normalized by total ion currents. Calibration spots (lactate-$^{13}C_3$) can be seen in blue at each time point and are scaled between 0–40%. (b) Calibration line, generated by spotting stable-labeled lactate-$^{13}C_3$ onto a control tissue, showing the linear response generated by MALDI-qMSI. (c) Box plots of lactate concentrations in tumors at different time points. The increase in the median lactate concentration at 2 h is attributed to a single tumor with a highly localized lactate response.

therefore, sodium L-lactate-$^{13}C_1$ was subsequently sourced and used for subsequent experiments. The proof-of-principle analysis was thus performed with normalization to total ion currents. Although it did not provide absolute quantitation of the lactate levels in the tissues, this at least provided the proof of principle that the qMSI methodology was suitable for use.

The analytical method performed well and confirmed that the technique was suitable for lactate quantitation within the tumor tissues, giving a linear response (R^2 = 0.997) across the calibration range (Figure 2b). Stable-isotope-labeled (lactate-$^{13}C3$) calibration spots can be seen in blue in Figure 2a. The dynamic range of the calibration line covered the lactate concentrations of the "unknown" tumor tissue (170.0–3525.6 μmol/kg). The lactate concentrations in the tumors at 30 min, 6 h, and 24 h were similar. The tumors taken at the 2 h time point had lactate levels that were slightly elevated compared with those of the other time points, which was attributed to a single tumor that had a large necrotic core with a high lactate concentration at this time point. Mean interanimal tumor lactate levels at each time point ranged between 490.6–2464.0 μmol/kg, giving a corresponding variation in C_v of 26.0–49.3% (n = 4 animals at each time point), indicating a high level of variation between the animals, especially at the 2 h time point (Figure 2c). Using the multiplex nature of MALDI-MSI, it was possible to simultaneously map the distribution of glutamate (Figure 2a) along with lactate within the same tumors. Glutamate was distributed throughout the tumors; this was in stark contrast to lactate, which was much more heterogeneously distributed and localized into the necrotic or prenecrotic regions (identified using H&E staining) of the tissues (Figure SI 1). Glutamate levels in these lactate-rich regions were much lower than those observed in the surrounding tissues, giving a visual representation of the Warburg effect.

Tumor-Model Screening. The NCI-H358 tumor model, which had a heterogeneous lactate distribution in the initial study, was shown to have high intertumor variation in lactate levels. This could be due to several factors, including the tumor-model metabolism profile or the duration for which the tumors were allowed to grow. High interanimal variation decreases the likelihood of detecting subtle differences in endogenous-metabolite levels in response to drug treatments when dosed animals are compared with vehicle-treated animals, which is required to evaluate efficacy.

For the testing of therapeutic compounds, a tumor model that has a more homogeneous lactate distribution would be highly desirable, as this should reduce the intertumor variability, give a more robust model to use in efficacy testing, and ultimately build a reliable PK–PD model. During this study, several different tumor models were selected for lactate qMSI screening. An NCI-H358 model, differentiated from the model in the initial study in that the tumor was allowed to grow for less time, thus minimizing the chance of necrosis; an MC38 model; a B16.F10.AP3 model; and an MC38-variant model were all screened using MALDI-qMSI for lactate quantitation and distribution. The evaluation of the lactate data highlighted an interest in tumor glutamate quantitation and distribution, and this analysis was subsequently performed at a collaborator site using adjacent tumor sections and a different MALDI instrument. MALDI-qMSI methods are multiplex, and ideally both the lactate and glutamate concentrations could be derived from the same tumor sections in the same analytical run; however, data from adjacent sections run under different conditions as distinct analytical batches can be used to draw valid conclusions from the data. Using the optimized sample-processing methods described earlier, the tumor models were analyzed in separate analytical batches (n = 4 for each metabolite). The data are summarized in Figure 3. Stable-labeled lactate and glutamate calibration lines gave consistent linear responses (R^2 = 0.9960–0.9978) with a gradient range of
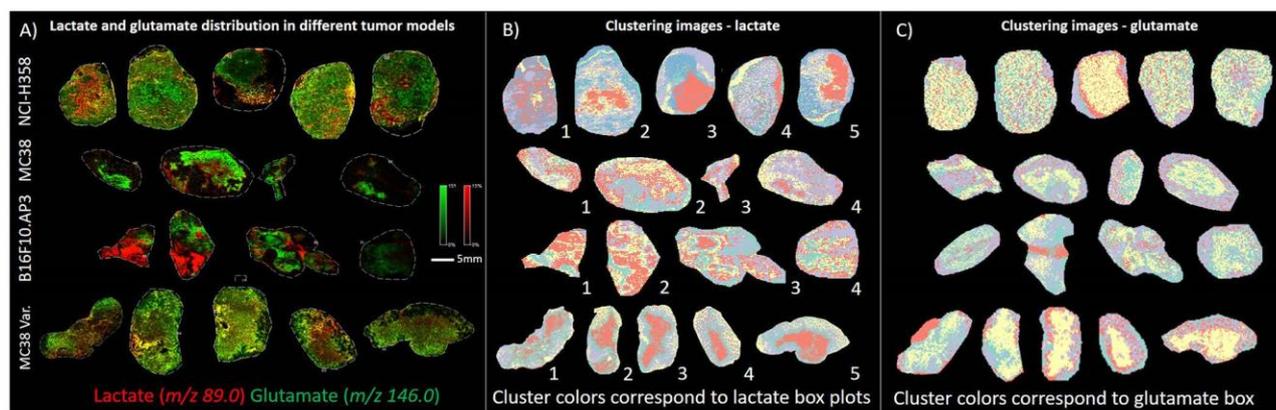
Figure 3. Comparison of four mouse tumor models showing (A) lactate (red) and glutamate (green) distributions generated by MALDI-qMSI, (B) clustering images of lactate in the different tumor model tissues, and (C) clustering images of glutamate in the different tumor model tissues. The clustering images give a visual representation of the spectrally diverse regions within the tumor tissues. The colors of the different clusters correspond to the colors used in the box plots in Figure 4. The lactate clustering and glutamate clustering are different because of the use of adjacent sections, different MALDI matrices, and different mass spectrometers.

0.0041−0.0098 and an intercept range of 0.0249−0.2649. Pixel-to-pixel normalization was performed on all the data using the response of a second stable-isotope-labeled version of lactate or glutamate that had been homogeneously sprayed across all the tissue sections. Ion images are shown in Figure 3a. Tumors from the MC38 and B16.F10.AP3 models showed heterogeneous lactate distributions throughout the tumor tissues, with little or no colocalization with glutamate. The MC38 tissue in particular had large areas of necrosis (confirmed by H&E). The B16.F10.AP3 tumors were less necrotic, but the lactate and glutamate distributions were very localized and patchy throughout the tissues. The NCI-H358 and MC38-variant tumors had more evenly distributed lactate and glutamate, even in areas that were confirmed to be necrotic by H&E staining. The lactate and glutamate concentrations across the tissue sections were largely in the same ranges for the different models, fluctuating between 81.7−2504.0 μmol/kg for lactate and 1095.5−7818.7 μmol/kg for glutamate.

Region-Specific qMSI. To better evaluate the heterogeneity of the lactate and glutamate biodistribution in the range of tumor models, spectral clustering was performed on each of the individual tissue sections from each model using k-means clustering with $k = 2$−5 ($k = 4$ shown), using the cosine distance metric. Region-specific clustering images are shown in Figure 3b,c. The clustering analysis allowed region-specific pixel-by-pixel quantitation of the lactate and glutamate levels, represented graphically in the box plots in Figure 4. According to the box plots of lactate and glutamate concentrations in each region of each tissue, the lactate concentrations were much more heterogeneous in the B15.F10.AP3 and MC38 models, as seen by the large boxes, whiskers, and many outliers. In comparison, the MC38-variant and NCI-H358 tumors had more homogeneously distributed lactate concentrations (smaller boxes), and the MC38 variant displayed lower intertumor median-lactate-concentration variability. The percent overlap for each cluster in each tissue section from each tumor model was calculated to assess the heterogeneity of the lactate and glutamate levels in the different models. The overlaps in the lactate clusters were in the ranges 16−99, 52−99, 23−99, and 21−97% for the NCI-H358, MC38, B16.F10.AP3, and MC38-variant models, respectively. This suggested that the MC38 tissue was the most homogeneous tumor model. However, the

MC38-variant model has a cluster with a much larger interquartile range than the other clusters (Figure 4) and is also different in terms of its lactate concentration (median of ~10^3 μmol/kg vs ~10^4 μmol/kg in the other three clusters). The outlying cluster has consistent median lactate concentrations among different tumors in the MC38-variant model, but the distribution of the cluster does not cover a significant area in each tissue section, compared with the equivalent clusters in the other models (Figure 3, cluster images), and is distributed around the periphery of the tissue suggesting, it could be attributable to off-tissue effects. Removal of the outlying cluster narrows the overlap data to 52−97% in the MC38-variant model, making it similar to the overlap observed in the MC38 model.

The glutamate concentrations in all the tissue models are overall less heterogeneous than the lactate concentrations, with the different models containing similar levels of heterogeneity, as seen in similar spreads of the data in the box plots. This is also reflected in the spectral overlaps, which are in similar ranges for all the different tumor models. The objective of the screening experiment was to identify a tumor model that had greater lactate homogeneity, lower lactate variability, and fewer areas of necrosis. The MC38-variant model was selected, as the analysis had shown that this model exhibited the most favorable properties of the four models tested. Subsequently, the MC38-variant model has allowed further efficacy studies to be performed. The more homogeneous lactate distribution and lower lactate-concentration variability in the MC38-variant model, highlighted by the qMSI analysis, has provided the confidence to analyze later studies using nonspatially resolved LC-MS with tissue homogenization. Lactate levels within the control tumors taken from the same study used in the qMSI experiment were measured by LC-MS and resulted in a mean concentration of 473.4 μmol/kg ±102.1 ($C_v = 21.6\%$) based on $n = 9$ control tumors from the MC38-variant model. This provides some validation that the qMSI analysis gives concentration results in the expected dynamic range within a tissue that is morphologically the same. The tumor model is now being effectively used to develop a PK−PD relationship to optimize efficacy in active drug-discovery and development projects.
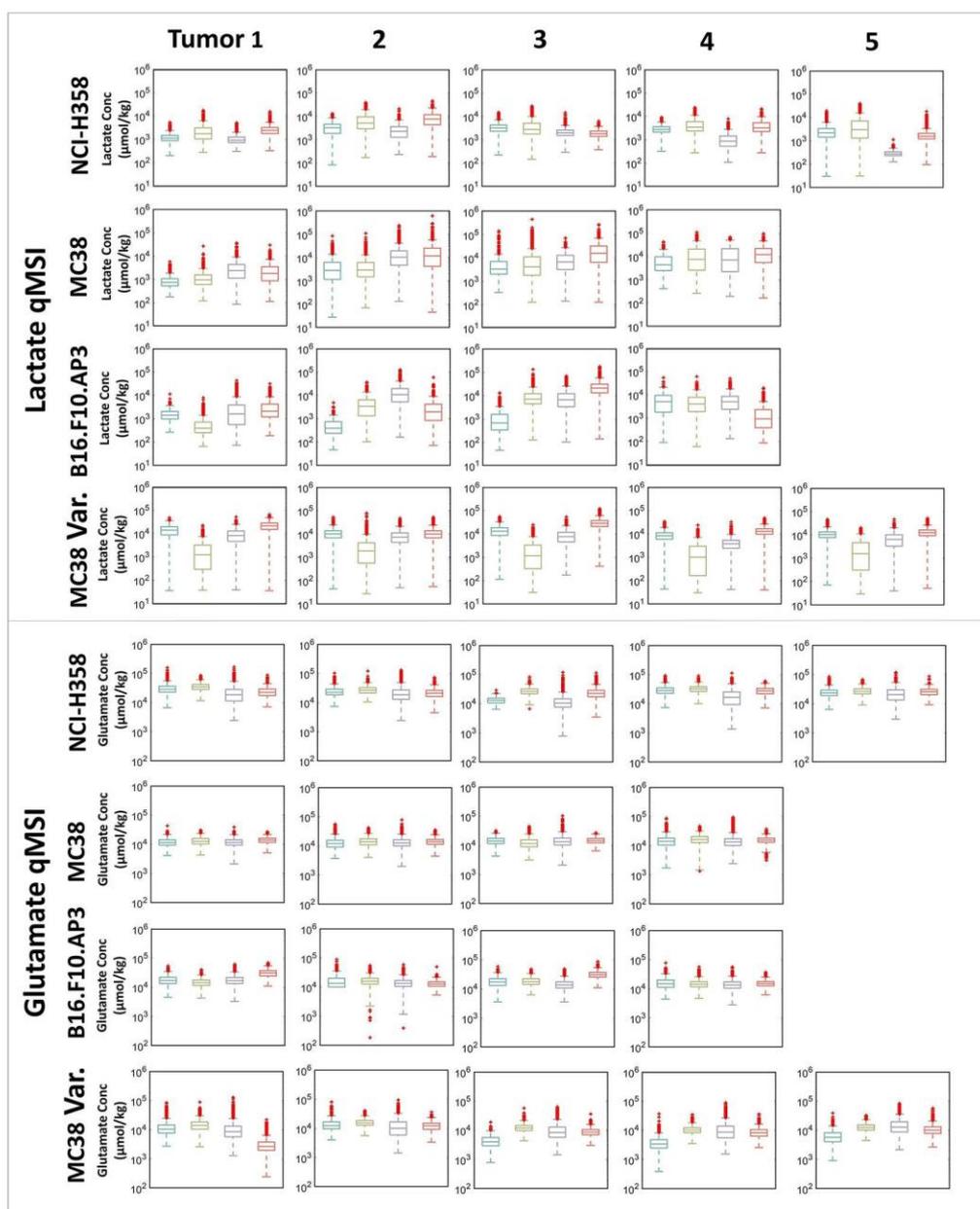
Figure 4. Box plots showing pixel-by-pixel region-specific lactate and glutamate concentrations. The box colors correspond to the colors used in the clustering images (representing different spectral clusters) in Figure 3b,c. The box plots show the differing heterogeneities of the concentrations of lactate and glutamate based on the different tumor models. The MC38-variant and NCI-H358 tumors have more homogeneously distributed lactate concentrations compared with the B16.F10.AP3 and MC38 models. The glutamate concentrations are more homogeneous than the lactate concentrations in all the models.

■ CONCLUSION

Early confirmation of drug efficacy is of great value to drug-discovery projects. Cellular or enzymatic assays can be used to determine compound potency but are rarely a substitute for in vivo experiments in preclinical animal models. Determination of efficacy end points that are directly related to the target pathway in the form of endogenous-metabolite differences in diseased human tissue is a gold standard. This can, however, be misleading in complex tissue environments such as tumor tissues because of the localization of the metabolites into different tissue compartments within the tumor.

Here, we have established sample-pretreatment protocols that minimize the degradation of endogenous metabolites within sectioned tissues; all tissues are handled in a standardized way and stored under the same conditions to ensure any degradation that occurs is uniform across all sections in the same experiment. We have demonstrated that MSI can be successfully used to assess the distribution and quantitation of endogenous metabolites within different tumor models; furthermore, we have shown how spectral clustering can be used to generate region-specific concentration data within tumor sections to give a more empirical illustration of tumor

heterogeneity. Quantitative MSI methods such as those reported in this work have the sensitivity to evaluate efficacy following a therapeutic intervention. The multiplex nature of the qMSI methods can allow the simultaneous quantitation of several endogenous compounds in the same tissue section, and it can also be used to encompass different endogenous compound classes, such as lipids, peptides, and proteins, that can modulate with disease state and give evidence of target engagement or drug efficacy in many other potential therapeutic targets.

■ ASSOCIATED CONTENT

⑤ Supporting Information

The Supporting Information is available free of charge on the ACS Publications website at DOI: 10.1021/acs.analchem.7b05239.

> Tissue-embedding methodology, cryo-sectioning details, MALDI-matrix application, details of the DESI-MSI methodology, and method used for tissue homogenization and analysis by LC-MS (PDF)

■ AUTHOR INFORMATION

Corresponding Author

*Email: john.swales@astrazeneca.com. Tel.: +44(0)1223 223417.

ORCID ⓘ

John G. Swales: 0000-0002-4792-0037

Alex Dexter: 0000-0001-8536-4417

Per E. Andren: 0000-0002-4062-7743

Author Contributions

P.M.G., M.M., and S.C. designed all the in vivo studies and contributed to the manuscript. F.M. developed the homogenization methodology and produced all the LC-MS data. J.G.S., G.H., A.N., and C.H. developed the quantitative MSI methodology and performed all of the imaging experiments. J.G.S. and N.S. designed and performed the stability experiments and DESI-MSI analysis. A.D. performed additional data processing. R.J.A.G., M.R.C., P.E.A., and J.B. contributed to the production of the manuscript, general methodology discussions, and support. J.G.S. wrote the manuscript with feedback from all authors.

Notes

The authors declare no competing financial interest.

■ ACKNOWLEDGMENTS

■ REFERENCES

(1) Warburg, O. *Science* **1956**, *123* (3191), 309−314.

(2) Vander Heiden, M. G.; Cantley, L. C.; Thompson, C. B. *Science* **2009**, *324* (5930), 1029−1033.

(3) Scott, K. E. N.; Cleveland, J. L. *Cell Metab.* **2016**, *24* (5), 649−650.

(4) Swales, J. G.; Wilkinson, G.; Gallagher, R.; Hammond, C.; O'Donnell, C.; Peter, R. *Int. J. High Throughput Screening* **2010**, *1*, 1−14.

(5) Coe, R. *Regul. Toxicol. Pharmacol.* **2000**, *31* (2), S1−S3.

(6) Rönquist-Nii, Y.; Edlund, P. O. *J. Pharm. Biomed. Anal.* **2005**, *37* (2), 341−350.

(7) Swales, J. G.; Tucker, J. W.; Strittmatter, N.; Nilsson, A.; Cobice, D.; Clench, M. R.; Mackay, C. L.; Andren, P. E.; Takats, Z.; Webborn, P. J.; Goodwin, R. J. *Anal. Chem.* **2014**, *86* (16), 8473−8480.

(8) Manicke, N. E.; Nefliu, M.; Wu, C.; Woods, J. W.; Reiser, V.; Hendrickson, R. C.; Cooks, R. G. *Anal. Chem.* **2009**, *81* (21), 8702−8707.

(9) van Remoortere, A.; van Zeijl, R. J.; van den Oever, N.; Franck, J.; Longuespee, R.; Wisztorski, M.; Salzet, M.; Deelder, A. M.; Fournier, L; McDonnell, L. A. *J. Am. Soc. Mass Spectrom.* **2010**, *21* (11), 1922−1929.

(10) Beine, B.; Diehl, H. C.; Meyer, H. E.; Henkel, C. Tissue MALDI Mass Spectrometry Imaging (MALDI MSI) of Peptides. In *Proteomics in Systems Biology: Methods and Protocols*; Reinders, J., Ed.; Springer: New York, NY, 2016; pp 129−150.

(11) Ashton, S.; Song, Y. H.; Nolan, J.; Cadogan, E.; Murray, J.; Odedra, R.; Foster, J.; Hall, P. A.; Low, S.; Taylor, P.; Ellston, R.; Polanska, U. M.; Wilson, J.; Howes, C.; Smith, A.; Goodwin, R. J.; Swales, J. G.; Strittmatter, N.; Takats, Z.; Nilsson, A.; Andren, P.; Trueman, D.; Walker, M.; Reimer, C. L.; Troiano, G.; Parsons, D.; De Witt, D.; Ashford, M.; Hrkach, J.; Zale, S.; Jewsbury, P. J.; Barry, S. T. *Sci. Transl. Med.* **2016**, *8* (325), 325ra17.

(12) Reyzer, M. L.; Hsieh, Y.; Ng, K.; Korfmacher, W. A.; Caprioli, R. M. *J. Mass Spectrom.* **2003**, *38* (10), 1081−1092.

(13) Takats, Z.; Wiseman, J. M.; Gologan, B.; Cooks, R. G. *Science* **2004**, *306* (5695), 471−473.

(14) Eikel, D.; Vavrek, M.; Smith, S.; Bason, C.; Yeh, S.; Korfmacher, W. A.; Henion, J. D. *Rapid Commun. Mass Spectrom.* **2011**, *25* (23), 3587−3596.

(15) Goodwin, R. J. A.; Nilsson, A.; Mackay, C. L.; Swales, J. G.; Johansson, M. K; Billger, M.; Andrén, P. E.; Iverson, S. L. *J. Biomol. Screening* **2016**, *21* (2), 187−193.

(16) Cobice, D. F.; Goodwin, R. J. A.; Andren, P. E.; Nilsson, A.; Mackay, C. L.; Andrew, R. *Br. J. Pharmacol.* **2015**, *172* (13), 3266−3283.

(17) Dekker, T. J.; Jones, E. A.; Corver, W. E.; van Zeijl, R. J.; Deelder, A. M.; Tollenaar, R. A.; Mesker, W. E.; Morreau, H.; McDonnell, L. A. *Anal. Bioanal. Chem.* **2015**, *407* (8), 2167−2176.

(18) Ait-Belkacem, R.; Bol, V.; Hamm, G.; Schramme, F.; Van Den Eynde, B.; Poncelet, L.; Pamelard, F.; Stauber, J.; Gomes, B. *SLAS Discovery* **2017**, *22* (10), 1182−1192.

(19) Chumbley, C. W.; Reyzer, M. L.; Allen, J. L.; Marriner, G. A.; Via, L. E.; Barry, C. E., 3rd; Caprioli, R. M. *Anal. Chem.* **2016**, *88* (4), 2392−2398.

(20) Kallback, P.; Shariatgorji, M.; Nilsson, A.; Andren, P. E. *J. Proteomics* **2012**, *75* (16), 4941−4951.

(21) Race, A. M.; Palmer, A. D.; Dexter, A.; Steven, R. T.; Styles, I. B.; Bunch, J. *Anal. Chem.* **2016**, *88* (19), 9451−9458.

(22) Dexter, A.; Race, A.; Styles, I.; Bunch, J. *Anal. Chem.* **2016**, *88*, 10893−10899.

(23) Bhattacharyya, A. *Bull. Calcutta Math. Soc.* **1943**, *35*, 99−109.

7.0 SUMMARY AND CONCLUSIONS

Mass spectrometry techniques have revolutionised pharmaceutical R&D. The industry has faced ever increasing pressure to develop and market drugs faster and with less attrition. To address this increased throughput a specific, sensitive, robust and versatile analytical technique was needed to keep up with the move to early, parallel elucidation of physiochemical and pharmacokinetic properties. By developing mass spectrometry based techniques for bioanalysis researchers were able to streamline sample preparation protocols capitalise on the multiplexed mass detection in order to simultaneously analyse several different analytes all in the same sample. This had a profound effect on how scientists conducted both *in vitro* and *in vivo* studies.

7.1 Cassette dosing and analysis (Chapter 3)

The ability of mass spectrometry techniques to analyse multiple compounds in a single analysis was a new paradigm in bioanalysis which in turn, allowed scientists to re-evaluate how they conducted animal studies. For the first time researchers could simultaneous dose several compounds to animals all at the same time, typically called cassette dosing (or N-in-one dosing). The technique quickly gained widespread use for the elucidation of both oral and intravenous pharmacokinetic parameters of new chemical entities. These high throughput bioanalytical techniques gave quick and robust information about compound bioavailability and residence time within the body, enabling drug discovery projects to rapidly adapt design, make, test cycles to optimise potential new drugs, but did not address the question of drug distribution or indeed, reveal any localisation of a drug or its metabolites in the bodies major organs.

Mass spectrometry imaging had the potential to address these short comings and provide spatially resolved distribution data directly from these high throughput cassette dosed studies. As part of this thesis a study was undertaken to assess the impact MSI could have on cassette dosed studies. Hans Wistar rats were dosed either orally (PO) or intravenously (IV) with a cassette containing 4 non-proprietary pharmaceutical compounds or discretely with a representative compound from the cassette. Tissue samples were taken at 15 mins post dose for intravenously dosed animals or 2 and 6 hrs post dose for orally dosed animals.

7.1.1 MSI of cassette dosed drugs – Intravenous administration

MALDI, DESI and LESA-MSI were used to assess the distribution of midazolam, bufuralol, clozapine and haloperidol in rat brain tissue sections after intravenous administration at 2 mg/kg/compound. The results from each platform are compared in chapter 3, figure 1. MALDI-MSI was initially used to analyse the samples, this technique successfully mapped the distribution of clozapine in brain but failed to detect the three other compounds in the cassette, despite experimentation with different MALDI matrices and solvent systems. DESI-MSI had more success, managing to detect bufuralol, clozapine and haloperidol and map the distribution of each compound in the brain tissue sections. Midazolam was detected in the brain sections but was of relatively low abunadance and it was not detected with sufficient mass accuracy to confirm identity. It was speculated that the limited positive detection rate of MALDI and DESI-MSI could be due to a variety of different reasons such as ion suppression or inherent low sensitivity of the MSI platforms to detect the compounds at the levels dosed and at the spatial resolution acquired (100 and 150 µm for MALDI and DESI

respectively) in the analysis. LESA-MSI, acquired at much lower spatial resolution, was successfully used to detect all of the four cassette dosed compounds in the brain tissue. The distribution profile of each drug was similar with all compounds showing relatively high abundance in the frontal cortex with little distribution into the rear left and right hemishperes of the cerebrum. The higher detection rate for LESA-MSI was attributed to the fundamentals of the technique, namely, wide chemical applicability due to the interface being based upon classical ESI, Increased sensitivity based on the lower spatial resolution and higher sampling area and the combination of the technique with a highly sensitive triple quadrupole mass spectrometer operating in low signal to noise ratio selected reaction monitoring mode.

7.1.2   MSI of cassette dosed drugs – Oral administration

A larger and more comprehensive study was designed to compare cassette dosing to discrete dosing after oral administration. Moxifloxacin, olanzapine, erlotinib and terfenadine were cassette dosed to Hans Wistar rats at 25, 10, 10 and 25 mg/kg respectively. In addition to the cassette dosing some animals were discretely dosed with either 25 mg/kg moxifloxacin or 10 mg/kg olanzapine. Plasma analysis by LC-MS/MS revealed that all of the animals were successfully exposed to the drugs and that plasma concentrations of moxifloxacin and olanzapine were comparable between the cassette and discretely dosed animals indicating that dosing in a cassette was valid and had not caused any drug-drug interactions resulting in differences in exposure.

Kidney sections were analysed using MALDI-MSI (chapter 3, figure 2). The detection rate for this analysis was 100% with all compound distributions being mapped at both

2 h and 6 h post dose for cassette and discretely dosed samples. All compounds showed a marked reduction in relative abundance between the 2 h and 6 h time point in the range 3-30 fold. This was reflected in the decrease in concentrations observed in the LC-MS/MS plasma analysis. Erlotinib and terfenadine were distributed in both the cortex and medulla of the kidneys whereas moxifloxacin and olanzapine were more localised in the medullary region. Consistent results between the discretely dosed moxifloxacin and olanzapine and the cassette dosed counterparts provided validation of the cassette dosing approach.

Adjacent sections to those analysed by MALDI-MSI were subsequently analysed using LESA-MSI (chapter 3, figure 3). This analysis was done to provide some validation of the MALDI-MSI results by a complementary imaging technique and further substantiate the use of cassette dosing and MSI as a viable drug distribution tool in pharmacokinetic studies. Results from LESA-MSI correlated with those generated in the MALDI-MSI analysis showing a clear difference between the relative abundance of the analytes at 6 h compared to 2 h and good reproducibility of the distribution between the discrete and cassette dosed compounds.

7.1.3   High Spectral and high spatial resolution MSI

The versatility of the MALDI-MSI was further explored using high spectral and high spatial resolution mass spectrometry imaging. Lung tissue sections were analysed from the oral study, the presence of the dosed analytes was confirmed by accurate mass and comparison with vehicle dosed control tissues. High spatial resolution MALDI-MSI was used on adjacent sections to exemplify the power of the technique.

Chapter 3, figure 4 shows the distribution of olanzapine in the lung tissue overlaid with the distribution of heme as a marker for the tissue vasculature.

7.2   Blood-brain barrier penetration studies (chapter 4)

Blood brain barrier penetration of potential new drugs has typically been difficult to accurately measure. Standard methods involve LC-MS/MS analysis of whole brain homogenates which yields a concentration of the drug throughout the entire brain but does not account for any localisation of the compound into specific compartments. If localisation does occur, the concentration of the drug is effectively diluted by the areas of the tissue where no drug is present leading to misleading results. Homogenate data is hindered further by the high levels of vasculature within the brain, the blood vessels contain residual blood which in turn contains drug, leading to an over-estimation of the brain concentration. MSI techniques can potentially mitigate these factors due to the inherent spatial resolution of the analysis and the multiplex nature of the techniques, allowing simultaneous mapping of blood markers (heme) to differentiate between residual blood contamination and real penetration of the drug substance into tissue. Liu et al. reported MALDI-MSI methodology that spatially resolved a compounds distribution across brain sections and correlated endogenous heme relative abundance to separate drug penetration in parenchymal tissue for residual blood contamination[208]. LESA-MSI had been shown in chapter 3 to be a useful technique to map the distribution of drugs in tissue, here the method is applied to BBB penetration studies and compared with gold standard LC-MS/MS analysis.

A study was designed to assess the BBB penetration of a set of non-proprietary drug compounds. The compounds were selected based on historical homogenisation data that suggested they were either brain penetrative (MK-0916 and SCH23390) or poorly penetrative (AZD4017 and AZD8329). The poorly penetrative compounds having a brain/plasma ratio of 0.01 and 0.02 respectively with corresponding brain concentrations of 0.07 and 0.1 µM that were attributed to residual blood contamination.

Compounds were dosed as cassettes containing a penetrative and poorly penetrative compound by either IV (SCH23390 and AZD8329) or PO (MK-0916 and AZD4017) administration. Animals were culled at either 30 min or 2 h post PO dose or 1 min and 30 min post IV admistration.

7.2.1 Assessing BBB penetration after oral administration

MALDI-MSI analysis detected both SCH23390 and MK-0916 and revealed a temporal difference between the early and late timepoints that reflected the known pharmacokinetics of the compounds (Chapter 4, figure 1). SCH23390 signal intensity was relatively high in the 1 min brain sample but was indistinguishable from vehicle dosed tissue at the 30 min timepoint. AZD4017 and AZD8329 were undetected by MALDI-MSI, this posed a unique opportunity to highlight the increased sensitivity LESA-MSI could deliver in this type of analysis, furthermore, the spatial resolution of LESA-MSI could be demonstrated to have significant advantages over homogenisation techniques.

LESA-MSI was performed on adjacent brain tissue sections to those analysed by MALDI-MSI. Mass spectrometry images of AZD4017 and MK-0916 can be seen in chapter 4, figure 2. MK-0916 distribution by LESA-MSI was comparable to the images generated by MALDI-MSI. LESA-MSI did however detect AZD4017, signal intensity of the compound was low but distinctly higher than the background response from vehicle dosed tissue. This confirmed the higher sensitivity of the technique over MALDI-MSI. Correlation of the AZD4017 signal intensity with the signal intensity of heme was good, suggesting the response could be attributed to residual blood contamination but examination of the images revealed that the compound had a low level homogeneous distribution throughout the brain tissue indicating it was brain

penetrative. This demonstrated the advantages of LESA-MSI over homogenisation techniques, which had classed AZD4017 as nonpenetrant and highlights the value spatially resolved analysis can have when assessing marginally BBB penetrative drugs.

7.2.2   Assessing BBB penetration after intravenous dosing

LESA-MSI successfully detected both SCH23390 and AZD8329 in brain tissue at both the 1 min and 30 min timepoints, again highlighting the higher sensitivity of the LESA-MSI technique over MALDI-MSI analysis. SCH23390 distribution was comparable to that observed in the 1 min sample analysed by MALDI–MSI. SCH23390 signal intensity in the brain sections at 30 min post dose was higher than that observed in vehicle dosed tissue. AZD8329 was detected at low signal intensities in both the 1 min and 30 min brain sections, again this was significantly higher than the background response in control tissue. AZD8329 signal intensity was consistent across the 1 min and 30 min timepoints with both also showing a homogeneous distribution of the compound throughout the tissue indicating the compound is poorly penetrant. Correlation of the compound signal intensity against that observed from heme confirmed the homogeneous distribution and penetration of the compound into brain tissue at low levels, a result that was missed using homogenisation methods.

7.2.3   Application of LESA-MSI in drug project BBB penetration studies

LESA-MSI was applied to the analysis of AZx, a compound being developed within the cardiovascular therapeutic area within AstraZeneca. The LESA-MSI analysis of rat brain tissue sections revealed that AZx was highly localised into various 'hot spots' throughout the tissue (chapter 3, figure 4). The signal intensity of AZx correlated well with heme indicating the response could be attributed to residual blood contamination. In addition the compound was not present in areas of the brain tissue which did not contain heme confirming the compound had very poor brain penetration. MALDI-MSI was used to analyse adjacent tissue sections confirming AZx co-location with heme, providing further validation of the LESA-MSI technique and indicating that LESA-MSI could be used to highlight localisation of drugs in tissues even at low (1000 µm) spatial resolution.

7.3   Quantitation of drugs in tissues using MSI (chapter 5)

Quantitative MSI techniques have been widely reported and discussed earlier in this thesis (chapter 1.5). LESA-MSI had been shown in chapters 3 and 4 to be an effective tissue imaging technique, generating low spatial resolution qualitative images that had been validated against MALDI and DESI-MSI as other representative imaging techniques. The next logical step was to assess the suitability of LESA-MSI to perform quantitation experiments of drugs in tissues.

A study was designed in Hans Wistar rats that dosed 1 animal with vehicle, 2 animals were dosed discretely with olanzapine (10 mg/kg) and 2 animals were dosed with a cassette of four compounds, moxifloxacin, olanzapine, erlotinib and terfenadine at 25, 10, 10 and 25 mg/kg respectively. Liver samples were taken at necropsy at 2 and 6 hrs post dose, post sectioning the amount of each drug in liver samples was quantified using LESA-MSI, DESI-MSI and by LC-MS/MS after homogenisation.

7.3.1   Mimetic tissues

LESA-MSI is a low resolution imaging method, typically creating images with a spatial resolution of 1000 µm pixel to pixel. The low spatial resolution of the technique rendered the qMSI 'spotting' technique unsuitable for use in this instance due to the limited size of the calibration spots, this would mean only a single extraction could be done at each calibration point. Instead, the tissue mimetic model was employed to provide homogenised tissue 'spiked' with the analytes at various calibration concentrations, these homogenates could then be frozen and sectioned to give tissue sections large enough to perform at least 10 extractions per calibration point.

7.3.2 Optimisation of LESA methods (Appendix II)

In order to establish a reliable, robust quantitation method it was necessary to firstly optimise the LESA extraction method. The LESA extraction solvent, tissue thickness, solvent dwell time and the effect of using an internal standard in the analysis were all explored. Mimetic liver tissue standards were used as representative homogeneous tissues to perform the optimisation experiments. The mimetics were spiked with a cassette of four compounds (clozapine, albendazole, tamoxifen and astemizole) to cover a LogD range between 2.9 and 4.0.

Optimisation of the extraction solution using isopropyl alcohol, methanol and acetonitrile was performed (appendix II, figure SI 1). Signal intensities of the extracted compounds varied significantly depending on which solvent was used in the solution and the proportion they were diluted with water. Acetonitrile mixed in a ratio of 60/40 *v/v* with water was found to be the optimum solvent composition in terms of extraction efficiency, robustness and reproducibility. Tissue thickness was found to only negligibly effect the intensity of compounds extracted from the mimetic tissues standards (appendix II, figure SI 2), 12 µm was subsequently used to maintain consistency with other MSI methods. Solvent dwell time was found to be optimal at 3 secs per extraction, shorter times resulting in lower signal intensities of drugs extracted and longer dwell times resulting in loss of the liquid micro-junction between the pipette tip and the tissue surface (appendix II, figure SI 3). The use of an internal standard (IS) either sprayed across the tissue (using a nubulising automated sprayer) or spiked directly into the extraction solvent was explored using both structurally similar and stable isotope-labelled versions of the analytes. The use of an IS sprayed over the tissue was shown to increase signal intensity variability using both the structurally similar compound and the stable isotope-labelled variant. Inclusion of the stable

labelled compound into the extraction solvent was found to improve variability (appendix II, SI table 1-3).

7.3.3   Quantitation of study samples using LESA-MSI

Rat liver sections taken from the vehicle, cassette and discretely dosed animals were analysed using LESA-MSI. Alongside these 'unknown' samples liver mimetics cassette spiked with different concentrations of each compound in the range 0 – 100 nmol/g were analysed in the same analytical run. The analytes were found to be distributed continuously but at various abundances throughout the study samples (chapter 5, figure 1). Calibration curves derived from the mimetic liver tissues were found to be acceptable in terms of linearity and linear range for subsequent back calculation of the compounds in the 'unknown' samples. Accuracy of the measured concentration versus the nominal concentration of each calibration standard was also found to be within the limits normally accepted for bioanalysis (chapter 5, figure 2). These results indicated that LESA-MSI could be used as a viable quantitative technique for the measurement of drug concentrations in tissues.

7.3.4 Comparison of LESA-qMSI with tissue homogenisation and DESI-qMSI

The mean intensity for each 'unknown' liver section was back calculated from the mimetic calibration curves for each compound giving a concentration value that could be directly compared to concentration values generated from the same sample of liver by homogenisation followed by analysis by LC-MS/MS. Adjacent tissue sections were also analysed using DESI-MSI, again, using the mimetic calibration standards alongside the 'unknowns'. Correlation between the results generated by LESA-MSI and those generated by LC-MS/MS ranged from 3.8 – 35.1% difference across the different compounds and time-points. These values are considered to be within the variance expected when comparing different analytical techniques and provided some validation of the LESA-MSI quantitation against what is recognised as the gold standard for quantitative measurement. DESI-MSI quantitation was performed as a direct comparison of LESA-MSI with another imaging technique. DESI-MSI compared well with LESA-MSI showing (using DESI as the standard) between 0.8 – 44.4% difference across the different compounds and timepoints. This gives further validation of the use of LESA-MSI as a quantitative technique. DESI-MSI was also compared to the data generated using LC-MS/MS displaying a range of 5.4 – 41.2% difference for olanzapine, moxifloxacin, erlotinib and terfenadine. This was the first time quantitative DESI-MSI had been reported in comparison with data generated by alternative techniques.

The data supported the use of LESA-MSI as a credible, quantitative technique for the measurement of drug concentrations in tissues, furthermore, it showed that the tissue mimetic model of calibration standard preparation worked across two different imaging

platforms, having already been used in MALDI-MSI analysis by Groseclose and Castellino[116] indicating its applicability across multple modes of qMSI.

7.4 Quantitation of endogenous metabolites in tumour tissues using MSI (chapter 6)

The research described in chapter 5 explored LESA and DESI-qMSI methodology and established the techniques as reliable quantitative methods to assess the concentration of drugs in tissues. The acquisition of drug concentrations in target tissues or at sites of toxicity is important information for researchers, allowing for example, evaluation of drug level coverage over an enzymatic IC_{50} in order to indicate the duration of effect or allowing calculation of toxicity dose margins. qMSI techniques have the potential not only monitor drug distribution and concentration but also monitor drug induced changes in endogenous molecule levels such as metabolites, lipids, proteins and peptides. Furthermore, insights into the distribution of these endogenous compounds could help with understanding the complex tissue architecture in diseases such as cancer.

Cellular metabolism is often different between healthy tissue and cancer cells. Drug targets often inhibit metabolic pathways leading to up and down regulation of key metabolic markers. Chapter 6 focusses on using qMSI techniques to quantify endogenous metabolites involved in cellular metabolism. Lactate and glutamate are intrinsically involved in cellular energy production in processes such as glycolysis, glutaminolysis and Krebs cycle. Measurement of any drug induced changes in these metabolites within tumours would offer direct evidence of compound efficacy. Quantitation of these key changes, together with drug levels can then be used to build accurate and robust *in-silico* pharmacokinetic/pharmacodynamic models to evaluate the potential efficacy of new chemical entities and reduce the number of *in vivo* experiments and animals used to develop new medicines.

7.4.1 Stabilisation of endogenous amino acids in tissues

In order to establish a reliable, robust quantitation platform it was necessary to ensure that any sample pre-treatment minimised any endogenous compound degradation within the tissues. An experiment was designed to evaluate the stability of four endogenous metabolites: lactate, glutamate, aspartate and glutamine, throughout the MSI pre-treatment workflow. Kidney sections were fixed and stored under different conditions over a 24 h period, either (1) left in the cryostat thaw-mounted at -16°C, (2) thaw-mounted, desiccated in N_2, vacuum packed and stored at room temperature, or (3) thaw-mounted desiccated in N_2, vacuum packed and stored at -80°C. Analysis was performed using DESI-MSI, a fresh kidney section was applied to each microscope slide directly prior to analysis to give a baseline abundance of the metabolites. Results can be seen in chapter 6, figure 1. Spectral clustering was used to define regions of interest for the cortex and medulla of each kidney and the mean relative abundance of the four amino acids in each region was extracted. The results indicated that kidneys treated and stored under conditions (3) showed far greater stability of the four metabolites in both the cortical and medullary regions of the kidney sections. Even with these protocols in place, degradation could still occur during the time taken to section multiple tissues onto the same microscope slide. To eliminate this risk multiple tissues were embedded in a suitable embedding media to allow the production of multiple tissue sections in a single cut of the cryostat blade, reducing the time the sections spend at temperatures less than -20°C and reducing sample preparation time.

7.4.2 Initial proof of principle for qMSI lactate quantitation

A study was performed in a NCI-H358 human xenograft mouse tumour model (n=20 animals). Animals were dosed with vehicle and euthanised at 0.5, 2, 6 and 24 h post dose to mimic a typical pharmacodynamic study design. Tumours were excised at necropsy, immediately snap frozen and stored at -80°C prior to sectioning. Tumours were sectioned using the protocols set out in section 7.4.1. MALDI-qMSI analysis applying spots of a stable isotope-labelled standard of lactate at different concentrations onto control tissue and forming a calibration line to back calculate lactate levels within the tumour sections from each animal at each time-point was carried out. The results from the analysis (chapter 6, figure 2) showed that the analytical method performed well. Due to the unavailability of a second, different stable-labelled version of lactate to perform pixel to pixel normalisation, the MSI data was normalised using total ion current. Further interpretation of the results revealed that the inter-tumour lactate levels in the tissue had a high level of variation. Lactate distribution was heterogeneous throughout the tissue sections and was present at higher concentration in areas of necrosis. Glutamate distribution was also extracted from the dataset. This was not part of the quantitative study but is of interest as another cellular metabolite involved in energy production. Glutamate distribution was much more homogeneous throughout the tissue sections compared with lactate.

7.4.3 Screening different tumour models for lactate and glutamate concentration and heterogeneity

The high concentration variability and heterogeneous distribution of lactate in the initial qMSI proof of principle study indicated that a tumour model that had lower variability

and a more homogeneous distribution of lactate may allow a more accurate assessment of the endogenous metabolite levels within the tumour tissues and make any modulation in later vehicle matched, drug dosed studies easier to detect. It was decided to screen four different tumour models. An NCI-H358 model, differentiated from the initial study by allowing the tumour to grow for less time and minimise the chance of necrosis, a MC38 model, a B16.F10.AP3 model and an MC38 variant model were all screened using MALDI-qMSI for both lactate and glutamate quantitation and distribution. Results of the analysis can be seen in chapter 6, figure 3a. Tumours from the MC38 and B16.F10.AP3 models showed heterogeneous lactate distribution throughout the tumour tissue with little or no co-localisation with glutamate. The MC38 tissue in particular had large areas of necrosis, B16.F10.AP3 tumours were less necrotic but lactate and glutamate distribution was very localised and 'patchy' throughout the tissue. The NCI-H358 and MC38 variant tumours had more evenly distributed lactate and glutamate even in areas that were confirmed to be necrotic by H&E staining.

Lactate and glutamate concentrations across each of the tissue sections were largely in the same range between the different models fluctuating between 81.7 – 2504.0 μM for lactate and 1095.5 – 7818.7 μM for glutamate.

7.4.4 Region-specific quantitation of lactate and glutamate and assessment of heterogeneity

Spectral clustering was performed on each of the individual tissue sections from each model. This analysis allowed region-specific pixel by pixel quantitation of the lactate and glutamate levels to be calculated, this is represented graphically in the box plots

in chapter 6, figure 4. From the box plots of lactate and glutamate concentration in each region of each tissue, the lactate concentration was much more heterogeneous in the B15.F10.AP3 and MC38 models as seen by the large boxes, whiskers and many outliers. In comparison, the MC38 variant and NCI-H358 tumours had a more homogeneously distributed lactate concentration (smaller boxes) with the MC38 variant displaying lower median inter-tumour lactate concentration variability. The glutamate concentration in all tissue models was overall less heterogeneous than the lactate concentration, with the different models containing similar levels of heterogeneity as seen by similar spreads of the data in the box plots.

The objective of the screening exercise was to identify a tumour model that had greater lactate homogeneity, lower lactate variability and fewer areas of necrosis. The MC38 variant model was selected as the analysis had shown this exhibited the most favourable properties of the four models tested. Subsequently, the MC38 variant model has allowed further efficacy studies to be performed. This was highlighted in initial efficacy study data which showed inter-tumour lactate concentration (measured by LC-MS) in control tumours varied by ±22%.

7.5   Final conclusions

The aim of this thesis was to investigate the use of mass spectrometry methods for profiling drug distribution in biofluids and whole tissues. The work reported herein has shown that mass spectrometry imaging techniques have wide applicability in the field of drug research and development, providing valuable insight into drug distribution, quantitation and efficacy. The techniques discussed were validated against traditional 'gold standard' LC-MS methods where appropriate. It is neither intended or expected

that MSI techniques will replace these tried and tested methods, but act in a complementary capacity when spatially resolved information is required to understand drug efficacy or toxicity. MSI is now being routinely applied to drug projects across the AstraZeneca development portfolio and within other large pharmaceutical development organisations.

References

1   Coe, R. Quantitative whole-body autoradiography. *Regulatory Toxicology and Pharmacology* **31**, S1-S3 (2000).

2   Cross, S. A., Groves, A. & Hesselbo, T. A quantitative method for measuring radioactivity in tissues sectioned for whole-body autoradiography. *The International journal of applied radiation and isotopes* **25**, 381-382 (1974).

3   Rönquist-Nii, Y. & Edlund, P. O. Determination of corticosteroids in tissue samples by liquid chromatography–tandem mass spectrometry. *Journal of pharmaceutical and biomedical analysis* **37**, 341-350 (2005).

4   Baratte, S. *et al.* Quantitation of SU11248, an oral multi-target tyrosine kinase inhibitor, and its metabolite in monkey tissues by liquid chromatograph with tandem mass spectrometry following semi-automated liquid–liquid extraction. *Journal of chromatography A* **1024**, 87-94 (2004).

5   Enthaler, B. *et al.* Improved sample preparation for MALDI-MSI of endogenous compounds in skin tissue sections and mapping of exogenous active compounds subsequent to ex-vivo skin penetration. *Analytical and bioanalytical chemistry* **402**, 1159-1167, doi:10.1007/s00216-011-5562-6 (2012).

6   Swales, J. G. *et al.* Mass spectrometry imaging of cassette-dosed drugs for higher throughput pharmacokinetic and biodistribution analysis. *Analytical chemistry* **86**, 8473-8480, doi:10.1021/ac502217r (2014).

7   Manicke, N. E. *et al.* Imaging of Lipids in Atheroma by Desorption Electrospray Ionization Mass Spectrometry. *Analytical chemistry* **81**, 8702-8707, doi:10.1021/ac901739s (2009).

8   van Remoortere, A. *et al.* MALDI imaging and profiling MS of higher mass proteins from tissue. *J Am Soc Mass Spectrom* **21**, 1922-1929, doi:10.1016/j.jasms.2010.07.011 (2010).

9   Beine, B., Diehl, H. C., Meyer, H. E. & Henkel, C. in *Proteomics in Systems Biology: Methods and Protocols*   (ed Jörg Reinders) 129-150 (Springer New York, 2016).

10   Karas, M., Bachmann, D. & Hillenkamp, F. Influence of the wavelength in high-irradiance ultraviolet laser desorption mass spectrometry of organic molecules. *Analytical chemistry* **57**, 2935-2939 (1985).

11   Caprioli, R., Farmer, T. & Gile, J. Molecular imaging of biological samples: localization of peptides and proteins using MALDI-TOF MS. *Analytical chemistry* **69**, 4751-4760 (1997).

12   Fenn, J., Mann, M., Meng, C., Wong, S. & Whitehouse, C. Electrospray ionization for mass spectrometry of large biomolecules. *Science* **246**, 64-71, doi:10.1126/science.2675315 (1989).

13   Hulme, H. E. *et al.* Mass spectrometry imaging identifies palmitoylcarnitine as an immunological mediator during Salmonella Typhimurium infection. *Scientific reports* **7** (2017).

14   Takats, Z., Wiseman, J. M., Gologan, B. & Cooks, R. G. Mass spectrometry sampling under ambient conditions with desorption electrospray ionization. *Science* **306**, 471-473, doi:306/5695/471 [pii]10.1126/science.1104404 (2004).

15   Shariatgorji, M. *et al.* Simultaneous imaging of multiple neurotransmitters and neuroactive substances in the brain by desorption electrospray ionization mass spectrometry. *NeuroImage* **136**, 129-138, doi:10.1016/j.neuroimage.2016.05.004 (2016).

16   Guenther, S. *et al.* Spatially resolved metabolic phenotyping of breast cancer by desorption electrospray ionization mass spectrometry. *Cancer research* **75**, 1828-1837, doi:10.1158/0008-5472.CAN-14-2258 (2015).

17   Swales, J. G. *et al.* Spatial quantitation of drugs in tissues using liquid extraction surface analysis mass spectrometry Imaging. *Scientific reports* **6**, 37648 (2016).

18   Duncan, K. D., Bergman, H. M. & Lanekoff, I. A pneumatically assisted nanospray desorption electrospray ionization source for increased solvent versatility and enhanced metabolite detection from tissue. *The Analyst* **142**, 3424-3431, doi:10.1039/c7an00901a (2017).

19   Cardoso-Palacios, C. & Lanekoff, I. Direct Analysis of Pharmaceutical Drugs Using Nano-DESI MS. *Journal of analytical methods in chemistry* **2016** (2016).

20   Bergman, H.-M. & Lanekoff, I. Profiling and quantifying endogenous molecules in single cells using nano-DESI MS. *The Analyst* (2017).

21   Atci, E., Ewing, T. & Beyenal, H. in *Meeting Abstracts.* 1849-1849 (The Electrochemical Society).

22   Laskin, J. *et al.* Chemical analysis of complex organic mixtures using reactive nanospray desorption electrospray ionization mass spectrometry. *Analytical chemistry* **84**, 7179-7187 (2012).

23   Lanshoeft, C. *et al.* Analysis of small molecule antibody–drug conjugate catabolites in rat liver and tumor tissue by liquid extraction surface analysis micro-capillary liquid chromatography/tandem mass spectrometry. *Rapid Communications in Mass Spectrometry* **30**, 823-832 (2016).

24   Sarsby, J., Martin, N., Lalor, P., Bunch, J. & Cooper, H. Top-Down and Bottom-Up Identification of Proteins by Liquid Extraction Surface Analysis Mass Spectrometry of Healthy and Diseased Human Liver Tissue. *Journal of the American Society for Mass Spectrometry*, 1-9, doi:10.1007/s13361-014-0967-z.

25   Quanico, J. *et al.* Development of liquid microjunction extraction strategy for improving protein identification from tissue sections. *Journal of proteomics* **79**, 200-218 (2013).

26   Van Berkel, G. J., Kertesz, V., Koeplinger, K. A., Vavrek, M. & Kong, A. N. T. Liquid microjunction surface sampling probe electrospray mass spectrometry for detection of drugs and metabolites in thin tissue sections. *Journal of mass spectrometry* **43**, 500-508 (2008).

27   Chandra, S., Smith, D. R. & Morrison, G. H. Subcellular imaging by dynamic SIMS ion microscopy. *Analytical chemistry* **72**, 104A-114A (2000).

28   Nemes, P. & Vertes, A. Laser ablation electrospray ionization for atmospheric pressure, in vivo, and imaging mass spectrometry. *Analytical chemistry* **79**, 8098-8106 (2007).

29   Muller, L. *et al.* Laser Desorption/Ionization Mass Spectrometric Imaging of Endogenous Lipids from Rat Brain Tissue Implanted with Silver Nanoparticles. *Journal of The American Society for Mass Spectrometry*, 1-13 (2017).

30   Paine, M. R. *et al.* Visualizing molecular distributions for biomaterials applications with mass spectrometry imaging: a review. *Journal of Materials Chemistry B* **5**, 7444-7460 (2017).

31   Jackson, S. N., Wang, H. Y. & Woods, A. S. Direct profiling of lipid distribution in brain tissue using MALDI-TOFMS. *Analytical chemistry* **77**, 4523-4527 (2005).

32   Prideaux, B. *et al.* High-sensitivity MALDI-MRM-MS imaging of moxifloxacin distribution in tuberculosis-infected rabbit lungs and granulomatous lesions. *Analytical chemistry* **83**, 2112-2118, doi:10.1021/ac1029049 (2011).

33   Garrett, T. J. P.-C., M.C.;Kovtoun, V.;Bui, H.; Izgarian, N.; Stafford, G.; Yost, R.A. Imaging of small molecules in tissue sections with a new intermediate-pressure MALDI linear ion trap mass spectrometer. *Int J Mass Spectrom* **260**, 166-176 (2007).

34   Cornett, D., Frappier, S. & Caprioli, R. MALDI-FTICR imaging mass spectrometry of drugs and metabolites in tissue. *Analytical chemistry* **80**, 5648-5653, doi:10.1021/ac800617s (2008).

35   Moor, D., Van De Plas, R. & Waelkens, E.   (Google Patents, 2011).

36   Svensson, M. *et al.* Heat stabilization of the tissue proteome: a new technology for improved proteomics. *Journal of proteome research* **8**, 974-981 (2009).

37   Goodwin, R. J. Sample preparation for mass spectrometry imaging: small mistakes can lead to big consequences. *Journal of proteomics* **75**, 4893-4911, doi:10.1016/j.jprot.2012.04.012 (2012).

38   Sugiura, Y., Shimma, S. & Setou, M. Thin sectioning improves the peak intensity and signal-to-noise ratio in direct tissue mass spectrometry. *Journal of the Mass Spectrometry Society of Japan* **54**, 45-48 (2006).

39   Wisztorski, M., Franck, J., Salzet, M. & Fournier, I. MALDI direct analysis and imaging of frozen versus FFPE tissues: what strategy for which sample? *Mass Spectrometry Imaging: Principles and Protocols*, 303-322 (2010).

40   Dreisewerd, K. The desorption process in MALDI. *Chemical reviews* **103**, 395-426 (2003).

41   Takats, Z., Wiseman, J. M. & Cooks, R. G. Ambient mass spectrometry using desorption electrospray ionization (DESI): instrumentation, mechanisms and applications in forensics, chemistry, and biology. *Journal of Mass Spectrometry* **40**, 1261-1275 (2005).

42   Espadas, G., Borràs, E., Chiva, C. & Sabidó, E. Evaluation of different peptide fragmentation types and mass analyzers in data-dependent methods using an Orbitrap Fusion Lumos Tribrid mass spectrometer. *Proteomics* **17** (2017).

43   Sleno, L., Volmer, D. A. & Marshall, A. G. Assigning product ions from complex MS/MS spectra: the importance of mass uncertainty and resolving power. *Journal of the American Society for Mass Spectrometry* **16**, 183-198 (2005).

44   Dilillo, M. *et al.* Ultra-High Mass Resolution MALDI Imaging Mass Spectrometry of Proteins and Metabolites in a Mouse Model of Glioblastoma. *Scientific reports* **7** (2017).

45   Colsch, B. & Woods, A. S. Localization and imaging of sialylated glycosphingolipids in brain tissue sections by MALDI mass spectrometry. *Glycobiology* **20**, 661-667, (2010).

46   Brulet, M. *et al.* Lipid mapping of colonic mucosa by cluster TOF-SIMS imaging and multivariate analysis in cftr knockout mice. *Journal of lipid research* **51**, 3034-3045, (2010).

47   Wiley, W. & McLaren, I. Rev. Sci. Instrum. (1955).

48   Guilhaus, M., Selby, D. & Mlynski, V. Orthogonal acceleration time-of-flight mass spectrometry. *Mass spectrometry reviews* **19**, 65-107 (2000).

49   Finnigan, R. E. Quadrupole mass spectrometers. *Analytical chemistry* **66**, 969A-975A (1994).

50   Poetzsch, M., Steuer, A. E., Roemmelt, A. T., Baumgartner, M. R. & Kraemer, T. Single hair analysis of small molecules using MALDI-triple quadrupole MS imaging and LC-MS/MS: investigations on opportunities and pitfalls. *Analytical chemistry* **86**, 11758-11765 (2014).

51   Williams, J. P. & Scrivens, J. H. Rapid accurate mass desorption electrospray ionisation tandem mass spectrometry of pharmaceutical samples. *Rapid Communications in Mass Spectrometry* **19**, 3643-3650 (2005).

52   Blatherwick, E. Q. *et al.* Utility of spatially-resolved atmospheric pressure surface sampling and ionization techniques as alternatives to mass spectrometric imaging (MSI) in drug metabolism. *Xenobiotica* **41**, 720-734 (2011).

53   Makarov, A. Electrostatic axially harmonic orbital trapping: a high-performance technique of mass analysis. *Analytical chemistry* **72**, 1156-1162 (2000).

54   Marshall, A. G., Hendrickson, C. L. & Jackson, G. S. Fourier transform ion cyclotron resonance mass spectrometry: a primer. *Mass spectrometry reviews* **17**, 1-35 (1998).

55   Nikolaev, E. N., Kostyukevich, Y. I. & Vladimirov, G. N. Fourier transform ion cyclotron resonance (FT ICR) mass spectrometry: Theory and simulations. *Mass spectrometry reviews* **35**, 219-258 (2016).

56   Fuchser, J., Cornett, S. & Becker, M. High resolution molecular imaging of pharmaceuticals at therapeutic levels. *Bruker Daltonik GmbH*, 4 (2008).

57   Weisbrod, C. R. *et al.* Front-End Electron Transfer Dissociation Coupled to a 21 Tesla FT-ICR Mass Spectrometer for Intact Protein Sequence Analysis. *Journal of The American Society for Mass Spectrometry* **28**, 1787-1795 (2017).

58   Hamm, G. *et al.* in *SFSM 2012*   (Orléans, 2012).

59   Solon, E. G., Schweitzer, A., Stoeckli, M. & Prideaux, B. Autoradiography, MALDI-MS, and SIMS-MS imaging in pharmaceutical discovery and development. *The AAPS journal* **12**, 11-26, doi:10.1208/s12248-009-9158-4 (2010).

60   Schwartz, S. A., Reyzer, M. L. & Caprioli, R. M. Direct tissue analysis using matrix-assisted laser desorption/ionization mass spectrometry: practical aspects of sample preparation. *Journal of mass spectrometry : JMS* **38**, 699-708 (2003).

61   Lemaire, R. *et al.* Direct analysis and MALDI imaging of formalin-fixed, paraffin-embedded tissue sections. *J Proteome Res* **6**, 1295-1305 (2007).

62   Groseclose, M. R., Massion, P. P., Chaurand, P. & Caprioli, R. M. High-throughput proteomic analysis of formalin-fixed paraffin-embedded tissue microarrays using MALDI imaging mass spectrometry. *Proteomics* **8**, 3715-3724, doi:10.1002/pmic.200800495 (2008).

63   Stauber, J. *et al.* MALDI imaging of formalin-fixed paraffin-embedded tissues: application to model animals of Parkinson disease for biomarker hunting. *J Proteome Res* **7**, 969-978, doi:10.1021/pr070464x (2008).

64   Carter, C. L., McLeod, C. W. & Bunch, J. Imaging of phospholipids in formalin fixed rat brain sections by matrix assisted laser desorption/ionization mass spectrometry. *J Am Soc Mass Spectrom* **22**, 1991-1998, doi:10.1007/s13361-011-0227-4 (2011).

65   Ly, A. *et al.* High-mass-resolution MALDI mass spectrometry imaging of metabolites from formalin-fixed paraffin-embedded tissue. *Nature protocols* **11**, 1428-1443 (2016).

66   Goodwin, R. J., Iverson, S. L. & Andren, P. E. The significance of ambient-temperature on pharmaceutical and endogenous compound abundance and distribution in tissues sections when analyzed by matrix-assisted laser desorption/ionization mass spectrometry imaging. *Rapid communications in mass spectrometry : RCM* **26**, 494-498, doi:10.1002/rcm.6125 (2012).

67   Goodwin, R. J. *et al.* Conductive carbon tape used for support and mounting of both whole animal and fragile heat-treated tissue sections for MALDI MS imaging and quantitation. *Journal of proteomics* **75**, 4912-4920 (2012).

68   Goodwin, R. J., Lang, A. M., Allingham, H., Borén, M. & Pitt, A. R. Stopping the clock on proteomic degradation by heat treatment at the point of tissue excision. *Proteomics* **10**, 1751-1761 (2010).

69   Blatherwick, E. Q., Svensson, C. I., Frenguelli, B. G. & Scrivens, J. H. Localisation of adenine nucleotides in heat-stabilised mouse brains using ion mobility enabled MALDI imaging. *International Journal of Mass Spectrometry* **345**, 19-27 (2013).

70   Agar, N. Y., Kowalski, J. M., Kowalski, P. J., Wong, J. H. & Agar, J. N. Tissue preparation for the in situ MALDI MS imaging of proteins, lipids, and small molecules at cellular resolution. *Methods in molecular biology* **656**, 415-431, doi:10.1007/978-1-60761-746-4_24 (2010).

71   Agar, N. Y., Yang, H. W., Carroll, R. S., Black, P. M. & Agar, J. N. Matrix Solution Fixation: Histology-Compatible Tissue Preparation for MALDI Mass Spectrometry Imaging. *Analytical chemistry* **79**, 7416-7423 (2007).

72   Chaurand, P., Norris, J. L., Cornett, D. S., Mobley, J. A. & Caprioli, R. M. New developments in profiling and imaging of proteins from tissue sections by MALDI mass spectrometry. *J Proteome Res* **5**, 2889-2900 (2006).

73   Strohalm, M. *et al.* Poly[N-(2-hydroxypropyl)methacrylamide]-based tissue-embedding medium compatible with MALDI mass spectrometry imaging experiments. *Analytical chemistry* **83**, 5458-5462, doi:10.1021/ac2011679 (2011).

74   Stoeckli, M., Chaurand, P., Hallahan, D. E. & Caprioli, R. M. Imaging mass spectrometry: a new technology for the analysis of protein expression in mammalian tissues. *Nat Med* **7**, 493-496 (2001).

75   Goodwin, R. J., Dungworth, J. C., Cobb, S. R. & Pitt, A. R. Time-dependent evolution of tissue markers by MALDI-MS imaging. *Proteomics* **8**, 3801-3808, doi:10.1002/pmic.200800201 (2008).

76   Taban, I. M. *et al.* Imaging of peptides in the rat brain using MALDI-FTICR mass spectrometry. *J Am Soc Mass Spectrom* **18**, 145-151 (2007).

77   Shariatgorji, M. *et al.* Controlled-pH tissue cleanup protocol for signal enhancement of small molecule drugs analyzed by MALDI-MS imaging. *Analytical chemistry* **84**, 4603-4607, doi:10.1021/ac203322q (2012).

78   Angel, P. M., Spraggins, J. M., Baldwin, H. S. & Caprioli, R. Enhanced sensitivity for high spatial resolution lipid analysis by negative ion mode matrix assisted laser desorption ionization imaging mass spectrometry. *Analytical chemistry* **84**, 1557-1564, doi:10.1021/ac202383m (2012).

79   Diehl, H. C. *et al.* The challenge of on-tissue digestion for MALDI MSI- a comparison of different protocols to improve imaging experiments. *Analytical and bioanalytical chemistry* **407**, 2223-2243, doi:10.1007/s00216-014-8345-z (2015).

80   Franck, J., El Ayed, M., Wisztorski, M., Salzet, M. & Fournier, I. On-tissue N-terminal peptide derivatizations for enhancing protein identification in MALDI mass spectrometric imaging strategies. *Analytical chemistry* **81**, 8305-8317, doi:10.1021/ac901043n (2009).

81   Holst, S. *et al.* Linkage-Specific in Situ Sialic Acid Derivatization for N-Glycan Mass Spectrometry Imaging of Formalin-Fixed Paraffin-Embedded Tissues. *Analytical chemistry* **88**, 5904-5913, doi:10.1021/acs.analchem.6b00819 (2016).

82   Toue, S. *et al.* Microscopic imaging mass spectrometry assisted by on-tissue chemical derivatization for visualizing multiple amino acids in human colon cancer xenografts. *Proteomics* **14**, 810-819, doi:10.1002/pmic.201300041 (2014).

83   Cobice, D. F. *et al.* Mass spectrometry imaging for dissecting steroid intracrinology within target tissues. *Analytical chemistry* **85**, 11576-11584, doi:10.1021/ac402777k (2013).

84   Manier, M. L. *et al.* Reagent precoated targets for rapid in-tissue derivatization of the anti-tuberculosis drug isoniazid followed by MALDI imaging mass spectrometry. *J Am Soc Mass Spectrom* **22**, 1409-1419, doi:10.1007/s13361-011-0150-8 (2011).

85   Shariatgorji, M. *et al.* Pyrylium Salts as Reactive Matrices for MALDI-MS Imaging of Biologically Active Primary Amines. *J Am Soc Mass Spectrom* **26**, 934-939, doi:10.1007/s13361-015-1119-9 (2015).

86   Teuber, K., Fedorova, M., Hoffmann, R. & Schiller, J. 2, 4-Dinitrophenylhydrazine as a new reactive matrix to analyze oxidized phospholipids by MALDI-TOF mass spectrometry. *Analytical Letters* **45**, 968-976 (2012).

87   Flinders, B., Morrell, J., Marshall, P. S., Ranshaw, L. E. & Clench, M. R. The use of hydrazine-based derivatization reagents for improved sensitivity and detection of carbonyl containing compounds using MALDI-MSI. *Analytical and bioanalytical chemistry* **407**, 2085-2094, doi:10.1007/s00216-014-8223-8 (2015).

88   Fournier, I., Day, R. & Salzet, M. Direct analysis of neuropeptides by in situ MALDI-TOF mass spectrometry in the rat brain. *Neuro Endocrinol Lett* **24**, 9-14 (2003).

89   Li, B., Comi, T. J., Si, T., Dunham, S. J. & Sweedler, J. V. A one-step matrix application method for MALDI mass spectrometry imaging of bacterial colony biofilms. *Journal of Mass Spectrometry* **51**, 1030-1035 (2016).

90   Tholey, A. & Heinzle, E. Ionic (liquid) matrices for matrix-assisted laser desorption/ionization mass spectrometry-applications and perspectives. *Analytical and bioanalytical chemistry* **386**, 24-37 (2006).

91   Zubair, F. *et al.* Trypsin and MALDI matrix pre-coated targets simplify sample preparation for mapping proteomic distributions within biological tissues by imaging mass spectrometry. *Journal of Mass Spectrometry* **51**, 1168-1179 (2016).

92   Cerruti, C. D., Benabdellah, F., Laprevote, O., Touboul, D. & Brunelle, A. MALDI imaging and structural analysis of rat brain lipid negative ions with 9-aminoacridine matrix. *Analytical chemistry* **84**, 2164-2171, doi:10.1021/ac2025317 (2012).

93   Eveque-Mourroux, M. *et al.*   (BMJ Publishing Group Ltd, 2017).

94   Sun, G. *et al.* Matrix-assisted laser desorption/ionization time-of-flight mass spectrometric analysis of cellular glycerophospholipids enabled by multiplexed solvent dependent analyte–matrix interactions. *Analytical chemistry* **80**, 7576-7585 (2008).

95   Thomas, A., Charbonneau, J. L., Fournaise, E. & Chaurand, P. Sublimation of new matrix candidates for high spatial resolution imaging mass spectrometry of lipids: enhanced information in both positive and negative polarities after 1,5-diaminonapthalene deposition. *Analytical chemistry* **84**, 2048-2054, doi:10.1021/ac2033547 (2012).

96   Debois, D., Bertrand, V., Quinton, L., De Pauw-Gillet, M. C. & De Pauw, E. MALDI-in source decay applied to mass spectrometry imaging: a new tool for protein identification. *Analytical chemistry* **82**, 4036-4045, doi:10.1021/ac902875q (2010).

97   Spraggins, J. M. *et al.* Next-generation technologies for spatial proteomics: Integrating ultra-high speed MALDI-TOF and high mass resolution MALDI FTICR imaging mass spectrometry for protein analysis. *Proteomics* **16**, 1678-1689 (2016).

98   Pagni, F. *et al.* Proteomics in thyroid cytopathology: Relevance of MALDI-imaging in distinguishing malignant from benign lesions. *Proteomics* **16**, 1775-1784 (2016).

99   Astigarraga, E. *et al.* Profiling and imaging of lipids on brain and liver tissue by matrix-assisted laser desorption/ionization mass spectrometry using 2-mercaptobenzothiazole as a matrix. *Analytical chemistry* **80**, 9105-9114 (2008).

100   de San Román, E. G., Manuel, I., Giralt, M., Ferrer, I. & Rodríguez-Puertas, R. Imaging mass spectrometry (IMS) of cortical lipids from preclinical to severe stages of Alzheimer's disease. *Biochimica et Biophysica Acta (BBA)-Biomembranes* (2017).

101   Bowrey, H. E. *et al.* Imaging mass spectrometry of the visual system: advancing the molecular understanding of retina degenerations. *PROTEOMICS-Clinical Applications* **10**, 391-402 (2016).

102   Giampà, M. *et al.* Maleic anhydride proton sponge as a novel MALDI matrix for the visualization of small molecules (< 250 m/z) in brain tumors by routine MALDI ToF imaging mass spectrometry. *Chemical Communications* **52**, 9801-9804 (2016).

103   Li, S. *et al.* Electrospray deposition device used to precisely control the matrix crystal to improve the performance of MALDI MSI. *Scientific reports* **6**, 37903 (2016).

104   Nakanishi, T., Ohtsu, I., Furuta, M., Ando, E. & Nishimura, O. Direct MS/MS analysis of proteins blotted on membranes by a matrix-assisted laser desorption/ionization-quadrupole ion trap-time-of-flight tandem mass spectrometer. *Journal of proteome research* **4**, 743-747 (2005).

105   Aerni, H. R., Cornett, D. S. & Caprioli, R. M. Automated acoustic matrix deposition for MALDI sample preparation. *Analytical chemistry* **78**, 827-834 (2006).

106   Schuerenberg, M. & Deininger, S.-O. in *Imaging Mass Spectrometry*   87-91 (Springer Japan, 2010).

107   Sugiura, Y., Honda, K. & Suematsu, M. in *Chronic Inflammation*   147-160 (Springer, 2016).

108   Anderson, D. M., Spraggins, J. M., Rose, K. L. & Schey, K. L. High spatial resolution imaging mass spectrometry of human optic nerve lipids and proteins. *J Am Soc Mass Spectrom* **26**, 940-947, doi:10.1007/s13361-015-1143-9 (2015).

109   Hankin, J. A., Barkley, R. M. & Murphy, R. C. Sublimation as a method of matrix application for mass spectrometric imaging. *Journal of the American Society for Mass Spectrometry* **18**, 1646-1652 (2007).

110   Hankin, J. A., Barkley, R. M. & Murphy, R. C. Sublimation as a method of matrix application for mass spectrometric imaging. *J Am Soc Mass Spectrom* **18**, 1646-1652, doi:10.1016/j.jasms.2007.06.010 (2007).

111   Goodwin, R. J., Scullion, P., Macintyre, L., Watson, D. G. & Pitt, A. R. Use of a solvent-free dry matrix coating for quantitative matrix-assisted laser desorption ionization imaging of 4-bromophenyl-1,4-diazabicyclo(3.2.2)nonane-4-carboxylate in rat brain and quantitative

analysis of the drug from laser microdissected tissue regions. *Analytical chemistry* **82**, 3868-3873, doi:10.1021/ac100398y (2010).

112   Goodwin, R. J. A. *et al.* Qualitative and Quantitative MALDI Imaging of the Positron Emission Tomography Ligands Raclopride (a D2 Dopamine Antagonist) and SCH 23390 (a D1 Dopamine Antagonist) in Rat Brain Tissue Sections Using a Solvent-Free Dry Matrix Application Method. *Analytical chemistry* **83**, 9694-9701, doi:10.1021/ac202630t (2011).

113   Ferguson, L. S., Creasey, S., Wolstenholme, R., Clench, M. R. & Francese, S. Efficiency of the dry–wet method for the MALDI-MSI analysis of latent fingermarks. *Journal of Mass Spectrometry* **48**, 677-684, doi:10.1002/jms.3216.

114   Grove, K. J., Frappier, S. L. & Caprioli, R. M. Matrix pre-coated MALDI MS targets for small molecule imaging in tissues. *Journal of The American Society for Mass Spectrometry* **22**, 192-195 (2011).

115   Nilsson, A. *et al.* Fine mapping the spatial distribution and concentration of unlabeled drugs within tissue micro-compartments using imaging mass spectrometry. *PloS one* **5**, e11411, doi:10.1371/journal.pone.0011411 (2010).

116   Groseclose, M. R. & Castellino, S. A mimetic tissue model for the quantification of drug distributions by MALDI imaging mass spectrometry. *Analytical chemistry* **85**, 10099-10106, doi:10.1021/ac400892z (2013).

117   Jadoul, L., Longuespee, R., Noel, A. & De Pauw, E. A spiked tissue-based approach for quantification of phosphatidylcholines in brain section by MALDI mass spectrometry imaging. *Analytical and bioanalytical chemistry* **407**, 2095-2106, doi:10.1007/s00216-014-8232-7 (2015).

118   Takai, N., Tanaka, Y., Watanabe, A. & Saji, H. Quantitative imaging of a therapeutic peptide in biological tissue sections by MALDI MS. *Bioanalysis* **5**, 603-612, doi:10.4155/bio.13.13 (2013).

119   Chumbley, C. W. *et al.* Absolute Quantitative MALDI Imaging Mass Spectrometry: A Case of Rifampicin in Liver Tissues. *Analytical chemistry* **88**, 2392-2398, doi:10.1021/acs.analchem.5b04409 (2016).

120   Pirman, D. A. & Yost, R. A. Quantitative Tandem Mass Spectrometric Imaging of Endogenous Acetyl-l-Carnitine from Piglet Brain Tissue Using an Internal Standard. *Analytical chemistry*, doi:10.1021/ac201949b (2011).

121   Pirman, D. A., Reich, R. F., Kiss, A., Heeren, R. M. A. & Yost, R. A. Quantitative MALDI Tandem Mass Spectrometric Imaging of Cocaine from Brain Tissue with a Deuterated Internal Standard. *Analytical chemistry* **85**, 1081–1089, doi:10.1021/ac302960j (2012).

122   Prideaux, B. A., S.J.; Carolan, V.A.; Morton, J.; Clench, M.R. Sample preparation and data interpretation procedures for the examination of xenobiotic compounds in skin by indirect imaging MALDI-MS. *Int J Mass Spectrom* **260**, 243-251 (2007).

123   Wang, H. Y., Jackson, S. N., McEuen, J. & Woods, A. S. Localization and analyses of small drug molecules in rat brain tissue sections. *Analytical chemistry* **77**, 6682-6686 (2005).

124   Hamm, G. *et al.* Quantitative mass spectrometry imaging of propranolol and olanzapine using tissue extinction calculation as normalization factor. *Journal of proteomics* **75**, 4952–4961 (2012).

125   Hsieh, Y. *et al.* Matrix-assisted laser desorption/ionization imaging mass spectrometry for direct measurement of clozapine in rat brain tissue. *Rapid communications in mass spectrometry : RCM* **20**, 965-972, doi:10.1002/rcm.2397 (2006).

126   Giordano, S. *et al.* Heterogeneity of paclitaxel distribution in different tumor models assessed by MALDI mass spectrometry imaging. *Scientific reports* **6**, 39284 (2016).

127   Takai, N., Tanaka, Y. & Saji, H. Quantification of small molecule drugs in biological tissue sections by imaging mass spectrometry using surrogate tissue-based calibration standards. *Mass spectrometry* **3**, A0025, doi:10.5702/massspectrometry.A0025 (2014).

128 Chen, J., Hsieh, Y., Knemeyer, I., Crossman, L. & Korfmacher, W. A. Visualization of first-pass drug metabolism of terfenadine by MALDI-imaging mass spectrometry. *Drug metabolism letters* **2**, 1-4 (2008).

129 Barré, F. P. *et al.* Derivatization strategies for the detection of triamcinolone acetonide in cartilage by using matrix-assisted laser desorption/ionization mass spectrometry imaging. *Analytical chemistry* **88**, 12051-12059 (2016).

130 Rompp, A. *et al.* imzML: Imaging Mass Spectrometry Markup Language: A common data format for mass spectrometry imaging. *Methods in molecular biology* **696**, 205-224, doi:10.1007/978-1-60761-987-1_12 (2011).

131 Schramm, T. *et al.* imzML A common data format for the flexible exchange and processing of mass spectrometry imaging data. *Journal of proteomics* (2012).

132 Race, A. M., Styles, I. B. & Bunch, J. Inclusive sharing of mass spectrometry imaging data requires a converter for all. *Journal of proteomics* **75**, 5111-5112 (2012).

133 Robichaud, G., Garrard, K. P., Barry, J. A. & Muddiman, D. C. MSiReader: an open-source interface to view and analyze high resolving power MS imaging files on Matlab platform. *Journal of the American Society for Mass Spectrometry* **24**, 718-721 (2013).

134 Bokhart, M. T., Nazari, M., Garrard, K. P. & Muddiman, D. C. MSiReader v1. 0: Evolving Open-Source Mass Spectrometry Imaging Software for Targeted and Untargeted Analyses. *Journal of The American Society for Mass Spectrometry*, 1-9 (2017).

135 Race, A. M. *et al.* SpectralAnalysis: Software for the Masses. *Analytical chemistry* **88**, 9451-9458, doi:10.1021/acs.analchem.6b01643 (2016).

136 Dexter, A., Race, A. M., Styles, I. B. & Bunch, J. Testing for Multivariate Normality in Mass Spectrometry Imaging Data: A Robust Statistical Approach for Clustering Evaluation and the Generation of Synthetic Mass Spectrometry Imaging Data Sets. *Analytical chemistry* **88**, 10893-10899, doi:10.1021/acs.analchem.6b02139 (2016).

137 Kallback, P., Shariatgorji, M., Nilsson, A. & Andren, P. E. Novel mass spectrometry imaging software assisting labeled normalization and quantitation of drugs and neuropeptides directly in tissue sections. *Journal of proteomics* **75**, 4941-4951, doi:10.1016/j.jprot.2012.07.034 (2012).

138 Arndt Asperger, D. N., Shibojyoti Lahiri, Axel Imhof, Shannon Cornett. *High-speed MALDI-TOF/TOF imaging of mouse brain tissue performed on intact proteins and after on-tissue digestion* (Bruker, http://scils.de/news/, 2017).

139 Chaurand, P. *et al.* Integrating histology and imaging mass spectrometry. *Analytical chemistry* **76**, 1145-1155 (2004).

140 Caldwell, R. L. & Caprioli, R. M. Tissue profiling by mass spectrometry: a review of methodology and applications. *Molecular & cellular proteomics : MCP* **4**, 394-401 (2005).

141 Puolitaival, S. M., Burnum, K. E., Cornett, D. S. & Caprioli, R. M. Solvent-free matrix dry-coating for MALDI imaging of phospholipids. *J Am Soc Mass Spectrom* **19**, 882-886, doi:S1044-0305(08)00119-0 [pii]10.1016/j.jasms.2008.02.013 (2008).

142 Yanagisawa, K. *et al.* Proteomic patterns of tumour subsets in non-small-cell lung cancer. *The Lancet* **362**, 433-439 (2003).

143 Cornett, D. S. *et al.* A novel histology-directed strategy for MALDI-MS tissue profiling that improves throughput and cellular specificity in human breast cancer. *Molecular & cellular proteomics : MCP* **5**, 1975-1983 (2006).

144 Thomas, A. *et al.* Histology-driven data mining of lipid signatures from multiple imaging mass spectrometry analyses: application to human colorectal cancer liver metastasis biopsies. *Analytical chemistry* **85**, 2860-2866, doi:10.1021/ac3034294 (2013).

145 Eberlin, L. S. *et al.* Molecular assessment of surgical-resection margins of gastric cancer by mass-spectrometric imaging. *Proceedings of the National Academy of Sciences* **111**, 2436-2441, doi:10.1073/pnas.1400274111.

146   Calligaris, D. *et al.* Application of desorption electrospray ionization mass spectrometry imaging in breast cancer margin analysis. *Proceedings of the National Academy of Sciences of the United States of America* **111**, 15184-15189, doi:10.1073/pnas.1408129111 (2014).

147   Ramos-Vara, J. A. & Miller, M. A. When Tissue Antigens and Antibodies Get Along. *Veterinary Pathology* **51**, 42-87, doi:doi:10.1177/0300985813505879 (2014).

148   Chughtai, K. *et al.* Fiducial markers for combined 3-dimensional mass spectrometric and optical tissue imaging. *Analytical chemistry* **84**, 1817-1823, doi:10.1021/ac203373h (2012).

149   Meistermann, H. *et al.* Biomarker discovery by imaging mass spectrometry: transthyretin is a biomarker for gentamicin-induced nephrotoxicity in rat. *Molecular & cellular proteomics : MCP* **5**, 1876-1886, doi:10.1074/mcp.M500399-MCP200 (2006).

150   Chang, Q. *et al.* Imaging Mass Cytometry. *Cytometry. Part A : the journal of the International Society for Analytical Cytology* **91**, 160-169, doi:10.1002/cyto.a.23053 (2017).

151   Bjornson, Z. B., Nolan, G. P. & Fantl, W. J. Single-cell mass cytometry for analysis of immune system functional states. *Curr Opin Immunol* **25**, 484-494, doi:10.1016/j.coi.2013.07.004 (2013).

152   Chang, Q. *et al.* Biodistribution of cisplatin revealed by imaging mass cytometry identifies extensive collagen binding in tumor and normal tissues. *Scientific reports* **6**, 36641, doi:10.1038/srep36641 (2016).

153   Kertesz, V. *et al.* Comparison of Drug Distribution Images from Whole-Body Thin Tissue Sections Obtained Using Desorption Electrospray Ionization Tandem Mass Spectrometry and Autoradiography. *Analytical chemistry* **80**, 5168-5177, doi:10.1021/ac800546a (2008).

154   Drexler, D. M., Tannehill-Gregg, S. H., Wang, L. & Brock, B. J. Utility of quantitative whole-body autoradiography (QWBA) and imaging mass spectrometry (IMS) by matrix-assisted laser desorption/ionization (MALDI) in the assessment of ocular distribution of drugs. *Journal of pharmacological and toxicological methods* **63**, 205-208, doi:10.1016/j.vascn.2010.10.003 (2011).

155   Goodwin, R. J. A. *et al.* Exemplifying the Screening Power of Mass Spectrometry Imaging over Label-Based Technologies for Simultaneous Monitoring of Drug and Metabolite Distributions in Tissue Sections. *Journal of Biomolecular Screening* **21**, 187-193, doi:10.1177/1087057115623740 (2016).

156   Franck, J. *et al.* Quantification-based mass spectrometry imaging of proteins by parafilm assisted microdissection. *Analytical chemistry* **85**, 8127-8134, doi:10.1021/ac4009397 (2013).

157   Schuster, D., Laggner, C. & Langer, T. Why drugs fail-a study on side effects in new chemical entities. *Current pharmaceutical design* **11**, 3545-3559 (2005).

158   Kubinyi, H. Drug research: myths, hype and reality. *Nature Reviews Drug Discovery* **2**, 665-668 (2003).

159   Troendle, F. J., Reddick, C. D. & Yost, R. A. Detection of pharmaceutical compounds in tissue by matrix-assisted laser desorption/ionization and laser desorption/chemical ionization tandem mass spectrometry with a quadrupole ion trap. *Journal of the American Society for Mass Spectrometry* **10**, 1315-1321 (1999).

160   Reyzer, M. L., Hsieh, Y., Ng, K., Korfmacher, W. A. & Caprioli, R. M. Direct analysis of drug candidates in tissue by matrix-assisted laser desorption/ionization mass spectrometry. *Journal of mass spectrometry : JMS* **38**, 1081-1092, doi:10.1002/jms.525 (2003).

161   Rohner, T. C., Staab, D. & Stoeckli, M. MALDI mass spectrometric imaging of biological tissue sections. *Mech Ageing Dev* **126**, 177-185 (2005).

162   Khatib-Shahidi, S., Andersson, M., Herman, J. L., Gillespie, T. A. & Caprioli, R. M. Direct molecular analysis of whole-body animal tissue sections by imaging MALDI mass spectrometry. *Analytical chemistry* **78**, 6448-6456, doi:10.1021/ac060788p (2006).

163   Stoeckli, M., Staab, D., Schweitzer, A., Gardiner, J. & Seebach, D. Imaging of a beta-Peptide Distribution in Whole-Body Mice Sections by MALDI Mass Spectrometry. *J Am Soc Mass Spectrom* **18**, 1921-1924, doi:10.1016/j.jasms.2007.08.005 (2007).

164   Trim, P. J. *et al.* Matrix-Assisted Laser Desorption/Ionization-Ion Mobility Separation-Mass Spectrometry Imaging of Vinblastine in Whole Body Tissue Sections. *Analytical chemistry* **80**, 8628-8634, doi:10.1021/ac8015467 (2008).

165   Shahidi-Latham, S. K., Dutta, S. M., Prieto Conaway, M. C. & Rudewicz, P. J. Evaluation of an accurate mass approach for the simultaneous detection of drug and metabolite distributions via whole-body mass spectrometric imaging. *Analytical chemistry* **84**, 7158-7165, doi:10.1021/ac3015142 (2012).

166   Chacon, A. *et al.* On-tissue chemical derivatization of 3-methoxysalicylamine for MALDI-imaging mass spectrometry. *Journal of mass spectrometry : JMS* **46**, 840-846, doi:10.1002/jms.1958 (2011).

167   Hsieh, Y., Chen, J. & Korfmacher, W. A. Mapping pharmaceuticals in tissues using MALDI imaging mass spectrometry. *Journal of pharmacological and toxicological methods* **55**, 193-200, doi:10.1016/j.vascn.2006.06.004 (2007).

168   Atkinson, S. J., Loadman, P. M., Sutton, C., Patterson, L. H. & Clench, M. R. Examination of the distribution of the bioreductive drug AQ4N and its active metabolite AQ4 in solid tumours by imaging matrix-assisted laser desorption/ionisation mass spectrometry. *Rapid communications in mass spectrometry : RCM* **21**, 1271-1276 (2007).

169   Ashton, S. *et al.* Aurora kinase inhibitor nanoparticles target tumors with favorable therapeutic index in vivo. *Sci Transl Med* **8**, 325ra317, doi:10.1126/scitranslmed.aad2355 (2016).

170   Swales, J. G. *et al.* Mapping drug distribution in brain tissue using liquid extraction surface analysis mass spectrometry imaging. *Analytical chemistry* **87**, 10146-10152, doi:10.1021/acs.analchem.5b02998 (2015).

171   Drexler, D. M. *et al.* Utility of imaging mass spectrometry (IMS) by matrix-assisted laser desorption ionization (MALDI) on an ion trap mass spectrometer in the analysis of drugs and metabolites in biological tissues. *Journal of pharmacological and toxicological methods* **55**, 279-288, doi:10.1016/j.vascn.2006.11.004 (2007).

172   Grove, K. J. *et al.* Application of Imaging Mass Spectrometry to Assess Ocular Drug Transit. *SLAS discovery* **22**, 1239-1245, doi:10.1177/2472555217724780 (2017).

173   Yamada, Y., Hidefumi, K., Shion, H., Oshikata, M. & Haramaki, Y. Distribution of chloroquine in ocular tissue of pigmented rat using matrix-assisted laser desorption/ionization imaging quadrupole time-of-flight tandem mass spectrometry. *Rapid communications in mass spectrometry : RCM* **25**, 1600-1608, doi:10.1002/rcm.5021 (2011).

174   Parson, W. B. *et al.* Analysis of chloroquine and metabolites directly from whole-body animal tissue sections by liquid extraction surface analysis (LESA) and tandem mass spectrometry. *Journal of mass spectrometry : JMS* **47**, 1420-1428, doi:10.1002/jms.3068 (2012).

175   Wiseman, J. M. *et al.* Desorption electrospray ionization mass spectrometry: Imaging drugs and metabolites in tissues. *Proceedings of the National Academy of Sciences of the United States of America* **105**, 18120-18125, doi:10.1073/pnas.0801066105 (2008).

176   Choo, E. F. *et al.* Role of P-glycoprotein on the brain penetration and brain pharmacodynamic activity of the MEK inhibitor cobimetinib. *Molecular pharmaceutics* **11**, 4199-4207, doi:10.1021/mp500435s (2014).

177   Porta, T., Grivet, C., Kraemer, T., Varesio, E. & Hopfgartner, G. Single hair cocaine consumption monitoring by mass spectrometric imaging. *Analytical chemistry* **83**, 4266-4272 (2011).

178   Mains, J., Wilson, C. G. & Urquhart, A. ToF-SIMS analysis of dexamethasone distribution in the isolated perfused eye. *Investigative ophthalmology & visual science* **52**, 8413-8419 (2011).

179   Matsumoto, T. *et al.* Distribution Analysis via Mass Spectrometry Imaging of Ephedrine in the Lungs of Rats Orally Administered the Japanese Kampo Medicine Maoto. *Scientific reports* **7**, 44098, doi:10.1038/srep44098 (2017).

180   Signor, L. *et al.* Analysis of erlotinib and its metabolites in rat tissue sections by MALDI quadrupole time-of-flight mass spectrometry. *Journal of mass spectrometry : JMS* **42**, 900-909, doi:10.1002/jms.1225 (2007).

181   Marko-Varga, G. *et al.* Drug localization in different lung cancer phenotypes by MALDI mass spectrometry imaging. *Journal of proteomics* **74**, 982-992, doi:10.1016/j.jprot.2011.03.019 (2011).

182   Castellino, S. *et al.* Central nervous system disposition and metabolism of Fosdevirine (GSK2248761), a non-nucleoside reverse transcriptase inhibitor: an LC-MS and Matrix-assisted laser desorption/ionization imaging MS investigation into central nervous system toxicity. *Chemical research in toxicology* **26**, 241-251, doi:10.1021/tx3004196 (2013).

183   Marshall, P. *et al.* Correlation of Skin Blanching and Percutaneous Absorption for Glucocorticoid Receptor Agonists by Matrix-Assisted Laser Desorption Ionization Mass Spectrometry Imaging and Liquid Extraction Surface Analysis with Nanoelectrospray Ionization Mass Spectrometry. *Analytical chemistry* **82**, 7787-7794, doi:10.1021/ac1017524 (2012).

184   Römpp, A., Guenther, S., Takats, Z. & Spengler, B. Mass spectrometry imaging with high resolution in mass and space (HR2 MSI) for reliable investigation of drug compound distributions on the cellular level. *Analytical and bioanalytical chemistry* **401**, 65-73 (2011).

185   Fehniger, T. E. *et al.* Direct demonstration of tissue uptake of an inhaled drug: proof-of-principle study using matrix-assisted laser desorption ionization mass spectrometry imaging. *Analytical chemistry* **83**, 8329-8336 (2011).

186   Bunch, J., Clench, M. R. & Richards, D. S. Determination of pharmaceutical compounds in skin by imaging matrix-assisted laser desorption/ionisation mass spectrometry. *Rapid communications in mass spectrometry : RCM* **18**, 3051-3060 (2004).

187   Castellino, S., Groseclose, M. R. & Wagner, D. MALDI imaging mass spectrometry: bridging biology and chemistry in drug development. *Bioanalysis* **3**, 2427-2441, doi:10.4155/bio.11.232 (2011).

188   D'Alvise, J., Mortensen, R., Hansen, S. H. & Janfelt, C. Detection of follicular transport of lidocaine and metabolism in adipose tissue in pig ear skin by DESI mass spectrometry imaging. *Analytical and bioanalytical chemistry* **406**, 3735-3742, doi:10.1007/s00216-014-7802-z (2014).

189   Shin, Y. G., Dong, T., Chou, B. & Menghrajani, K. Determination of loperamide in mdr1a/1b knock-out mouse brain tissue using matrix-assisted laser desorption/ionization mass spectrometry and comparison with quantitative electrospray-triple quadrupole mass spectrometry analysis. *Archives of pharmacal research* **34**, 1983-1988, doi:10.1007/s12272-011-1119-7 (2011).

190   Dekker, L. J. *et al.* A mass spectrometry based imaging method developed for the intracellular detection of HIV protease inhibitors. *Rapid Communications in Mass Spectrometry* **23**, 1183-1188 (2009).

191   Koeniger, S. L. *et al.* A quantitation method for mass spectrometry imaging. *Rapid communications in mass spectrometry : RCM* **25**, 503-510, doi:10.1002/rcm.4891 (2011).

192   Bouslimani, A., Bec, N., Glueckmann, M., Hirtz, C. & Larroque, C. Matrix-assisted laser desorption/ionization imaging mass spectrometry of oxaliplatin derivatives in heated intraoperative chemotherapy (HIPEC)-like treated rat kidney. *Rapid Communications in Mass Spectrometry* **24**, 415-421 (2010).

193   Salphati, L. *et al.* Distribution of the phosphatidylinositol 3-kinase inhibitors Pictilisib (GDC-0941) and GNE-317 in U87 and GS2 intracranial glioblastoma models-assessment by matrix-

assisted laser desorption ionization imaging. *Drug metabolism and disposition: the biological fate of chemicals* **42**, 1110-1116, doi:10.1124/dmd.114.057513 (2014).

194   Sun, N. *et al.* Pharmacokinetic and pharmacometabolomic study of pirfenidone in normal mouse tissues using high mass resolution MALDI-FTICR-mass spectrometry imaging. *Histochemistry and cell biology* **145**, 201-211 (2016).

195   Nilsson, A. *et al.* Investigating nephrotoxicity of polymyxin derivatives by mapping renal distribution using mass spectrometry imaging. *Chemical research in toxicology* **28**, 1823-1830, doi:10.1021/acs.chemrestox.5b00262 (2015).

196   McClure, R. A. *et al.* Vol. 2   620-629 (2013).

197   Takai, N., Tanaka, Y., Inazawa, K. & Saji, H. Quantitative analysis of pharmaceutical drug distribution in multiple organs by imaging mass spectrometry. *Rapid Commun Mass Spec.* **26**, 1549-1556, doi:10.1002/rcm.6256 (2012).

198   Boudon, S. M. *et al.* Evaluation of sparfloxacin distribution by mass spectrometry imaging in a phototoxicity model. *J Am Soc Mass Spectrom* **25**, 1803-1809, doi:10.1007/s13361-014-0947-3 (2014).

199   Végvári, Á. *et al.* Essential tactics of tissue preparation and matrix nano-spotting for successful compound imaging mass spectrometry. *J Proteom.* **73**, 1270-1278 (2010).

200   Zecchi, R. *et al.* Impact of drug administration route on drug delivery and distribution into the lung: an imaging mass spectrometry approach. *European journal of mass spectrometry* **19**, 475-482, doi:10.1255/ejms.1254 (2013).

201   Bartelink, I. H. *et al.* Heterogeneous drug penetrance of veliparib and carboplatin measured in triple negative breast tumors. *Breast cancer research : BCR* **19**, 107, doi:10.1186/s13058-017-0896-4 (2017).

202   Ait-Belkacem, R. *et al.* Microenvironment Tumor Metabolic Interactions Highlighted by qMSI: Application to the Tryptophan-Kynurenine Pathway in Immuno-Oncology. *SLAS discovery* **0**, 1-11, doi:10.1177/2472555217712659 (2017).

203   Kreye, F. *et al.* MALDI-TOF MS imaging of controlled release implants. *Journal of Controlled Release* **161**, 98-108 (2012).

204   Munteanu, B. *et al.* Label-free in situ monitoring of histone deacetylase drug target engagement by matrix-assisted laser desorption ionization-mass spectrometry biotyping and imaging. *Analytical chemistry* **86**, 4642-4647, doi:10.1021/ac500038j (2014).

205   Balog, J. *et al.* Intraoperative tissue identification using rapid evaporative ionization mass spectrometry. *Science translational medicine* **5**, 194ra193-194ra193 (2013).

206   Liu, X., Weaver, E. M. & Hummon, A. B. Evaluation of therapeutics in three-dimensional cell culture systems by MALDI imaging mass spectrometry. *Analytical chemistry* **85**, 6295-6302, doi:10.1021/ac400519c (2013).

207   Harvey, A. *et al.* MALDI-MSI for the analysis of a 3D tissue-engineered psoriatic skin model. *Proteomics* **16**, 1718-1725, doi:10.1002/pmic.201600036 (2016).

208   Liu, X. *et al.* Molecular imaging of drug transit through the blood-brain barrier with MALDI mass spectrometry imaging. *Sci. Rep.* **3** (2013).

Word Count

Chapter 1 (Introduction): 12457

Chapter 2: 166

Chapter 3: 6064

Chapter 4: 5453

Chapter 5: 5799

Chapter 6: 5855

Chapter 7 (Summary and conclusion): 4385

Total word count: 40179

Appendix I – Supplementary Information to Chapter 3

Mass spectrometry imaging of cassette dosed drugs for higher throughput pharmacokinetic and biodistribution analysis

John G. Swales[1, 5], James W. Tucker[1], Nicole Strittmatter[4], Anna Nilsson[3], Diego Cobice[4],

Malcolm R. Clench[5], C. Logan Mckay[4], Per E. Andren[3], Zoltán Takáts[4], Peter J.H. Webborn[1],

Richard J.A. Goodwin[1]

[1] Drug Safety & Metabolism, Innovative Medicines, AstraZeneca R&D, Alderley Park, UK.
[2] SIRCAMS, School of Chemistry, University of Edinburgh, Edinburgh, U.K.
[3] Biomolecular Imaging and Proteomics, National Center for Mass Spectrometry Imaging,
   Department of Pharmaceutical Biosciences, Uppsala University, Uppsala, Sweden
[4] Department of Surgery and Cancer, Sir Alexander Fleming Building, Imperial College, London SW7 2AZ, UK
[5] Biomedical Research Centre, Sheffield Hallam University, Howard Street, Sheffield S1 1WB, UK

Table of Contents

1

1. Supplementary Methods

1.1 Bioanalytical Stock Solution Preparation. Stock solutions of test compounds were prepared in DMSO to give a final concentration of 2 mM. Compounds were mixed into a cassette to a final concentration of 0.2 mM and were subsequently serially diluted to form working solutions for use in calibration curve construction. Samples for the standard curves and quality controls were prepared from different solutions by spiking control rat plasma with the appropriate working solution. Calibration standards (50 μL) were prepared in control rat plasma at 1, 5, 10, 20, 50, 100, 500, 1000, 2000, 5000 and 10000 nM. Duplicate quality controls (50 μL) were spiked at 10, 100 and 2000 nM in control rat plasma and were interspersed at regular intervals throughout the analytical batches. The calibration standards were injected at the beginning and end of the analytical run and were subsequently used to construct a calibration curve and quantify the unknowns and quality controls. Analytical batches were considered successful if calibration standards and quality controls (a minimum of 2/3) were within 25% of the nominal concentration. 50 μL of plasma was protein precipitated with 200 μL of chilled acetonitrile containing internal standard (generic from the AZ compound library). The samples were then vortex mixed and centrifuged at 4500g for 10 mins. 50 μL of supernatant was then mixed with 300 μL of distilled water prior to analysis by LC-MS/MS.

1.2 Bioanalytical Method. A TSQ Quantum Vantage (Thermo Fisher Scientific, San Jose, CA, USA) mass spectrometer operating with a heated electrospray ionization interface was used for the LC-MS/MS determination of the compounds dosed discretly and in cassettes. The mass transitions monitored for compounds dosed orally were m/z 472.3>436.4, 313.1>256.1, 394.1>278.1, 402.1>384.3 for terfenadine, olanzapine, erlotinib and moxifloxacin, corresponding collision energies were 25, 22, 31 and 21 eV respectively. The sheath gas and

2

auxiliary gas were set at 80 and 40 (Arb) respectively. An Agilent 1200SL HPLC pump (Agilent, Stockport, UK) and a CTC Analytics HTC PAL autosampler (Presearch Ltd., Basingstoke, UK) were used to introduce the samples to the mass spectrometer. Chromatography was performed on a Eclipse plus (50mm×2.1mm ID, 5μm) HPLC column (Agilent, Cheadle, UK) with mobile phase consisting of eluent (A) water containing 0.1% formic acid and (B) methanol containing 0.1% formic acid. The linear gradient used was (T = minutes): at T = 0.0, 95%A:5%B, T = 3.0, 5%A:95%B, T = 4.0, 5%A:95%B, T = 4.1, 95%A:5%B, T = 5.0, 95%A:5%B. The flow rate used was 750 μL/min. Concentration-time data was processed using QuickCalc/GMSU (Gubbs Inc, Alpharetta, Georgia, USA) to quantify peak areas. Pharmacokinetic parameters were calculated using non-compartmental analysis performed in WinNonlin 5.2.1 (Pharsight Corp., Mountain View, California, USA).

3

Figure S-1. Plasma concentrations (ng/mL) of moxifloxacin and olanzapine after oral dosing at 25 and 10 mg/kg, respectively, as part of a cassette dose and a discrete dose. Plasma concentration/time profiles for cassette and disctretly dosed compounds can be seen to be identical for moxifloxacin (black) and olanzapine (red) after oral dosing.
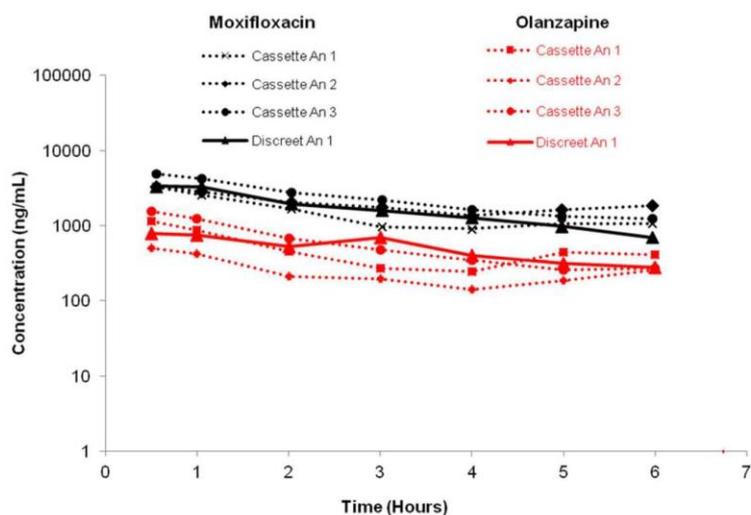
Table S-1: Pharmacokinetic parameters of pharmaceutical compounds after oral cassette or discrete dosing to male Hans Wistar rats.

	Erlotinib			Moxifloxacin			
Parameter	Cassette 1	Cassette 2	Cassette 3	Cassette 1	Cassette 2	Cassette 3	Discreet 1
Dose (mg/kg)	10	10	10	25	25	25	25
Cmax (ng/mL)	4354	3081	5576	3746	3787	5657	3777
Tmax (h)	0.5	0.5	0.5	0.5	0.5	0.5	0.5
Half-life (h)	9.5	13.1	5.6	3.2	5.6	2.6	2.3
AUC0-t (hr*ng/mL)	16711	13160	21701	9719	12898	16045	11480
AUCinf (hr*ng/mL)	55064	54488	46179	15129	29806	21099	13991

	Terfenadine			Olanzapine			
Parameter	Cassette 1	Cassette 2	Cassette 3	Cassette 1	Cassette 2	Cassette 3	Discreet 1
Dose (mg/kg)	25	25	25	10	10	10	10
Cmax (ng/mL)	43	32	79	1162	507	1562	791
Tmax (h)	1.0	0.5	2.0	0.5	0.5	0.5	0.5
Half-life (h)	3.5	2.4	1.4	3.8	4.7	2.0	3.7
AUC0-t (hr*ng/mL)	155	71	261	2879	1438	3618	3032
AUCinf (hr*ng/mL)	245	102	288	5131	3193	4418	4530

4

Figure S-2 Sample spectra confirming exposure in lung tissue of A) moxifloxacin, B) olanzapine, C) erlotinib and D) terfenadine by accurate mass and comparison of each with a vehicle dosed control sample. The mass accuracy of each analyte confirms the response obtained can only be from the compounds dosed.
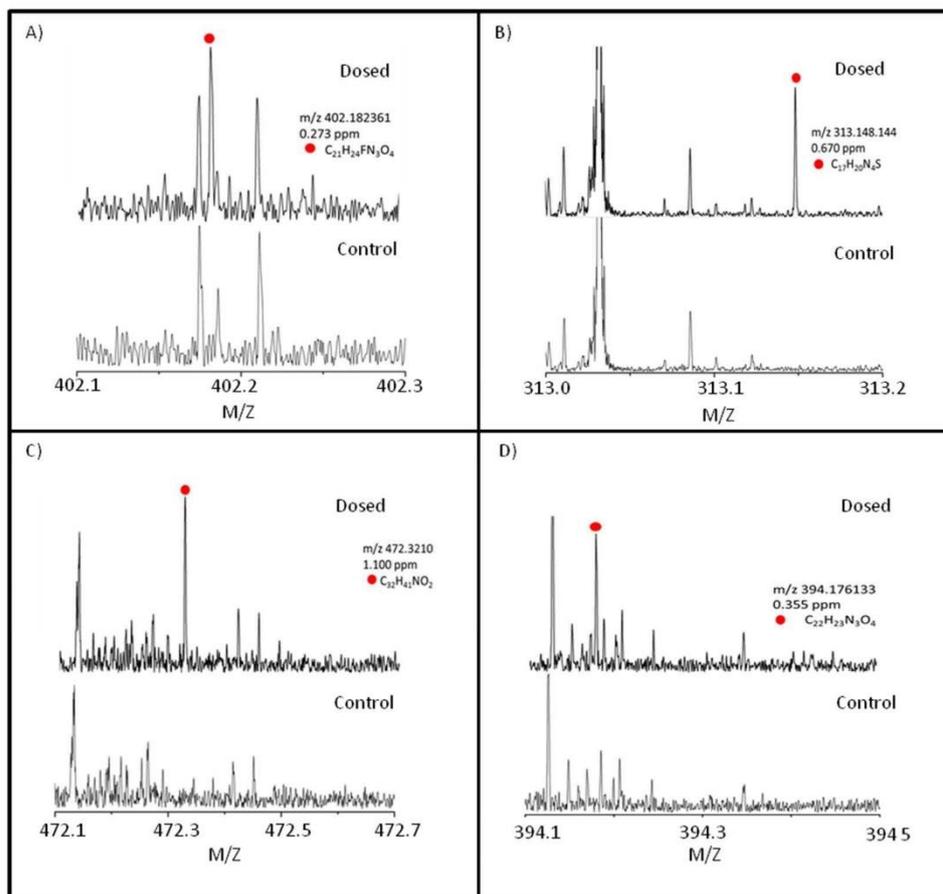
Appendix II – Supplementary Information to Chapter 5

Supplementary Information

Spatial Quantification of Drugs in tissues using Liquid Extraction Surface Analysis Mass Spectrometry Imaging.

John G. Swales[1, 2], Nicole Strittmatter[1], James W. Tucker[1], Malcolm R. Clench[2], Peter J.H.

Webborn[1], Richard J.A. Goodwin[1]

[1] Drug Safety & Metabolism, AstraZeneca R&D, Cambridge Science Park, Cambridge, CB4 0WG, UK
[2] Biomedical Research Centre, Sheffield Hallam University, Howard Street, Sheffield S1 1WB, UK

Short title: Quantification of drugs by LESA

Keywords: LESA, DESI, MSI, Imaging

Corresponding author:

Email: john.swales@astrazeneca.com
Address: AstraZeneca, Darwin Building, Cambridge Science Park, Milton Road, Cambridge, Cambridgeshire, CB4 0WG, UK
Tel. +44(0)1223 223417

Liver homogenate preparation

Liver homogenates were prepared by adding deionised water to one cerebral hemisphere at a 3:1 v/w ratio in a Precellys CK28 – 7mL tissue homogenising tube (KT03961-11302.7) and subjecting to rapid multi directional motion using a Precellys Evolution homogeniser (Bertin Technologies, Montigney-le-Bretonneux, FR).

LC-MS/MS bioanalytical method

Preparation of calibration standards and quality controls

Calibration (Cal) (0.1 – 100 nmol/L) and quality control (QC) (1, 25, 75 nmol/L) samples were prepared by serial dilution of separate 2 mM DMSO stock solutions in either control plasma or control liver homogenate. Calibration samples were prepared fresh on the day of analysis, QC samples were prepared in advance and stored at -20 °C alongside homogenised test samples where-by being subjected to the same freeze/thaw cycle.

Bioanalytical Method

On the day of analysis 50 μL of test, Cal or QC sample was subjected to protein precipitation with 150 μL of acetonitrile containing 1 μg/mL of the assay internal standard, a structurally unrelated compound from the AZ compound library. Following mixing and centrifugation 50 μL of the resulting supernatant was transferred to the well of a 96 deep well plate containing 300 μL of water.

50 μL of the resulting extracts were injected onto a gradient UHPLC system (Accela, Thermo Scientific, Hemel Hempstead, Herts, UK) compromising of 0.1% v/v formic acid (aq) as mobile phase A, 0.1% v/v formic acid in methanol as mobile phase B and a Phenomenex Max-RP 50 x 2.1mm column (Phenomenex, Macclesfield, Cheshire, UK) as the stationary phase. Detection was performed using a TSQ Vantage (Thermo Scientific, Hemel

Hempstead, Herts, UK) mass spectrometer operating in selected reaction monitoring mode (SRM) with an electrospray ionisation source (ESI). The mass transitions monitored for compounds dosed orally were the same as detailed in the main manuscript for LESA analysis. Analyte/internal standard peak area ratios were calculated and the calibration data fitted using a linear regression with a $1/x^2$ weighted fit. Test and QC sample concentrations were back calculated from the fitted line. Analytical batches was considered acceptable if 75% of the calibration levels fell within 15% of their nominal concentrations and a minimum of 4 out of 6 of the back calculated QC samples fell within 15% of their nominal concentrations.

LESA optimization experiments

Solvent composition

Figure SI 1 - Graph showing mean intesity of clozapine, albendazole, tamoxifen and astemizole after LESA extraction (n=10) with different solvent compositions of a) Isopropyl alcohol, b) methanol and c) Acetonitrile.
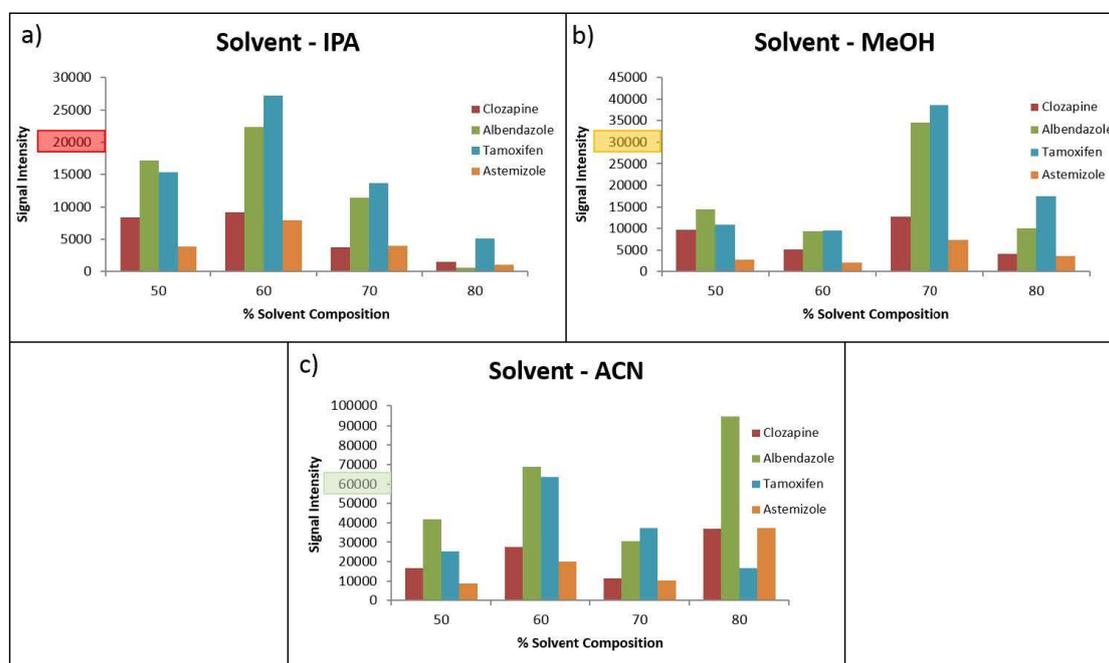
Tissue thickness

Figure SI 2 – Graph showing the effect of tissue thickness on mean signal intensity after LESA extraction (n=10).
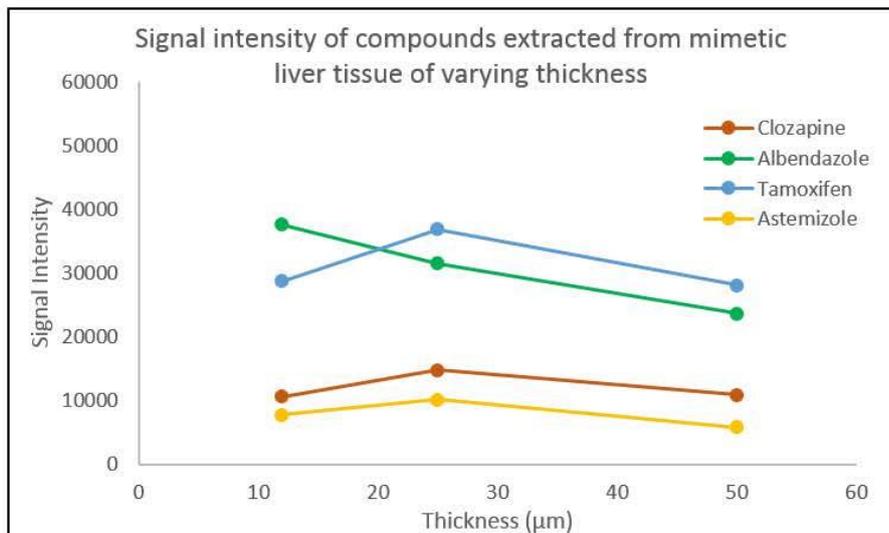
Solvent dwell time

Figure SI 3 – Graph showing the effect of solvent dwell time on mean signal intesity of SCH-23390 after LESA extraction (n=10).
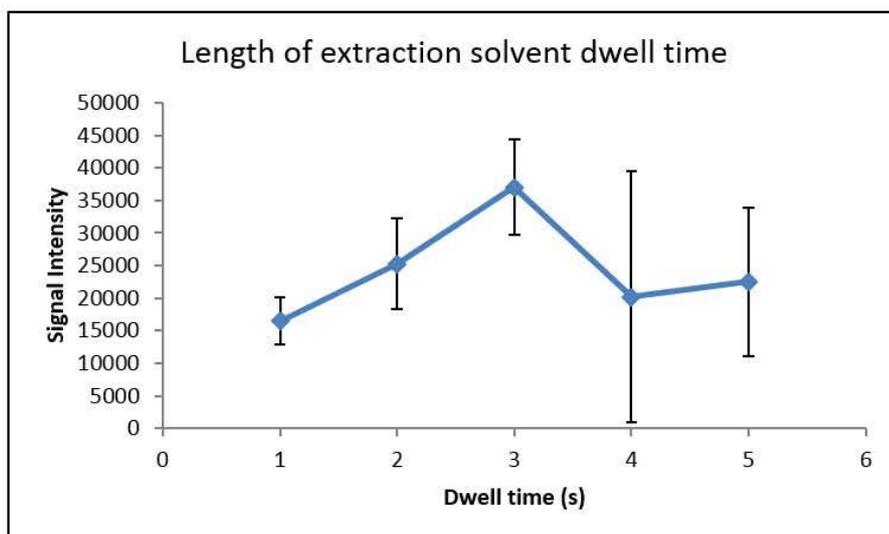
Use of an internal standard

Table SI 1 – Coefficient of variation comparison for tamoxifen, clozapine, albendazole and astemizole after LESA extraction at random points (n=10) on mimetic liver calibration standards with and without an unlabelled internal standard sprayed over the tissue.

Cal Level	Tamoxifen		Clozapine		Albendazole		Astemizole	
	No IS	With IS	No IS	With IS	No IS	With IS	No IS	With IS
0.1	23.2	27.1	33.2	39.8	30.3	36.5	24	28.2
0.5	17.3	27.5	19.9	32.4	11.4	32.4	20.8	34.3
1	8.6	18.6	18.1	33.3	20.2	36.2	17.2	19.5
5	11.7	37.8	28.4	28.5	26.8	24.4	26.6	27.4
10	41.8	42.5	28.6	38.1	23.1	31.1	23.3	35.4
20	23.9	32	21.3	30.5	18.2	29.7	26.1	35.6
50	20.6	23.3	17.7	24.2	15.4	22.6	16.2	21.9
100	25.3	42.5	15	34.6	17.7	35.6	30.2	32.3

Table SI 2 – Coefficient of variation comparison for clozapine after LESA extraction at random points (n=10) on mimetic liver calibration standards with and without (deuterated) clozapine-d4 internal standard sprayed over the tissue.

Cal Level	Clozapine	
	No IS	With IS
0.1	38.8	64.1
0.5	39.9	43.9
1	43.7	46.1
5	19.3	17.1
10	28.7	43.1
20	22.6	31.5
50	44.0	56.5
100	34.7	35.1

Table SI 3 – Coefficient of variation comparison for clozapine after LESA extraction at random points (n=10) on mimetic liver calibration standards with and without (deuterated) clozapine-d4 internal standard spiked into the LESA extraction solvent..

Cal Level	Clozapine	
	No IS	With IS
0.1	12.8	19.7
0.5	40.3	41.1
1	25.4	13.0
5	46.3	31.8
10	41.8	32.7
20	31.1	19.7
50	45.9	38.7
100	31.1	18.6

The reasons for the differences in the Coefficient of variation between different concentrations in tables SI 1-3 are unknown and are likely to be the sum of many contributing factors such as ion suppression, instrument variability and inherent variation in the LESA technique. The differences do not follow a normal distribution.

Appendix III – Supporting information to Chapter

Supporting Information

Quantitation of endogenous metabolites in mouse tumors using mass spectrometry imaging

John G. Swales[1, 3], Alex Dexter[4], Gregory Hamm[1], Anna Nilsson[5], Nicole Strittmatter[1],

Filippos N. Michopoulos[2], Christopher Hardy[1], Pablo Morentin-Gutierrez[2], Martine Mellor[2],

Per E. Andren[5], Malcolm R. Clench[3], Josephine Bunch[4], Susan Critchlow[2], Richard J.A.

Goodwin[1]

[1] Pathology, Drug Safety & Metabolism, IMED Biotech Unit, AstraZeneca, Cambridge, UK
[2] Oncology Bioscience, IMED Biotech Unit, AstraZeneca, Cambridge, UK
[3] Centre for Mass Spectrometry Imaging, Biomolecular Research Centre, Sheffield Hallam University, Sheffield, UK
[4] National Centre of Excellence in Mass Spectrometry Imaging (NiCE-MSI), National Physical Laboratory, Teddington, TW11 0LW, United Kingdom
[5] Biomolecular Mass Spectrometry Imaging, National Resource for MSI, Science for Life Laboratory, Dept. of Pharmaceutical Biosciences, Uppsala University, Sweden

Short title: Quantitation of endogenous small molecules by MALDI-MSI

Keywords: MALDI, MSI, Imaging, Quantitation, Lactate, Glutamate

Corresponding author:

Email: john.swales@astrazeneca.com
Address: AstraZeneca, Darwin Building, Cambridge Science Park, Milton Road, Cambridge, Cambridgeshire, CB4 0WG, UK
Tel. +44(0)1223 223417

Tissue Embedding

To minimize any potential degradation of the endogenous analytes, all tumors from each model were embedded together in a plastic mould (VWR International Ltd, Lutterworth, Leicestershire, UK) using 10% w/v gelatin solution. Gelatin blocks were stored at -80°C prior to cryosectioning.

Sectioning

Gelatin embedded tissues were cryosectioned on a CM3050S cryomicrotome (Leica Biosystems, Nussloch, Germany) at a thickness of 10 μm and thaw mounted onto indium tin oxide (ITO) coated MALDI target slides (Bruker Daltonics, Bremen, Germany). Thaw-mounted slides were immediately dessicated using a stream of dry N_2 prior to vacuum packing and storage at −80°C until analysis.

Tumor sections used in the stability experiment were sectioned onto ITO coated glass slides (Fisher Scientific, Loughborough, Leicestershire, UK) for subsequent MALDI-MSI analysis. Tissue sections were taken at approximately equal depth from all samples.

Homogenization and Quantitation of Lactate Levels by LC-MS

Whole tissue lysates were obtained after homogenization and extraction with 1 mL ACN/MeOH/H2O v/v/v per 50 mg of tissue on Precellys Fast Prep-24 temperature controlled device (Fisher Scientific, Loughborough, UK) using CKMix50R-2 ml tubes. Tissue homogenization was completed after 3x20 second cycles at 5000rpm with 30 seconds pause in between. After centrifugation at 0°C for 5 mins at 10621 g (Eppendorf 5417R) a maximum of 700 μL clear supernatant was placed in a centrifuge tube and the extraction procedure was repeat as described above. The second fraction of clear supernatant was combined in the same centrifuge tube with the first extract before storing at -20°C.

S-2

Prior to LC-MS analysis 5 µL of tissue extract was diluted with 45 µL of 55 µM $^{13}C_3$ Lactic

acid (Dilution A). 5µL of diluent A was mixed in a polypropylene HPLC vial with 45 µL

H_2O, followed by quick vortex and 10min centrifugation at 3273 g (4°C).

Lactic acid was chromatographically resolved from matrix interferences under isocratic

elution conditions with 20% eluent B (Eluent A: 10 mM tributylamine, 15 mM acetic acid in

H_2O, Eluent B: Isopropanol/MeOH 20/80 *v/v*) using a HSS T3 C_{18} column (2.1x100mm,

1.8µm) and quantification results were obtained over a linear range of 0.5-160 µM

concentration. Batch validation completed on quality control samples (QC) prepared by

mixing equal aliquots of all tissue lysate and spiked with $^{13}C_3$ Lactic acid at concentration of

0.5, 1, 5, 40 and 120 µM. Validation QCs at each concentration were injected at the

beginning, middle and end of the analytical batch to obtain accuracy (<7% bias) and

precision (<7% CV) values.

Figure SI 1: Lactate and glutamate distribution alongside H&E stained images highlighting the co-localization of necrotic and pre-necrotic regions with areas of high lactate concentration.
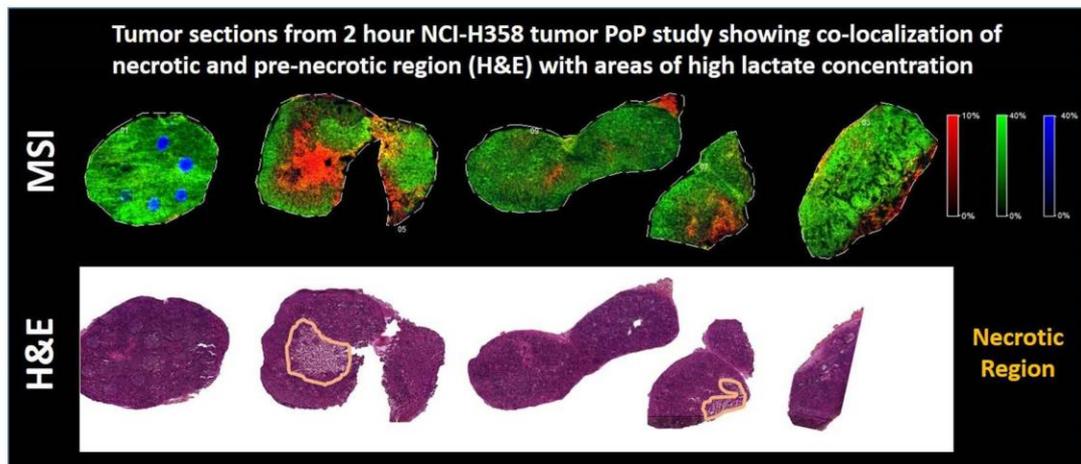
Appendix IV – Copyright Permissions

ACS Publications
Most Trusted. Most Cited. Most Read.

Title: Quantitation of Endogenous Metabolites in Mouse Tumors Using Mass-Spectrometry Imaging

Author: John G. Swales, Alex Dexter, Gregory Hamm, et al

Publication: Analytical Chemistry

Publisher: American Chemical Society

Date: May 1, 2018

PERMISSION/LICENSE IS GRANTED FOR YOUR ORDER AT NO CHARGE